Aus der

Kinderklinik und Kinderpoliklinik im Dr. von Haunerschen Kinderspital
Direktor: Prof. Dr. Dr. Christoph Klein

In Zusammenarbeit mit dem

Helmholtz Zentrum München, Deutsches Forschungszentrum für Gesundheit und Umwelt,
Comprehensive Pneumology Center

# Phenotypic characterization of CCR2$^{+}$ T cells in experimental pulmonary fibrosis




HelmholtzZentrum münchen
Deutsches Forschungszentrum für Gesundheit und Umwelt

CPC Comprehensive Pneumology Center

**Dissertation**

zum Erwerb des Doktorgrades der Medizin
an der Medizinischen Fakultät der
Ludwig-Maximilians-Universität zu München

Vorgelegt von

Eva Alice Brudy

aus
Oberkirch

2014

Mit Genehmigung der Medizinischen Fakultät

Der Universität München

| | |
|---|---|
| Berichterstatter: | PD Dr. Susanne Krauss-Etschmann |
| Mitberichterstatter: | PD Dr. Antje Menssen |
| | Prof. Dr. Clemens Schacky auf Schönfeld |
| Mitbetreuung durch promovierten Mitarbeiter: | Yingyan Yu; PhD |
| Dekan: | Prof. Dr. med. Dr. h.c. M. Reiser, FACR, FRCR |

Tag der mündlichen Prüfung: 18.12.2014

# Contents


**1 Abbreviations ..... 7**

**2 Introduction ..... 8**

*2.1 Interstitial lung diseases ..... 8*

2.1.1 Classification ..... 8

2.1.2 Idiopathic pulmonary fibrosis ..... 8

2.1.2.1 Clinical specifications ..... 8

2.1.2.2 Concepts of pathogenesis ..... 11

*2.2 The role of CCR2 in pulmonary fibrosis ..... 13*

**3 Hypothesis and Aims ..... 15**

**4 Materials and Methods ..... 16**

*4.1 Materials ..... 16*

4.1.1 Equipment ..... 16

4.1.2 Software ..... 16

4.1.3 Consumables ..... 16

4.1.4 Reagents ..... 17

4.1.5 Narcotics and Antidote ..... 17

4.1.6 Antibodies ..... 17

*4.2 Methods ..... 19*

4.2.1 Mice ..... 19

4.2.2 Induction of pulmonary fibrosis ..... 19

4.2.2.1 Preparation of Reagents ..... 19

4.2.2.2 Treatment procedure ..... 19

4.2.3 Sampling of lung, spleen and BALF ..... 20

4.2.3.1 Preparation of reagents ..... 20

4.2.3.2 Organ removal ..... 20

4.2.4 Preparation of cells for FACS ..... 21

4.2.4.1 Preparation of Reagents ..... 21

4.2.4.2 BAL ..... 21

4.2.4.3 Spleen ..... 21

4.2.4.4 Lung ..... 22

4.2.5 Experimental settings ..... 22

4.2.5.1 Compensating for spectral overlap of fluorochromes ..... 22

4.2.5.2 Longitudinal assessment of T cell percentages after BLM treatment ..... 24

4.2.5.3 Assessment of CCR/CXCR co-expression on lung T cells ..... 25

4.2.6 Data Analysis ..... 26
4.2.6.1 Analysis of FACS data ..... 26
4.2.6.1.1 Longitudinal assessment of T cell percentages after BLM treatment ..... 27
4.2.6.1.2 Assessment of chemokine receptor co-expression ..... 30
4.2.6.2 Statistical Analysis ..... 32
4.2.7 Histology ..... 32
4.2.7.1 Haematoxylin Eosin (HE) staining ..... 32
4.2.7.2 Masson Goldner's Trichrom staining ..... 33

**5 Results ..... 34**

*5.1 Experimental outline ..... 34*

*5.2 Characterization of the animals ..... 34*
5.2.1 Animal numbers ..... 34
5.2.2 Change of body weight ..... 35
5.2.3 Histology ..... 36

*5.3 Longitudinal assessment of T cells ..... 38*
5.3.1 Spleen ..... 38
5.3.1.1 Percentages of $CD4^+$ and $CD8^+$ T cells ..... 38
5.3.1.2 Naïve, central memory and effector memory $CD4^+$ T cells ..... 38
5.3.1.3 CCR2 expression ..... 39
5.3.2 BALF ..... 40
5.3.2.1 Cell count ..... 40
5.3.2.2 $CD4^+$ and $CD8^+$ T cells ..... 40
5.3.3 Lung ..... 42
5.3.3.1 $CD4^+$ and $CD8^+$ T cells ..... 42
5.3.3.2 Naïve, central memory, effector memory T cells ..... 43

*5.4 Maximal increase of the percentage of $CCR2^+$ T cells after bleomycin treatment ..... 45*
5.4.1 BALF ..... 45
5.4.1.1 Percentage of CCR2 expressing BAL lymphocytes ..... 45
5.4.2 Lung ..... 46
5.4.2.1 $CCR2^+$cells within total $CD4^+$ and $CD8^+$ T cells ..... 46
5.4.2.2 $CCR2^+$cells within $CD4^+$ T cell subtypes ..... 48
5.4.2.3 Maximal content of $CCR2^+$ T cells ..... 50

*5.5 Chemokine Receptor Co-expression ..... 51*
5.5.1 CCR2 ..... 51
5.5.2 CCR3 ..... 51
5.5.3 CCR4 ..... 52
5.5.4 CCR5 ..... 53

5.5.5 CCR6 ..... 54
5.5.6 CCR7 ..... 55
5.5.7 CCR9 ..... 56
5.5.8 CCR10 ..... 57
5.5.9 CXCR3 ..... 57
5.5.10 CXCR4 ..... 58
5.5.11 CXCR5 ..... 59
5.5.12 CXCR6 ..... 60

**6 Discussion ..... 62**

*6.1 Mouse model ..... 62*
6.1.1 Mice with fibrotic disease show body weight loss but no systemic immune response ..... 64

*6.2 T-cell kinetics in BAL and lung tissue during time course ..... 64*
6.2.1 $CD4^+$ and $CD8^+$ T cells ..... 64
6.2.2 Increase of effector memory T cells following bleomycin treatment in lung tissue ..... 65
6.2.3 $CCR2^+CD4^+$ T cells are increased and show $CD62L^{low}CD44^{hi}$ phenotype ..... 66

*6.3 Chemokine receptors ..... 68*
6.3.1 CCR6 ..... 68
6.3.2 CCR7 ..... 69
6.3.3 CCR3 and CCR4 ..... 71
6.3.4 CXCR5 ..... 72
6.3.5 CCR5 ..... 73
6.3.6 CXCR4 ..... 74
6.3.7 CCR9 and CCR10 ..... 75
6.3.8 CXCR6 ..... 76
6.3.9 CXCR3 ..... 77

*6.4 Conclusion ..... 78*

**7 Summary ..... 80**

**8 Zusammenfassung ..... 82**

**9 Appendix ..... 84**

*9.1 References ..... 84*

*9.2 Illustrations ..... 96*

*9.3 Tables ..... 97*

**Danksagung ..... 98**

**Eidesstattliche Versicherung ..... 99**

# 1 Abbreviations

| | |
|---|---|
| 7AAD | 7-Aminoactinomycin |
| AH | Armenian hamster |
| APC | Allophycocyanin |
| APC H7 | Allophycocyanin horizon 7 |
| BLM | Bleomycin |
| CCR | Cc-motive chemokine receptor |
| CXCR | Cxc-motive chemokine receptor |
| EDTA | Ethylenediaminetetraacetic acid |
| EMT | Epithelial to mesenchyal transition |
| FACS | Fluorescence activated cell sorting |
| FITC | Fluorescinisothiocyanat |
| FSC | Forward scatter |
| HRCT | High resolution computed tomography |
| IC | Isotype control |
| IgG | Immunoglobulin G |
| IIP | Idiopathic interstitial pneumonia |
| IL | Interleukin |
| ILD | Interstitial lung disease |
| ip | intraperitoneal |
| IPF | Idiopathic pulmonary fibrosis |
| It | intratracheal |
| iv | Intravenous |
| MCP-1 | Macrophage chemoattractant protein 1 |
| MMP | Matrix metallo proteinase |
| NSIP | Nonspecific interstitial pneumonia |
| PB | Pacific blue |
| PBS | Phosphate buffered saline |
| PE | Phycoerythin |
| RB-ILD | Respiratory bronchiolitis associated interstitial lung disease |
| SSC | Side scatter |
| $T_{cm}$ | Central memory T cell |
| $T_{em}$ | Effector memory T cell |
| TGFβ | Transforming growth factor β |
| Th | T helper cell |
| tLT | Tertiary lymphoid tissue |
| $T_{naive}$ | Naïve T cell |
| $T_{reg}$ | Regulatory T cell |
| wt | Wild type |
| α-SMA | α smooth muscle actin |

# 2 Introduction

## 2.1 Interstitial lung diseases

### 2.1.1 Classification

Interstitial lung diseases (ILD) are a group of diverse chronic inflammatory lung disorders which are characterized by restrictive impairment of lung function and diffuse lung infiltration (Figure 1).

An important, although rare group of ILD are the idiopathic interstitial pneumonias (IIP), as some of them are extremely rapidly progressive and lead to death within less than 10 years following diagnosis. By definition, their origin is not known. Furthermore, there is no curative treatment available for most of them, and the standard anti-inflammatory strategies do not lead to a sufficient control of symptoms. The following will concentrate on IPF which presents the most frequent entity of IIPs.

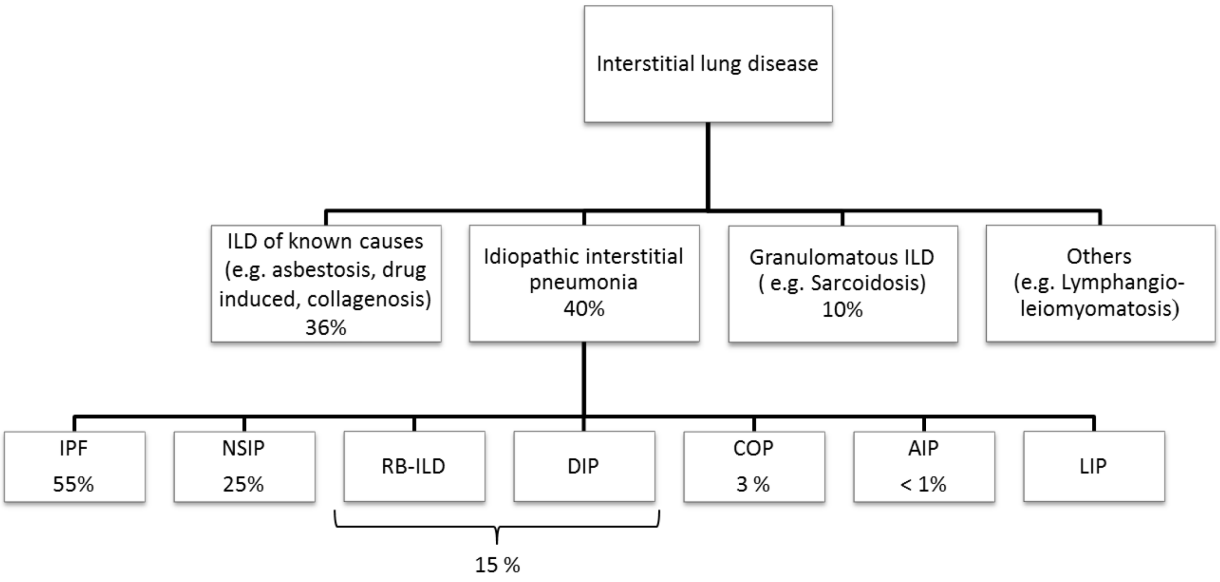



**Figure 1 Classification of ILD and relative frequency of subgroups***; modified from (1, 2); IPF: idiopathic pulmonary fibrosis; NSIP: nonspecific interstitial pneumonitis; RB-ILD: respiratory bronchiolitis associated interstitial lung disease; DIP: desquamative interstitial pneumonia; COP: cryptogenic organizing pneumonitis; AIP: acute interstitial pneumonia; LIP: lymphoid interstitial pneumonia*

### 2.1.2 Idiopathic pulmonary fibrosis

#### 2.1.2.1 *Clinical specifications*

"Idiopathic pulmonary fibrosis is defined as a specific form of chronic, progressive fibrosing interstitial pneumonia of unknown cause, occurring primarily in older adults, limited to the

lungs, and associated with the histopathologic and/or radiologic pattern of usual interstitial pneumonia (UIP)" (ATS and ERS 2011 (3)).

The median survival time of IPF is estimated to be 2 to 3 years from the day of diagnosis (4, 5). A study from the USA estimated a prevalence of 14 to 42 per 100 000 persons and an incidence of 6.8 to 16 per 100 000 persons (6). Another study from the UK found a lower incidence of 4.6 per 100 000 people but observed an increase in incidence for the period between 1991 and 2003 (7).

IPF patients present with unspecific symptoms like a chronic dry cough, dyspnea at exertion, and bibasilar crackles in the physical examination. Lung function tests show a restrictive pattern with a decreased vital capacity and impaired gas exchange.

The clinical course of IPF is characterized either by a subacute or more rapid loss of lung function or by an intermittant disease course with phases of acute exacerbations, which eventually lead to a rapid respiratory failure and death (8, 9).

The main diagnostic tool is the "high resolution computed tomography" (HRCT), which shows the typical UIP pattern, defined by the combination of basal subpleural reticular opacity, honeycombs and bonchiectasis (10, 11).

If the radiological features are not sufficient to confirm the suspicion of IPF, the diagnostic is completed by the histopathologic evaluation of a surgical lung biopsy. The histologic UIP-pattern is characterized by a heterogeneous appearance in lower magnifications, reflecting areas with different stages of fibrotic areas next to regions of normal lung parenchyma. In higher magnifications, fibrotic areas are marked by fibroblast foci and accumulation of collagen. The inflammatory reaction is represented by a patchy infiltrate of lymphocytes and plasma cells in combination with a hyperplasia of type II alveolar cells and bronchial epithelial cells. (1, 3, 12)

None of the currently available treatment options provides a curative approach or even sufficient symptom control for the majority of affected patients. Immunosupressive therapy with corticoids or immunosuppressive drugs like azathioprine used for other interstitial lung diseases seem to have no beneficial effects in IPF. Uniquely for patients with acute exacerbations immunosupressive treatment could possibly decrease mortality (13).

The ATS/ERS/JRS/ALAT guideline from 2011 recommeded a combination therapy with immunomodulators and acetylcysteine was for selected patients (3). Meanwhile, this recommendation was withdrawn, as a trial comparing the treatment with prednisone,

azathioprine and acetylcyteine versus acetylcysteine alone showed a higher risk for hospitalisation and death in the group treated with the combination therapy (14).

The only curative approach in IPF is lung transplantation. However, due to the lack of donor organs and contraindications at the side of the patients it is only applicable to a very defined group of patients (15). In 2011 pirfenidone, the first drug specifically for the treatment of IPF, has been approved in the European Union. Patients treated with pirfenidone showed decreased loss of forced vital capacity (FVC) compared to patients receiving placebo, but the drug could not stop the disease progression (16, 17). Beneath these poor treatment options only symptomatic, supportive therapies like oxygen supplementation ot physical therapy reamain (3).

### 2.1.2.2 *Concepts of pathogenesis*

As indicated by the word “idiopathic” the origin of IPF is unknown. Former concepts of pathogenesis assumed that IPF is a chronic inflammatory disease. The failure of immunosuppressive therapies let to another hypothesis which proposes repeated injuries of the alveolar epithelium being the starting point of the disease (18). Several risk factors were found to be often associated with IPF, such as smoking (19), environmental exposures like different types of dusts (20), chronic viral infections in particular herpes virus infection (21), and gastro oesophageal reflux (22). These factors might contribute to the initial lung injury, but up to now, none of them could be identified as the main factor for the development of IPF.

As consequence of the chronic injury, the development of the fibrotic reaction is thought to be the result of impaired wound healing processes through the loss of basement membrane integrity (23). These processes are driven by different components of the lung tissue. A dysfunction of the alveolar epithelium leads to apoptosis of epithelial cells. Mesenchymal components lead to an overwhelming extracellular matrix production. Different cytokines secreted by epithelial and mesenchymal cells attract immune cells.

Based on observations made in familial cases of IPF, the contribution of genetic alterations in the pathogenesis of IPF was suspected, but only a minority of patients presented similar mutations (24, 25). However, one common phenomenon found more frequently in sporadic and familial cases of IPF is a shortening of telomeres in peripheral blood leucocytes and alveolar epithelial cells. Interestingly, in the majority of these patients with sporadic IPF no mutation in the telomerase gene was found. This telomere shortening is thought to promote apoptosis of pulmonary epithelial cells, and could provide an explanation for the late onset of the disease (25-27).

A dysregulation of matrix metallo proteinases (MMPs) activity seems to play a role in the destruction of the basement membrane and the imbalance of the tissue remodeling processes in the lung. MMP2 and MMP9, which degrade the collagen IV of the basement membrane, were overexpressed in lung tissue and BALF of patients with interstitial lung diseases (28). MMP7 was overexpressed in lung tissue of patients with pulmonary fibrosis and $MMP7^{-/-}$ mice were protected from pulmmonary fibrosis (29).

A number of different cytokines and other mediators were identified as pro-fibrotic factors in interstitial lung diseases. Among these, TGFβ is one of the best characterized. It was found

to be involved in collagen production, epithelial cell apoptosis (30), epithelial to mesenchymal transition (EMT) (31, 32) and fibroblast differentiation into myofibroblasts (33). Myofibroblasts are suggested to be the source of the overwhelming extracellular matrix production in IPF. Their origin is not yet clarified. The concepts reach from transdifferentiation of resident fibroblasts over EMT (34) to recruitment of bone marrow derived mesenchymal stem cells (35).

The contribution of the immune system to fibrogenesis is multifactorial. Besides many other cell types and pathways, T cells seem to play an important role in the pathogenesis of IPF. There is evidence that a Th2 polarized immune response has profibrotic effects, whereas a Th1 response might be antifibrotic (36). Furthermore, IL17 produced by Th17 and γδ T cells was found to have profibrotic effects in the early phase of bleomycin (BLM) induced fibrosis in mice (37). Mice overexpressing the Th2 cytokine IL13 showed spontanous subepithelial pulmonary fibrosis (38), while blocking of IL13 resulted in decreased fibrosis following *Aspergillus fumigatus* (39) or bleomycin challenge (40). IL13 might act via induction of TGFβ production in pulmonary epithelial cells and its activation (41). In mouse models, as well as in human disease, there are hints for a dominance of Th2 cytokines in pulmonary fibrosis (40, 42). However, this Th2 polarization is not uncontroversial since lung fibroblasts were shown to produce predominantly Th1 related cytokines (43). IFNγ, a cytokine produced by Th1 cells, as well as IL10, produced by $T_{reg}$, were shown to have anti fibrotic effects (44-47). IL10 gene polymorphisms resulting in reduced IL10 production were found in IPF patients (48). In turn, IL10 delivery to the lung attenuates BLM induced pulmonary fibrosis in mice (46).

These and many other processes finally lead to the owerwhelming matrix production and consequently to a thickening of the alveolar walls and a loss of the lung elasticity.

## 2.2 The role of CCR2 in pulmonary fibrosis

CC-motive chemokine receptor 2 (CCR2) is a member of the group of seven transmembrane-spanning G protein coupled chemokine receptors. It is constitutively expressed on macrophages and monocytes but also on lymphocyte subsets (49) and fibrocytes (50, 51). It binds the chemokines CCL2, 7, 8, 13 and 16 with CCL2, also known as monocyte chemoattractant protein-1 (MCP-1), being the major ligand. In turn, CCR2 is the only known receptor for CCL2 unlike most other chemokines that bind to multiple receptors (52). CCL2 is expressed by a variety of cell types like epithelial cells, including pulmonary epithelium (53), endothelial and smooth muscle cells (54), fibroblasts (55), and in particular macrophages (49).

In peripheral blood of BALB/c mice CCR2 was expressed on approximately 5 to 15 % of $CD4^+$ T cells and 2 to 8% of $CD8^+$ T cells, but in inflamed tissue sites the percentage of CCR2 expressing T cells increased up to 50 % (56).

The diverse functions of the CCR2/CCL2 axis are not fully understood, yet. Classically, CCR2 is classified as pro-inflammatory chemokine receptor. Among others, it participates in leukocyte recruitment and T cell polarization (57, 58).

The content of $CCR2^+$ T cells was found increased in different chronic inflammatory disorders like Crohn's disease (59), rheumatoid arthritis (60) or multiple sclerosis (61). In a mouse model of collagen induced arthritis $CCR2^+$ T cells gained regulatory functions (62).

There is evidence that the CCR2/CCL2 axis plays also a role in the pathogenesis of pulmonary fibrosis. CCR2 and its ligand are considered to have pro-fibrotic effects. *In vitro* studies showed that CCL2 promotes collagen deposition and production of TGFβ in fibroblasts (63). Furthermore, it induced fibrocyte proliferation and production of α-SMA in cultured fibrocytes of murine and human origin (51). In turn, fibroblasts from CCR2 knock-out mice showed less α-SMA production upon stimulation by TGFβ than those from wt mice (64). CCL2 was increased in the BALF of mice treated with BLM (65). CCR2 deficiency, as well as blockade of CCL2 resulted in attenuated bleomycin induced fibrosis in mice (64, 66). In the lungs of these mice, decreased levels of TGFβ and α-SMA mRNA were detected (64). Fibrocyte migration to the murine lung in response to FITC induced lung injury was dependent on CCR2, as CCR2 deficient mice showed lower fibrocyte migration to the lung, and thus were protected from FITC induced pulmonary fibrosis. However, the inflammatory

reaction was similar in $CCR2^{+/+}$ and $CCR2^{-/-}$ mice (50, 66). Also, the expression of MMP2 and MMP9 was reduced in lung tissue from BLM treated CCR2-/- mice compared to wt (67).

On the other hand, one study reported that mice transgenic for hCCL2 were protected from mortality after bleomycin induced fibrosis. Thus, they showed higher monocytes/macrophages and lymphocytes in BALF compared to wt mice, while the accumulation of neutrophils was restricted following BLM treatment. CCL2 transgenic mice deficient for CCR2 were not protected from pulmonary fibrosis, which indicated that the effect was dependent on CCR2 (65). The reason for the discrepancy of these results is not evident and needs further investigation, but these conflicting observations may strengthen the hypothesis of differential functions of the CCR2/CCL2 axis.

CCL2 as well as $CCR2^{+}$ T cell percentages were increased in children with different forms of ILDs (68). However, the role of these specific lymphocytes in the context of pulmonary fibrosis is not clear. Thus, it is unknown if they contribute to the pathogenesis of disease or, on the contrary, represent an unsuccessful attempt of the immune system to limit the disease.

# 3 Hypothesis and Aims

As outlined above, there is evidence for an important role of CCR2 in ILD, but the specific contribution of $CCR2^+$ T cells in the pathogenesis of ILD is unclear.

In the present work, we hypothesize that, pulmonary $CCR2^+$ T cells have specific functional properties.

Therefore, the aim of this study was to perform a phenotypic characterization of pulmonary $CCR2^+$ T cells using an animal model of bleomycin-induced pulmonary fibrosis.

In particular, we asked:

- How does the relative content of $CCR2^+$ T cells change in the lung after bleomycin treatment?
- What is the phenotype of pulmonary $CCR2^+$ T cells in bleomycin induced fibrotic lung disease?
- Are pulmonary $CCR2^+$ T cells a naïve T cell population or do they express markers of effector or central memory T cells?
- Which chemokine receptors are co-expressed on $CCR2^+$ T cells?
- Are there changes of the phenotype of spleen T cells, as indicator of a systemic T cell response after bleomycin treatment?

# 4 Materials and Methods

## 4.1 Materials

### 4.1.1 Equipment

| | |
|---|---|
| Balance XS205 | Mettler Toledo, Gießen, Germany |
| Centrifuge Mikro 200R | Hettich, Tuttlingen, Germany |
| Centrifuge Rotina 420R | Hettich, Tuttlingen, Germany |
| Eppendorf mini spin plus | Eppendorf, Hamburg, Germany |
| Forceps | Fine Science Tools , Heidelberg, Germany |
| High pressure syringe | Penn Century, Wyndmoor, USAa |
| LSR II Flow Cytometer | BD Biosciences, San Jose, USA |
| Microm EC350-2 embedding station | Thermo scientific, Walldorf, Germany |
| Microm STP 420D- tissue processor | Thermo scientific, Walldorf, Germany |
| Microscope Axiovert 40C | Zeiss, Oberkochen, Germany |
| Microtom Hyrax 55 | Zeiss, Oberkochen, Germany |
| Mirax SCAN | Zeiss, Oberkochen, Germany |
| Multipette stream | Eppendorf, Hamburg, Germany |
| Neubauer Improved 0.1 mm depth | Brand, Wertheim, Germany |
| Pipettes Research plus | Eppendorf, Hamburg, Germany |
| Scissors | Fine Science Tools , Heidelberg, Germany |

### 4.1.2 Software

| | |
|---|---|
| Excel 2010 | Microsoft, Redmond, USA |
| FACSDiva Version 6.1.3 | BD Biosciences, San Jose, USA |
| GraphPad Prism Version 5.00 | GraphPad Software, San Diego USA |
| Mirax scan | Zeiss, Oberkochen, Germany |
| Mirax viewer | Zeiss, Oberkochen, Germany |
| Word 2010 | Microsoft, Redmond, USA |

### 4.1.3 Consumables

| | |
|---|---|
| 1.5 ml tube | Eppendorf, Hamburg, Germany |
| 10 ml syringe discardit II | BD Medical, Franklin Lakes, USA |
| 2.5 ml tube | Eppendorf, Hamburg, Germany |
| 20G venous catheter Introcan | B.Braun, Melsungen, Germany |
| 20G/27G BD microlance 3 | BD Medical, Franklin Lakes, USA |
| 5 ml polystyrene round bottom tubes | BD Biosciences, San Jose, USA |
| 50 ml /15 ml tubes | BD Biosciences, San Jose, USA |
| Cell strainer 40/70/100µm | BD Biosciences, San Jose, USA |
| Cover glasses 24x60 mm | Menzel, Braunschweig, Germany |
| Embedding cassetes Rotilabo | ROTH, Karlsruhe, Germany |
| Micro Slides | Hecht- Assistant, Sondheim, Germany |

| | |
|---|---|
| Pipette tips (10/20/100/1000 µl) | Eppendorf, Hamburg, Germany |

### 4.1.4 **Reagents**

| | |
|---|---|
| 7- Aminoactinomycin | Sigma-Aldrich, Saint-Louis, USA |
| Acetic acid 100% | ROTH, Karlsruhe, Germany |
| BD PharmLyse | BD Biosciences, San Jose, USA |
| Bleomycin | Sigma-Aldrich, Saint-Louis, USA |
| Collagenase A | Roche Applied Science, Mannheim, Germany |
| DNase I | AppliChem, Darmstadt, Germany |
| EDTA 0.5M | Life Technologies, Darmstadt, Germany |
| FCS | GE Healthcare, Buckinghamshire, UK |
| Formaldehyd 4% | Pharmacy LMU Munich, Germany |
| NaCl 0.9 % | B.Braun, Melsungen, Germany |
| Paraffin | Thermo scientific, Walldorf, Germany |
| PBS | Life Technologies, Darmstadt, Germany |
| RPMI 1640 Glutamine - | Life Technologies, Darmstadt, Germany |
| Trypan blue | Sigma-Aldrich, Saint-Louis, USA |

### 4.1.5 **Narcotics and Antidote**

| | |
|---|---|
| Atipamezol (Antisedan) | Pfizer, New York, USA |
| Fentanyl-Janssen 0.5 mg | Janssen-Cilag, Neuss, Germany |
| Flumazenil (Anexate) | Roche, Basel, Swizerland |
| Ketamin 10 % | Medistar, Ascheberg, Germany |
| Medetomidin (Dormitor) 1mg/ml | Pfizer, New York, USA |
| Midazolam –HCL 15mg/3ml | Ratiopharm, Ulm, Germany |
| Naloxon 0.4mg/ml | Inresa, Freiburg, Germany |
| Xylazin 2% (Rompun) | Bayer Health Care, Leverkusen, Germany |

### 4.1.6 **Antibodies**

| | |
|---|---|
| Anti-mouse CCR10 PE | R&D Systems, Minneapolis, USA |
| Anti-mouse CCR3 PE | R&D Systems, Minneapolis, USA |
| Anti-mouse CXCR4 PE | R&D Systems, Minneapolis, USA |
| Anti-mouse CXCR5 PE | R&D Systems, Minneapolis, USA |
| Anti-mouse CXCR6 PE | R&D Systems, Minneapolis, USA |
| APC H7 rat IgG2b, κ isotype control | BD Biosciences, San Jose, USA |
| APC-H7 rat anti mouse CD4 | BD Biosciences, San Jose, USA |
| FITC anti-mouse CD8b | Biolegend, San Diego, USA |
| FITC anti-mouse/human CD44 | Biolegend, San Diego, USA |
| FITC rat IgG2b, κ isotype control | Biolegend, San Diego, USA |
| Monoclonal anti-mouse CCR2 APC | R&D Systems, Minneapolis, USA |
| Pacific Blue anti-mouse CD3 | Biolegend, San Diego, USA |
| Pacific Blue Rat IgG2b, κ | Biolegend, San Diego, USA |
| PE anti-mouse CD 194 (CCR4) | Biolegend, San Diego, USA |

| | |
|---|---|
| PE anti-mouse CD 195 (CCR5) | Biolegend, San Diego, USA |
| PE anti-mouse CD 196 (CCR6) | Biolegend, San Diego, USA |
| PE anti-mouse CD183 (CXCR3) | Biolegend, San Diego, USA |
| PE anti-mouse CD62L | Biolegend, San Diego, USA |
| PE Armenian Hamster IgG isotype contol | Biolegend, San Diego, USA |
| PE Rat IgG2a, κ | Biolegend, San Diego, USA |
| PE-anti-mouse CD 197 (CCR7) | Biolegend, San Diego, USA |
| PE-anti-mouse CD 199 (CCR9) | Biolegend, San Diego, USA |
| Rat IgG2a isotype control PE | R&D Systems, Minneapolis, USA |
| Rat IgG2b isotype control APC | R&D Systems, Minneapolis, USA |
| Rat IgG2b isotype control PE | R&D Systems, Minneapolis, USA |

## 4.2 Methods

### 4.2.1 Mice

For all experiments, 8 to 11 week old C57BL/6 mice were used. Mice were housed in the animal facility of the Institute of Lung Biology and Disease, Helmholtz Zentrum Munich, Neuherberg. Cages were implemented with 2 to 4 mice; standard food and water were available ad libitum. The experiments were approved by the District Government of Upper Bavaria.

### 4.2.2 Induction of pulmonary fibrosis

#### 4.2.2.1 *Preparation of Reagents*

For anaesthesia during the treatment procedure, a mixture of Midazolam, Medetomidin and Fentanyl (MMF) was used because all of the components can be antagonized. In this way the anaesthetization time could be held short.

The stock solution was prepared using 1ml Midazolam (5mg/ml), 0.5 ml Medetomidin (1mg/ml), 1ml Fentanyl (50µg/ml).

Antidote was prepared using 3 ml Naloxon (0.4mg/ml), 0.5ml Atipamezol (5mg/ml), 5ml Flumazenil (0.5mg/5ml). Bleomycin was prepared as stock solution of 3U/ml in sterile NaCl 0.9% and stored at -20°C in aliquots of 350µl.

For one mouse of 20g 33.4 µl of stock solution was diluted with 166 µl sterile NaCl 0.9%, resulting in 0,1 U in 200 µl solution (0.5U/ml) correspondent to 5U/kg body weight.

#### 4.2.2.2 *Treatment procedure*

Body weight was recorded before mice were anesthetized by intraperitoneal injection of the MMF mixture according to their body weight. For example, a mouse of 20g received 50µl.

After confirmation of anaesthesia by checking the reaction to pain, mice underwent intratracheal intubation using a 21G venous catheter. Correct intubation was controlled by observation of thoracic excursions during mechanical ventilation. 200µl sterile NaCl 0.9% or 200µl of the prepared Bleomycin solution were instilled as aerosol, using a pneumatic pressure device for controlled application of pressure on the high pressure syringe.

Anaesthesia was antagonized by subcutaneous injection of Naloxon, Atipamezol, Flumazenil solution, according to the body weight (for example 170µl for a mouse of 20 g).

### 4.2.3 **Sampling of lung, spleen and BALF**

#### 4.2.3.1 ***Preparation of reagents***

Because it was not necessary to antagonize the anaesthesia, a mixture of Ketamin and Xylazin was used to anaesthetize mice for the organ removal. The stock solution was prepared by adding 1ml of Ketamin 10% and 0.25ml of Xylazin 10% to 6ml PBS.

Collagenase was prepared as stock solution of 5mg/ml. For 20 ml of stock solution 100 mg of CollagenaseA lyophilizate were dissolved in 20 ml PBS and the solution was stored at 4°C.

For preparation of DNAse stock solution 10ml of 0.15M NaCl solution were prepared by dissolving 87.66mg of NaCl in 10 ml aqua dest, 10mg of lyophilized DNAse was dissolved in the prepared NaCl solution, resulting in a concentration of 1mg/ml. The stock solution was stored in aliquots at -20°C.

For lung digestion, 3.8 ml of RPMI 1640 medium were transferred to a 50 ml tube. Then, 700µl of CollagenaseA stock solution (0.7mg/ml) and 500µl of DNAse (0.1mg/ml) stock solution were added.

For digestion of spleens, 4.6 ml of RPMI 1640 medium were transferred to a 50ml tube and 234µl of CollagenaseA stock solution and 167µl of DNAse stock solution was added, resulting in 5 ml medium with a concentration of 0.234 mg/ml collagenase and 33.4 µg/ml DNAse.

#### 4.2.3.2 ***Organ removal***

To detect body weight changes at the different time points after bleomycin treatment, the body weight was recorded again. Then, the Ketamin/Xylazin mixture was injected ip according to the body weight, for a mouse of 20g this were 200µl. Deep anaesthesia was confirmed by checking the reaction to pain. The abdomen was opened, and then the spleen was removed and transferred to a petri dish containing 5 ml digestion medium. The spleen was dissected with forceps and the cell suspension was transferred to a 50ml tube.

Mice were sacrificed by exsanguination through cutting the abdominal aorta. For collection of bronchio-alveolar lavage fluid (BALF), the trachea was exposed and a 20G venous catheter was placed in the trachea. BAL was performed by instilling and aspirating of 1ml PBS three times, using a 1 ml syringe. BALF was stored on ice until further processing.

To remove the lungs, the chest was opened and the blood in the pulmonary vessels was removed from the lung by lung perfusion through injection of 10 ml PBS in the right heart ventricle.

Lungs were removed and either both lungs were transferred to 5 ml of the digestion medium or formalin was instilled in the right lung for histology and the left lung was transferred to a petri dish with digestion- medium. The lung tissue was dissected using forceps and the plunger of a 1ml syringe. The tissue-medium mixture was transferred to a 50ml tube.

### 4.2.4 **Preparation of cells for FACS**

#### 4.2.4.1 ***Preparation of Reagents***

BD PharmLyse reagent was diluted 1:10 with milliQ water. For preparation of the staining buffer 2ml of 0.5M EDTA and 2.5 ml FCS were added to 500ml PBS resulting in 2mM EDTA and 0.5% FCS solution.

#### 4.2.4.2 ***BAL***

The amount of aspirated BALF was recorded. BALF was centrifuged at 350G for 10 min to obtain BAL cells. Cells were resuspended in 200 µl staining medium.

10µl of the cell suspension were diluted 1:2 with 10µl of Trypan blue/4% acidic acid. Living cells were counted using a Neubauer haemocytometer. Four big squares were counted and cell number was calculated regarding the size of the haemocytometer:

$$\frac{counted\ cells}{4} * 10^4 * dilution * volume(ml)$$

#### 4.2.4.3 ***Spleen***

The cell suspension was incubated at 37°C and 80 RPM for 10 minutes. After incubation, the spleen cell suspension was passed through 70µm and 40µm cell strainers, and each was washed with 2.5 ml of staining buffer. An aliquot of 10µl was taken out for cell counting.

The suspension was centrifuged at 200G for 10 min. The supernatant was discarded, and the cell pellet was resuspended to a concentration of $10^7$cells/ml.

For counting, the aliquot was diluted 1:10 with staining buffer. 10 µl of the dilution was mixed 1:2 with trypan blue 4% acidic acid, resulting in a final dilution of 1:20. Living cells were counted as described above.

#### 4.2.4.4 *Lung*

Lungs from saline-treated animals were incubated for 30 minutes, lungs from bleomycin treated mice were incubated for 40 minutes at 37°C and 80 RPM. After incubation, the tissue-medium mixture was passed through a 20G cannula using a 10ml Syringe to get a single cell suspension. The suspension was then passed through a 100µm and a 70µm cell strainer, and each was washed with 2.5ml staining medium. An aliquot of 40µl was taken for cell counting. For this, 10µl of the aliquot were diluted 1:2 with trypan blue 4% acidic acid.

The cell suspension was centrifuged at 200G for 10 min. The supernatant was discarded and the pellet was resuspended to a concentration of $10^7$cells/ml.

### 4.2.5 **Experimental settings**

#### 4.2.5.1 ***Compensating for spectral overlap of fluorochromes***

For multi-colour FACS experiments, a compensation for the overlap of emission spectra of different fluorochromes is necessary. The principle of this compensation is the subtraction of the so-called “spilled over” signal (Figure 2).

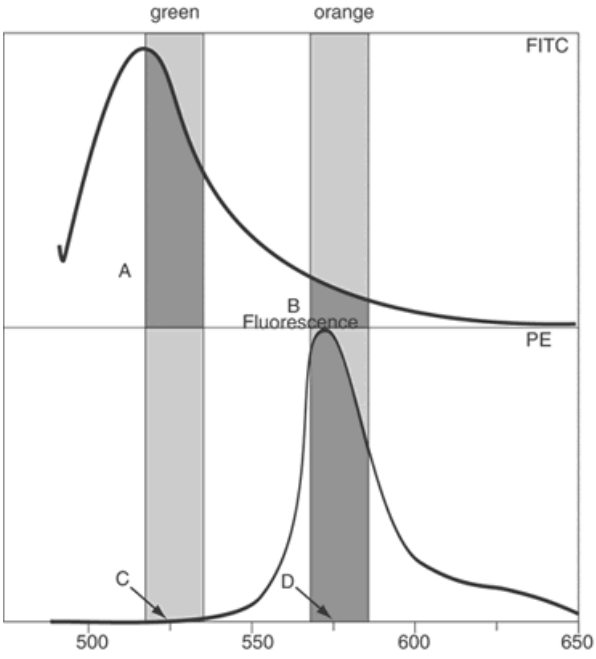



**Figure 2 Emission spectra of FITC and PE with respective filter bandpass***; illustration adapted from (69) A) contigency of FITC signal which is detected in the FITC channel (green); B) contigency of FITC signal “spilling over” into the PE channel (orange), which has to be subtracted from the detected PE signal; C) only a very small portion of the PE signal is spilling into the FITC channel; D) contingency of PE signal which is detected in the PE channel*

To assess this signal spill-over, it is necessary to use one unstained sample and samples that are each stained with one single fluorochrome.

Different cell types in spleen and lung result in different background fluorescence. Therefore, the compensation for spectral overlap was set up separately for the different organs.

Cells were prepared as described above. 50µl of cell suspension (0.5 x$10^6$ cells) were transferred to 5 ml round bottom tubes and antibodies were added (Table 1).

*Table 1 Antibodies and set-up used to compensate for spectral overlap of fluorochromes*

| | **CD3-PB (1:10)** | **CD4 APC-H7** | **CD8-PE (1:10)** | **CD8-FITC (1:10)** | **CD45-APC** | **7-AAD** |
|---|---|---|---|---|---|---|
| **1** | | | | | | |
| **2** | 2.5 µl | | | | | |
| **3** | | 0.625 µl | | | | |
| **4** | | | 3.125 µl | | | |
| **5** | | | | 3.125 µl | | |
| **6** | | | | | 0.625 µl | |
| **7** | | | | | | 3 µl |

After staining, cells were incubated for 20 min at 4° C. Contaminating erythrocytes were lysed by adding 2 ml of BD PharmLyse followed by 5 min incubation at room temperature. The lysis reagent was removed after a centrifugation step at 200G and 5°C, and cells were washed with 2 ml staining buffer. After another 5 min of centrifugation the cell pellet was suspended in 300 µl staining buffer

The FACS Diva software provides an automated tool for setting up the compensation. These settings were used for all FACS experiments done in this study.

This automatic compensation setup using FACS Diva software gave the following results for spectral overlap of fluorochromes in percent of the recorded signal (Table 2 and Table 3).

*Table 2 Spectral overlap for spleen samples*

| **Percent** | **FITC** | **PE** | **7-AAD** | **PB** | **APC** | **APC H7** |
|---|---|---|---|---|---|---|
| **FITC** | 100 | 1.15 | 0.05 | 0.20 | 0 | 0.03 |
| **PE** | 20.57 | 100 | 0.64 | 0 | 0 | 0 |
| **7-AAD** | 2.98 | 21.08 | 100 | 0 | 1.09 | 0 |
| **PB** | 0.02 | 0 | 0 | 100 | 0 | 0 |
| **APC** | 0.06 | 0.04 | 4.17 | 0.47 | 100 | 0.88 |
| **APC H7** | 0.01 | 0 | 2.37 | 0.15 | 19.37 | 100 |

*Table 3 Spectral overlap for lung samples*

| Percent | FITC | PE | 7-AAD | PB | APC | APC H7 |
|---|---|---|---|---|---|---|
| **FITC** | 100 | 1.16 | 0 | 3.42 | 0.03 | 0.37 |
| **PE** | 20.01 | 100 | 1.72 | 2.66 | 0.01 | 0.10 |
| **7-AAD** | 2.58 | 20.28 | 100 | 0.95 | 1.09 | 0.12 |
| **PB** | 0.05 | 0.01 | 0 | 100 | 0.02 | 0.07 |
| **APC** | 0.09 | 0.04 | 4.04 | 2.29 | 100 | 1.16 |
| **APC H7** | 0.02 | 0 | 2.27 | 0 | 17.82 | 100 |

#### 4.2.5.2 ***Longitudinal assessment of T cell percentages after BLM treatment***

For BAL cells, 200µl of cell suspension were divided in two 5ml round bottom tubes. Cells were stained with directly labelled antibodies (Table 4).

*Table 4 Antibodies used for BAL samples*

| Antibody (dil) | 1 | 2 |
|---|---|---|
| **CD3-PB (1:10)** | 2.5 µl | 2.5 µl |
| **CD4-APC-H7** | 0.625 µl | 0.625µl |
| **CD8-FITC (1:10)** | 1.25 µl | 1.25 µl |
| **CCR2-APC** | 1.25 µl | |
| **Rat IgG2b-APC** | | 1.25 µl |
| **7-AAD** | 3 µl | 3 µl |

For spleen and lung samples, 25µl of the cell suspension ($10^7$ cells/ml) were transferred to each 5 ml tube resulting in 250 000 cells per tube and the antibodies were added to the tubes (Table 5).

*Table 5 Antibodies used for spleen and lung samples*

| Antibody (dil.) | 1 | 2 | 3 | 4 |
|---|---|---|---|---|
| **CD3-PB (1:10)** | 2.5 µl | 2.5 µl | 2.5 µl | 2.5 µl |
| **CD4-APC-H7** | 0,625 µl | 0,625 µl | 0,625 µl | 0,625 µl |
| **CD8-FITC (1:10)** | 1,25 µl | 1,25 µl | | |
| **CD44-FITC (1:10)** | | | 2,5 µl | 2,5 µl |
| **CD62L-PE (1:10)** | | | 3,125 µl | 3,125 µl |
| **CCR2-APC** | 1,25 µl | | 1,25 µl | |
| **Rat IgG2b-APC** | | 1,25 µl | | 1,25 µl |
| **7AAD** | 3 µl | 3 µl | 3 µl | 3 µl |

Samples were incubated for 20 min at 4°C in the dark. 2 ml 1:10 diluted BDpharmLyse reagent was added to each tube for red blood cell lysis, followed by 5 min incubation at room temperature in the dark. The lysis reagent was removed by centrifugation at 200g for 5

min and an additional washing step with 2 ml staining buffer. The cell pellet was resuspended in 300 µl staining buffer. Samples were analysed on a BD LSRII Flow cytometer.

#### 4.2.5.3 *Assessment of CCR/CXCR co-expression on lung T cells*

Due to the paucity of pulmonary $CCR2^+$ T cells, it was not possible to co-stain all chemokine receptors of interest in one single experiment. Therefore, the experiment was subdivided into three staining panels. Each, one mouse was used per panel with a total of 6 to 7 mice per panel.

For the assessment of the cytokine receptor co-expression, cells were also resuspended to a concentration of $10^7$ cells/ml. 100 to 200µl of cell suspension, depending on counted cell numbers, were transferred to each 5 ml tube. Antibodies were added to the tube (Table 6). Incubation, red blood cell lysis and washing steps were performed as described above in section 4.2.5.2.

*Table 6 Antibodies used for assessment of chemokine receptor expression*

| **Amount for $10^6$ cells** | | | | | | | | |
|---|---|---|---|---|---|---|---|---|
| **All tubes** | 1 | 2 | 3 | 4 | 5 | 6 | 7 | 8 |
| **CD3-PB** | 1 µl | 1 µl | 1 µl | 1 µl | 1 µl | 1 µl | 1 µl | |
| **CD4-APC H7** | 2.5 µl | 2.5 µl | 2.5 µl | 2.5 µl | 2.5 µl | 2.5 µl | 2.5 µl | |
| **CD8-FITC** | 0.5 µl | 0.5 µl | 0.5 µl | 0.5 µl | 0.5 µl | 0.5 µl | 0.5 µl | |
| **7-AAD** | 10 µl | 10 µl | 10 µl | 10 µl | 10 µl | 10 µl | 10 µl | |
| | | | | | | | | |
| **Panel 1** | 1 | 2 | 3 | 4 | 5 | 6 | 7 | |
| **CCR2-APC** | 5 µl | 5 µl | 5 µl | 5 µl | 5 µl | 5 µl | | |
| **Rat IgG2b-APC** | | | | | | | 5 µl | |
| **CCR4-PE** | | 5 µl | | | | | | |
| **CCR5-PE** | | | 2.5 µl | | | | | |
| **CCR6-PE** | | | | 5 µl | | | | |
| **CXCR3-PE** | | | | | 1.25 µl | | | |
| **AH-IgG-PE** | | | | | | 5 µl | 5 µl | |
| | | | | | | | | |
| **Panel 2** | 1 | 2 | 3 | 4 | 5 | 6 | 7 | 8 |
| **CCR2-APC** | 5 µl | 5 µl | 5 µl | 5 µl | 5 µl | 5 µl | | |
| **Rat IgG 2b-APC** | | | | | | | 5 µl | 5 µl |
| **CXCR5** | 5 µl | | | | | | | |
| **CCR3** | | 5 µl | | | | | | |
| **Rat IgG2a-PE** | | | 5 µl | | | | 5 µl | |
| **CCR7** | | | | 10 µl | | | | |
| **CCR9** | | | | | 5 µl | | | |
| **Rat IgG2a, κ-PE** | | | | | | 10 µl | | 10 µl |
| | | | | | | | | |

| **Panel 3** | 1 | 2 | 3 | 4 | 5 |
|---|---|---|---|---|---|
| **CCR2-APC** | 5 µl | 5 µl | 5 µl | 5 µl | |
| **Rat IgG2b-APC** | | | | | 5 µl |
| **CCR10** | 5 µl | | | | |
| **CXCR4** | | 5 µl | | | |
| **CXCR6** | | | 5 µl | | |
| **Rat IgG2b-PE** | | | | 5 µl | 5 µl |

### 4.2.6 **Data Analysis**

#### 4.2.6.1 ***Analysis of FACS data***

For analysis of FACS data BD FACS Diva Software was used.

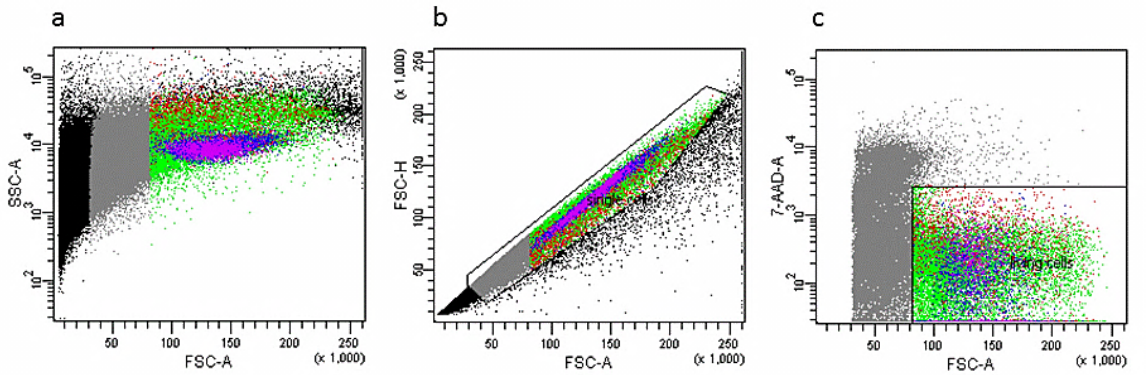



**Figure 3 First step in the analysis of FACS data; example of a lung sample***; a) dot plot of all measured events; b)dot plot of all measured events gate is drawn for separation of single cells and excludes particles of small size; c) dot plot of single cells, gate is selecting living cells*

Cells adhering together can alter the result of FACS experiments, since they can mimic a cell population which does not exist. For example $CD4^+$ cells adhering to $CD8^+$ cells may mimic a population of $CD4^+CD8^+$ cells, because in this case, the detectors for both fluorochromes bound to the different antibodies detect a signal.

These adhering cells can be excluded using a dot plot showing the area scaled FSC (FSC-A) versus the height scaled FSC (FSC-H). Adhering cells appear below the diagonal because the ratio of the height of the FSC signal compared to the area is lower (Figure 3b).

To exclude these biases, only events appearing near the diagonal were taken into the analysis and were selected in the first electronic gate. For the next step, these single cells were shown in a dot plot with FSC-A versus the fluorescence of 7AAD. The gate for living cells was drawn for cells negative for 7AAD fluorescence and considering FSC-A signal to exclude death cells and also cell trash which give high background fluorescence (Figure 3c). This procedure was followed for all samples.

#### 4.2.6.1.1 Longitudinal assessment of T cell percentages after BLM treatment

For the identification of T lymphocytes, living cells were shown in a histogram and $CD3^+$ cells were selected according to the intensity of the PB signal (Figure 4).

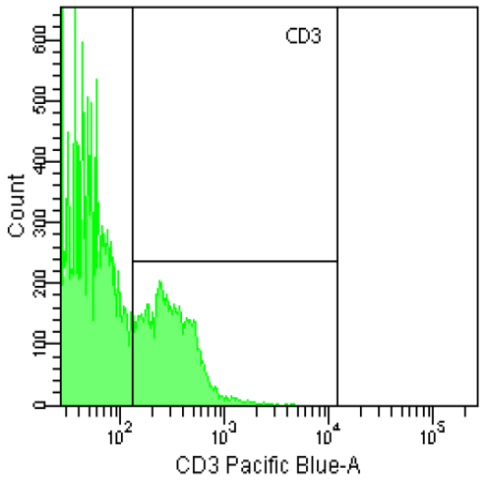



**Figure 4 Histogram showing living cells**; *x-axis showing PB fluorescence intensity; gate selecting $CD3^+$ cells*

For spleen and lung samples, histograms showing only $CD3^+$ cells were drawn. $CD4^+$ cells were selected in an electronic gate according to the APC-H7 signal, $CD8^+$ cells according to the FITC fluorescence (Figure 5).

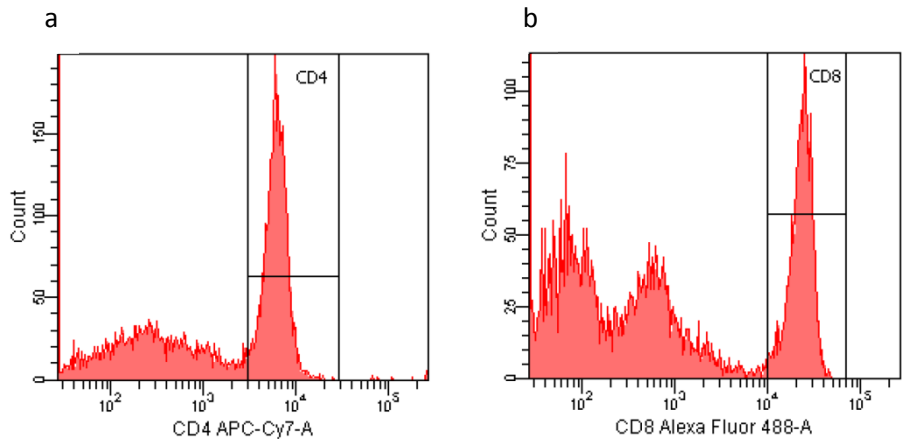



**Figure 5 Histograms showing $CD3^+$ cells** *a) APC-H7 fluorescence intensity on the x-axis; gate selecting $CD4^+$ cells; b) FITC fluorescence intensity on the x-axis; gate selecting $CD8^+$ cells; the $CD8^{low}$ population presumably represents NK cells*

BAL samples contain many cells emitting background fluorescence in all channels. For this reason, it was not possible to exclude these cells with the CD3 gate. To be able to exclude

this population which gave a signal in both, the FITC and the APC-Cy7 channel, for BAL samples, $CD3^+$ cells were shown in a dot plot with FITC intensity for $CD8^+$ T cells versus APC-H7 intensity for $CD4^+$ T cells. Events only positive for APC-H7 fluorescence were selected as $CD4^+$ T cells. Events only positive for FITC fluorescence were selected as $CD8^+$ T cells (Figure 6).

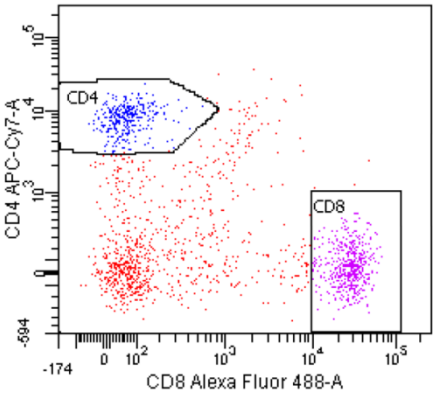



**Figure 6: BAL sample; Dot plot showing $CD3^+$ cells**, *gates selecting CD4+ or CD8+ cells*

For the assessment of percentages of $CCR2^+$ T cells, histograms showing only $CD4^+$ or $CD8^+$ cells were used. The percentage of CCR2 expressing cells was determined according to the APC signal intensity. For this, the sample stained with the specific antibody was compared to a sample stained with the appropriate isotype control (Figure 7).

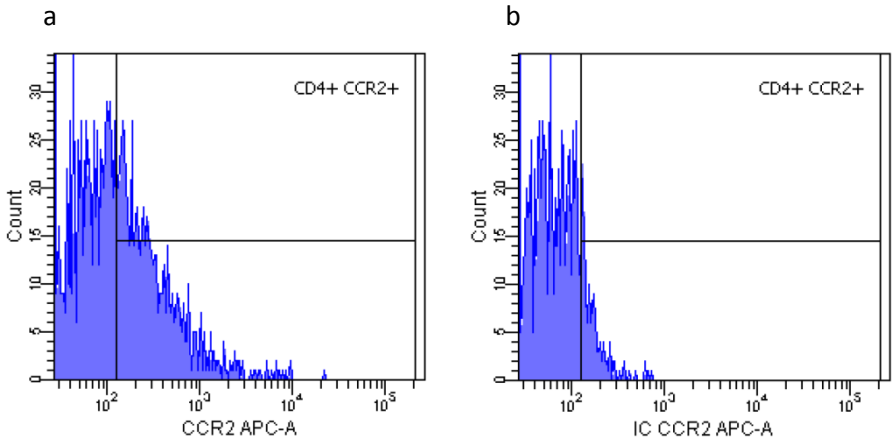



**Figure 7 Histograms showing $CD4^+$ cells**; *APC fluorescence intensity on the x-axis, a) sample stained with antibody binding to CCR2, b) sample stained with an appropriate isotype control*

For spleen and lung samples, $CD4^+$ T cell subtypes were analysed additionally. $CD3^+$, $CD4^+$ T cells, and CCR2 expressing $CD4^+$ T cells were selected as described above.

Naïve, central memory, and effector memory T cells were detected through the expression of CD44 and CD62L. $CD4^+$ cells were shown in a dot plot drawing CD44-FITC signal versus CD62L-PE fluorescence intensity. $CD44^{low}CD62L^{high}$ expressing cells were considered as naïve cells ($T_{naive}$). $CD44^{high}CD62L^{high}$ cells were considered as central memory cells ($T_{cm}$) and $CD44^{high}CD62L^{low}$ cells as effector memory cells ($T_{em}$) (Figure 8).

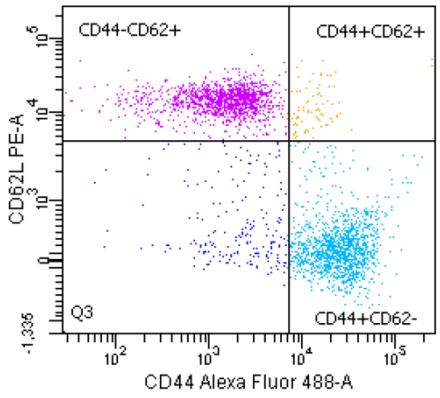



**Figure 8 Dot plot showing $CD4^+$ T cells, quadrants determining $CD4^+$ T cell subtypes**, *upper left quadrant: naïve T cells, upper right quadrant central memory T cells, lower right quadrant effector memory T cells*

The percentage of $CCR2^+$ cells within CD4 T cell subpopulations was assessed using histograms showing naïve, central memory or effector memory CD4 T cells. The percentages of $CCR2^+$ cells were determined by comparison of samples stained with the specific antibody to samples stained with an appropriate isotype control (Figure 9).

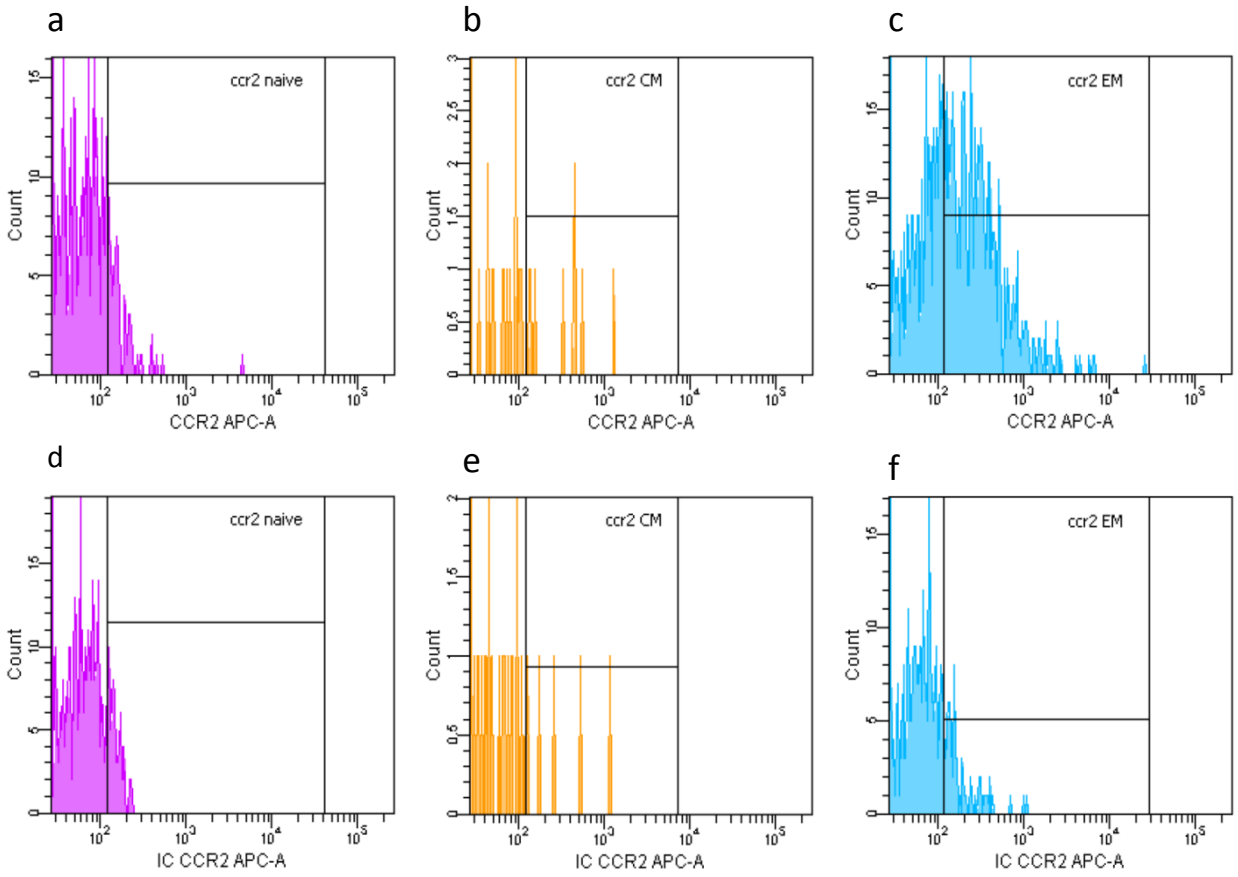



**Figure 9 Histograms showing T-cell subtypes, in lung samples**; *upper row showing a sample stained with an antibody specific for CCR2; lower row showing a sample stained with an approproate isotype control; a+d ) naïve CD4$^+$ T cells; b+e) central memory CD4 T cells; central memory T cells were too rare to be assessed adequately; c+f) effector memory cells*

#### 4.2.6.1.2 Assessment of chemokine receptor co-expression

To be able to identify the CD3$^+$ population more clearly, an additional lymphocyte gate was introduced. Living cells were shown in a dot plot showing FSC-A versus SSC-A. The lymphocyte gate was drawn based on the granularity (SSC) and the size (FSC) of the lymphocyte population (Figure 10).

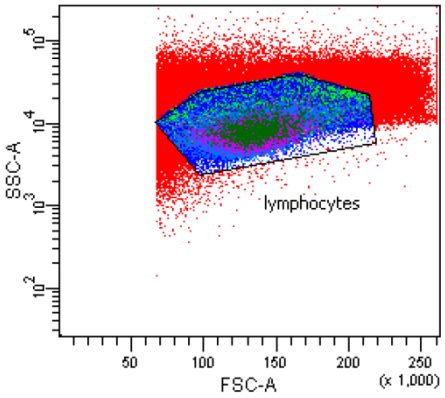



**Figure 10 Dot plot showing living cells**; *gate selecting lymphocytes*

This selected population was then transferred in a histogram to select of $CD3^+$ cells- $CD4^+$, $CD8^+$ and $CCR2^+$ populations were selected using electronic gates as described above (Figure 4, Figure 5 and Figure 7)

The next step was to determine the expression of the other chemokine receptors on $CD4^+$ and $CD8^+$ T cells. For this, the same strategy was used as for the assessment of CCR2 expression, but using PE as fluorocrome.

CCR2 (APC) was plotted against other chemokine receptors (PE) within $CD4^+$ or $CD8^+$ T cells. To calculate percentages of cells expressing CCR2 as well as the other chemokine receptor, the tube stained with both specific antibodies was compared to two isotype samples (Figure 11).

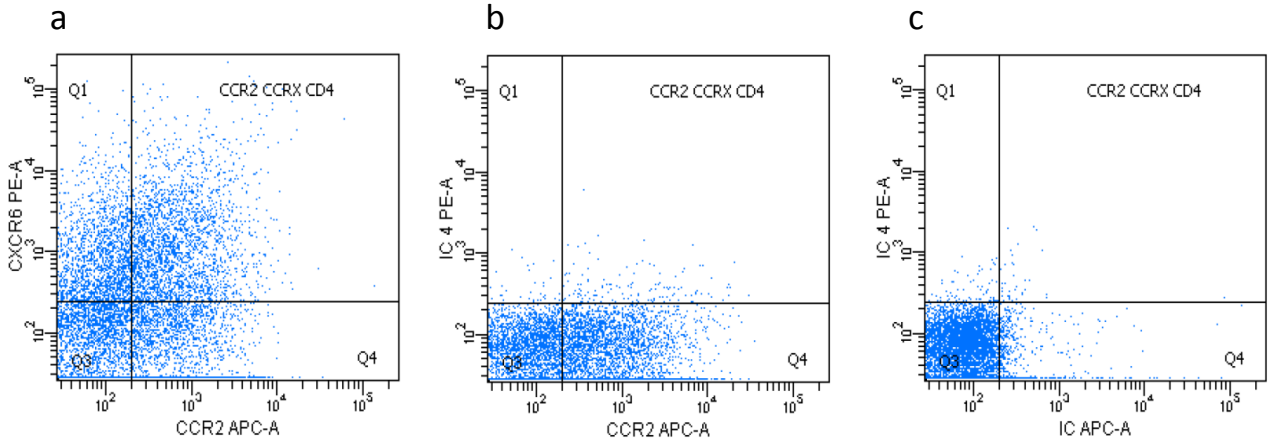



**Figure 11 Example for assessment of chemokine receptor co-expression with CCR2**, *Dot plots show $CD4^+$ cells stained with a) both chemokine receptor-specific antibodies b) the isotype control for CXCR6-PE and the antibody specific for CCR2 c) both isotype controls*

As basis for the statistical analysis, the percentages of cell populations given by the statistic view of FACS Diva software were used. Percentages of $CD4^+$ and $CD8^+$ T cells were calculated back to living cells. For parameters detected more than once for one animal, means were calculated and taken into the analysis.

#### 4.2.6.2 *Statistical Analysis*

Due to the low number of samples in most of the experimental groups, a normal distribution could not be assumed. Therefore, nonparametric tests were used for statistical analysis. For comparison of body weight before and after treatment, Wilcoxon signed rank test was used. For comparison of two unpaired groups, nonparametric Mann Whitney U test was performed. Comparisons of the groups in the longitudinal experiments were done using Kruskal Wallis test followed Dunn's multiple comparison test. By this test, treatment groups at the different time points were compared to the control group. For all calculations, GraphPad Prism software was used. Significance was accepted for $p < 0.05$.

### 4.2.7 **Histology**

For histology, the right lung was cut from the whole lung and 4%formalin was instilled in the main bronchus for fixation. The lung was put into a 50 ml tube containing 4% formaldehyde solution and incubated overnight.

The next day, the lung was cut into superior, middle, inferior, and postcaval lobe. The four lobes were arranged in an imbedding cassette, paraffinated overnight, and imbedded in a parrafine block. Blocks were cut to 3 µm slices and transferred to a glass slide. For deparaffination, the slides were washed for 5 minutes in xylol, and then they were washed two times for one minute in 100% ethanol and one minute in each, 90%, 80% and 70% ethanol.

#### 4.2.7.1 *Haematoxylin Eosin (HE) staining*

Slides were rinsed shortly with Aqua dest and then stained for 5 minutes with Mayer's Hämatoxylin. They were rinsed shortly with water and 0.3% HCl-alcohol followed by 10 to 15 minutes washing in tap water. After rinsing again with Aqua dest; slides were stained with Eosin Y for 8 minutes. For dehydration, the samples were washed shortly in 70% and 80% ethanol, followed by washing steps in 90%, 96% and 100% ethanol for one minute, each. Finally they were washed for two minutes in 100% ethanol and two times for 5 minutes in Xylol. Slides were covered with cover glasses using entellan.

#### 4.2.7.2 *Masson Goldner's Trichrom staining*

For Masson Goldner's Trichrom staining, slides were stained with Weigert's Hämatoxylin for 10 minutes, followed by washing for 3 min in tap water. After 1 min incubation in 0.3% HCl-alcohol, slides were washed again for 3 minutes in tap water. Slides were rinsed shortly with Aqua dest before staining in ponceau fuchsin acid for 6 minutes. They were rinsed shortly with Aqua dest, 1% acetic acid, and again with Aqua dest followed by 5 minutes incubation in phosphormolybdic acid-orange g. Slides were rinsed again shortly with 1% acetic acid and stained with light green 0.2%. The staining was finished by rinsing again with 1% acetic acid and aqua dest. Dehydration was performed as described for HE staining.

# 5 Results

## 5.1 Experimental outline

The overall aim of this project was to characterize the phenotype of $CCR2^+$ T cells in the context of experimental interstitial lung disease. For this, a widely common model for pulmonary fibrosis based on the intratracheal administration of Bleomycin was used. The experimental outline for the longitudinal analysis is shown in Figure 12.

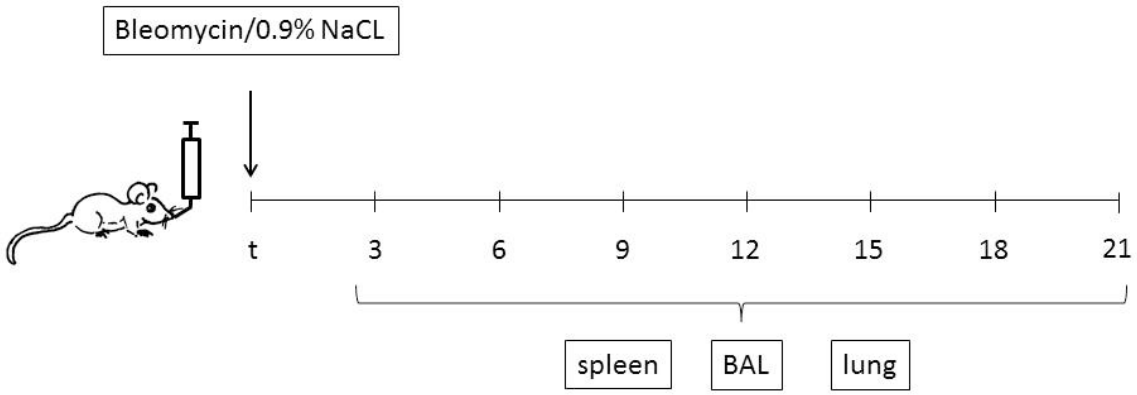



**Figure 12 Experimental outline of bleomycin induced Lung fibrosis**; *200µl of bleomycin solution or 0.9% NaCl was instilled intratracheally; mice were sacrificed at the indicated time points. Spleen, BAL and lung were taken for analysis at each time point.*

The first goal was to investigate changes of the composition of T cells and T cell subtypes in spleen, lung, and BALF during the longitudinal development of fibrosis. Furthermore, we wanted to determine the time point with maximal pulmonary $CCR2^+$ T cell content in order to set the optimal time point for further examination of this population.

In a second step, the percentages of $CCR2^+$ $CD4^+$ and $CD8^+$ T cells also expressing other chemokine receptors were investigated at the time point chosen from the results of the different time points.

## 5.2 Characterization of the animals

### 5.2.1 Animal numbers

Table 7 gives an overview of sampled tissues at the different time points. From day 12 on an increasing death rate of 11% at day 12 to 61% at day 21 was observed in the group of BLM treated animals.

*Table 7 Number of animals for time course experiments*

| | Saline | Day 3 | Day 6 | Day 9 | Day 12 | Day 15 | Day 18 | Day 21 |
|---|---|---|---|---|---|---|---|---|
| ***Treated animals*** | *14* | *10* | *17* | *15* | *18* | *14* | *19* | *18* |
| **BALF only** | 4 | 3 | 5 | 5 | 5 | 1 | | |
| **BALF & lung** | | | | | | 2 | 4 | 2 |
| **Lung & BALF& spleen** | 3 | 2 | 3 | 2 | 3 | 1 | 1 | 3 |
| **Lung & spleen** | 7 | 2 | 9 | 8 | 8 | 4 | 5 | 2 |
| **Lung only** | | 3 | | | | | | |
| **excluded** | | | | | | 1 | 1 | |
| **died** | | | | | 2 | 5 | 8 | 11 |
| ***Final animal numbers analysed*** | | | | | | | | |
| **BALF** | 7 | 5 | 8 | 7 | 8 | 4 | 4 | 5 |
| **Lung** | 10 | 7 | 12 | 10 | 11 | 7 | 6 | 7 |
| **spleen** | 10 | 4 | 12 | 10 | 11 | 5 | 6 | 5 |
| **Body weight**[#] | 12 | 10 | 13 | 15 | 13 | 9 | 11 | 7 |

[#]Body weight was not detected in the first run of time course: 2 saline treated animals, 4 BLM treated day 6 and 3 BLM treated Day 12.

### 5.2.2 **Change of body weight**

The body weight change was assessed as indicator of disease severity. Most mice lost body weight following BLM treatment (Table 10).

*Table 8 Body weight on D0 and the different time points*

| | | BW D0 (g)[*] | BW D 3 to 21 (g) | p-value[#] |
|---|---|---|---|---|
| **Sal** | n = 12 | 20.2 (19.0-23.0) | 20.8 (18.7-23.2) | 0.15 |
| **Day 3** | n = 10 | 19.7 (18.6-21.1) | 19.1 (18.0-19.8) | **0.002** |
| **Day 6** | n = 13 | 19.8 (18.9-22.0) | 17.9 (13.2-23.3) | **0.004** |
| **Day 9** | n = 15 | 20.0 (17.8-21.5) | 18.0 (13.1-20.2) | **0.0003** |
| **Day 12** | n = 13 | 19.0 (17.9- 22.3) | 19.0 (13.5-21.0) | 0.3 |
| **Day 15** | n = 9 | 19.4 (18.0-21.0) | 17.5 (12.7-19.8) | **0.04** |
| **Day 18** | n = 11 | 19.9 (17.5-21.0) | 19.1 (13.3-22.1) | 0.19 |
| **Day 21** | n = 7 | 18.7 (18.0-19.9) | 17.5 (13.0-21.6) | 0.3 |

* Values are expressed as median (range)

[#] p-values indicate significance of body weight difference at different time point vs. day 0 by Wilcoxon paired rank test.

At days 3, 6, 9, and 15, mice showed a significant loss of body weight compared to the body weight measured at day 0. At the other time points, the body weight change was more inhomogeneous with some mice extensively loosing body weight (up to 8.8 g) and others keeping their weight or even gaining body weight. The body weight in the control group was stable (Table 8).

When the body weight change was compared between the different time points after bleomycin treatment and the control group, a significant loss of body weight was found at days 6, 9, and 15 (Figure 13).

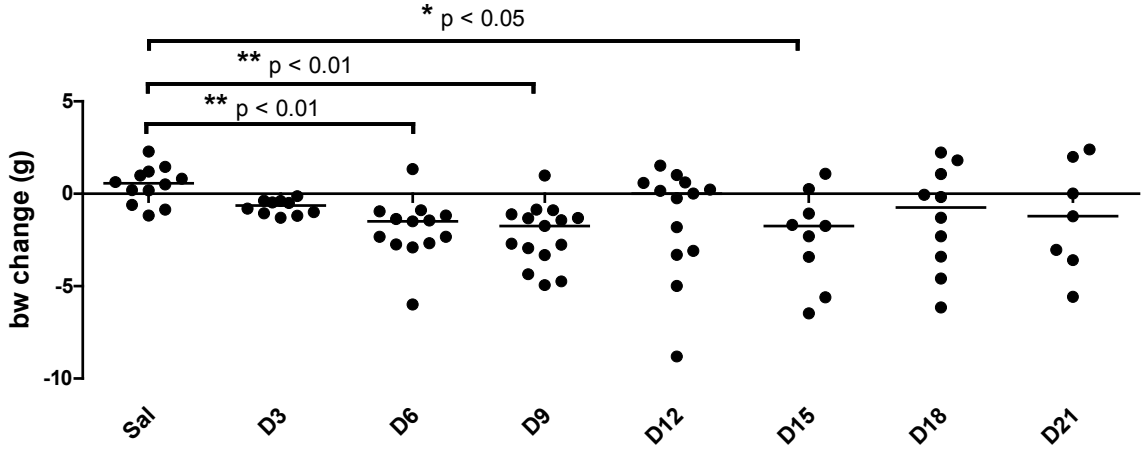



**Figure 13 Body weight change over time course***; indicated p-values obtained by Dunn Multiple Comparison test; Kruskal Wallis test: **p<0.01*

### 5.2.3 **Histology**

Histology sections were done to assess the distribution and severity of fibrotic lesions in the lungs of BLM treated mice.

Figure 14 shows Goldner's masson tricrome staining of histological sections from right lungs at the time points examined after BLM treatment. The pictures show representative areas affected from lung injury at the indicated time points. All sections also contained areas of histologically unaffected tissue to a variable extend. In sections from saline treated mice there were no inflammatory or fibrotic lesions. At days 3 and 6, the accumulation of inflammatory cells dominated over fibrotic lesions reflecting the initial inflammatory phase of BLM induced fibrosis. From day 9, thickening of alveolar walls and markedly enhanced collagen deposition were the leading features. The distribution of the lesions was mainly peri-bronchial, although in some sections also sub-pleural alterations were observed.

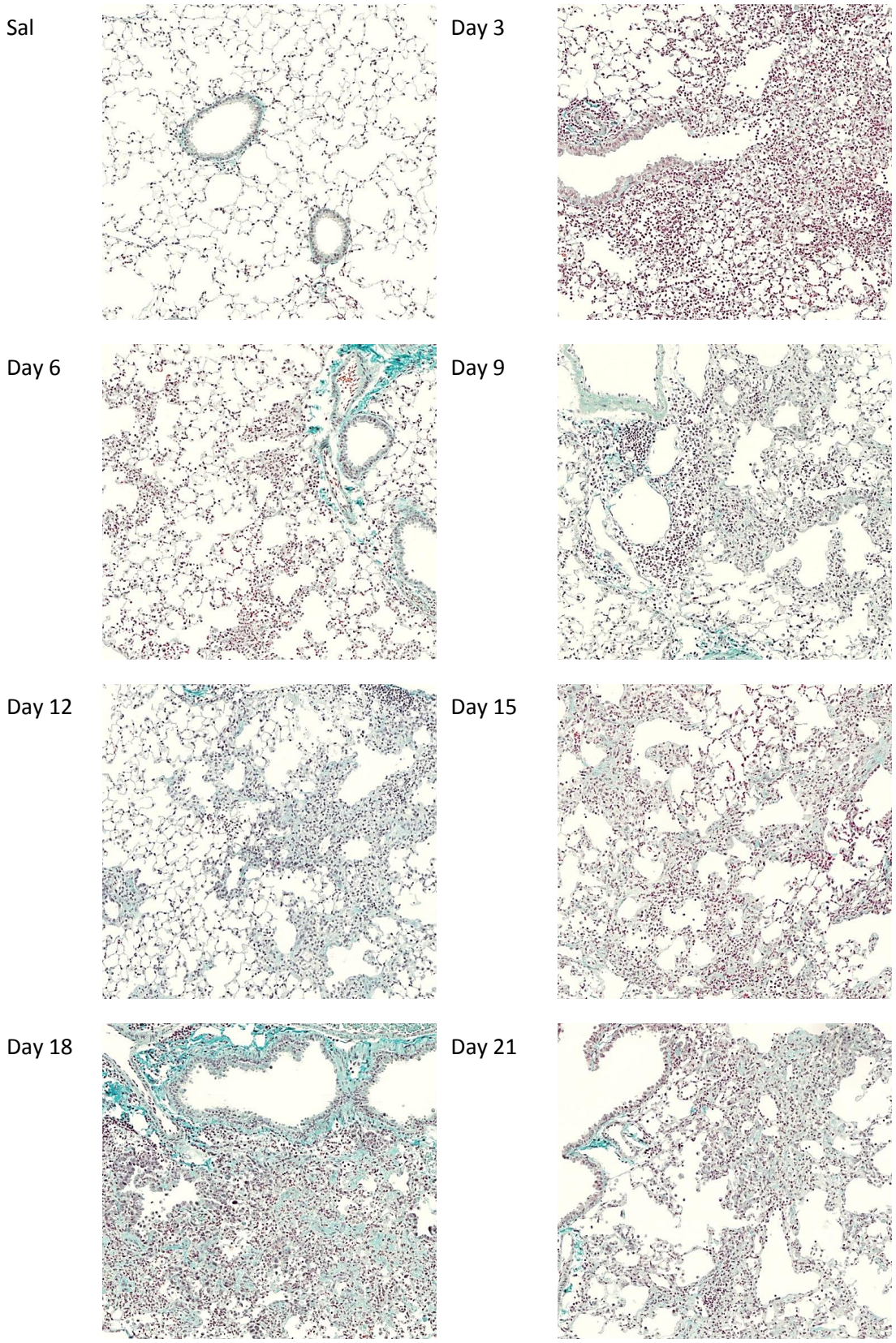



**Figure 14 Masson Goldner's Tricrom stain of histological sections of lung tissue from saline or BLM treated mice**

## 5.3 Longitudinal assessment of T cells

### 5.3.1 Spleen

#### 5.3.1.1 *Percentages of CD4$^+$ and CD8$^+$ T cells*

To investigate if BLM treatment evokes a systemic T cell response, spleen cells were analysed. The relative content of CD4$^+$and CD8$^+$ T cells within the spleen cell populations did not change significantly at the time points examined (Table 9). Thus there was no hint for a systemic reaction of the T cells at the quantitative level.

*Table 9 Percentages of CD4$^+$ and CD8$^+$ T cells within total living cell population in spleen samples*

| | | CD4* | CD8 |
|---|---|---|---|
| **Sal** | n = 10 | 22.3 (18.2-25.4) | 15.7 (7.4-20.0) |
| **Day 3** | n = 4 | 20.5 (18.2-23.4) | 10.22 (9.0-15.1) |
| **Day 6** | n = 12 | 23.9 (18.8-27.7) | 15.7 (12.1-28.8) |
| **Day 9** | n = 10 | 21.7 (17.5-27.6) | 14.1 (11.0-21.5) |
| **Day 12** | n = 11 | 19.5 (15.0-28.1) | 15.7 (9.8-22.5) |
| **Day 15** | n = 5 | 21.3 (21.1-21.7) | 17.7 (11.9-23.9) |
| **Day 18** | n = 6 | 22.8 (18.5-30.9) | 17.7 (13.3-22.1) |
| **Day 21** | n = 5 | 19.9 (17.6-26.6) | 13.3 (9.5-18.7) |

* Values are expressed as median (range)

#### 5.3.1.2 *Naïve, central memory and effector memory CD4$^+$ T cells*

To asses also changes in the spleen T cell activation status, T cell memory subtypes were analysed. Naïve T cells were the main CD4$^+$ T cell population with about 80%, followed by effector memory CD4$^+$ T cells (about 10%). Among the different time points, there was no change in the relation of the different subsets (Table 10).

*Table 10 Percentages of CD4$^+$ T-cell subtypes within total CD4$^+$ T cells in spleen*

| | | Naïve* | CM | EM |
|---|---|---|---|---|
| **Sal** | n = 10 | 81.3 (71.4-83.1) | 3.2 (2.2-4.8) | 9.9 (9.0-16.2) |
| **Day 3** | n = 4 | 80.2 (79.6-81.1) | 2.4 (2.1-3.1) | 8.9 (7.2-9.8) |
| **Day 6** | n = 12 | 78.9 (74.2-83.6) | 3.5 (1.5-5.1) | 10.6 (7.9-15.6) |
| **Day 9** | n = 10 | 80.4 (68.0-86.7) | 3.1 (2.2-4.9) | 9.2 (6.9-17.6) |
| **Day 12** | n = 11 | 79.0 (57.1-83.4) | 3.4 (1.8-5.9) | 11.7 (8.8-20.7) |
| **Day 15** | n = 5 | 84.8 (80.8-85.9) | 2.3 (1.1-3.0) | 8.7 (6.8-10.7) |
| **Day 18** | n = 6 | 83.7 (78.9-87.9) | 2.3 (1.6-4.0) | 8.6 (6.3-12.6) |
| **Day 21** | n = 5 | 77.3 (76.8-84.0) | 3.0 (2.0-4.3) | 12.2 (9.1-14-2) |

* Values are expressed as median (range)

#### 5.3.1.3 *CCR2 expression*

CCR2 was only expressed on a small population of spleen T cells. The relative content of $CCR2^+$ cells was nearly similar within $CD4^+$ and $CD8^+$ T cells, and did not differ significantly among different time points (Table 11).

*Table 11 Percentages of CCR2 expressing $CD4^+$ or $CD8^+$ cells within total $CD4^+$ and $CD8^+$ cells in spleen*

| | | CCR2 to CD4* | CCR2 to CD8 |
|---|---|---|---|
| **Sal** | n = 10 | 2.1 (1.1-5.8) | 1.2 (0.0-5.5) |
| **Day 3** | n = 4 | 2.1 (0.94-2.3) | 1.5 (0.82-2.5) |
| **Day 6** | n = 12 | 3.2 (2.1-4.1) | 1.8 (0.78-3.6) |
| **Day 9** | n = 10 | 1.7 (0.74-3.9) | 1.2 (0.0-3.3) |
| **Day 12** | n = 11 | 4.1 (0.0-5.0) | 2.2 (0.0-4.3) |
| **Day 15** | n = 5 | 1.8 (1.6-2.5) | 1.9 (1.2-3.8) |
| **Day 18** | n = 6 | 1.1 (0.1-2.9) | 0.88 (0.0-3.3) |
| **Day 21** | n = 5 | 2.4 (1.4-5.5) | 1.1 (0.0-2.2) |

* Values are expressed as median (range)

Table 12 shows percentages of naïve, central memory and effector memory $CD4^+$ T cells expressing CCR2. CCR2 was predominantly expressed on $T_{em}$ cells. Within naïve T cells only a small population expressed CCR2. Among the time points, there was no significant difference in the percentage of $CCR2^+$ cells within the different subsets.

*Table 12 Percentages of CCR2 expression within $CD4^+$ T-cell subtypes in spleen*

| | | Naïve | CM | EM |
|---|---|---|---|---|
| **Sal** | n = 10 | 0.46 (0.00-6.7) | 4.3 (0.00-21) | 11 (7.6-20) |
| **Day 3** | n = 4 | 1.0 (0.65-1.4) | 4.6 (0.00-7.5) | 16 (14-21) |
| **Day 6** | n = 12 | 1.0 (0.00-2.2) | 5.7 (0.00-33) | 19 (7.9-29) |
| **Day 9** | n = 10 | 0.85 (0.00-1.7) | 5.9 (2.2-8.1) | 15 (7.5-2) |
| **Day 12** | n = 11 | 0.08 (0.00-2.0) | 5.9 (2.5-18) | 12 (7.5-36) |
| **Day 15** | n = 5 | 0.53 (0.00-1.6) | 5.2 (4.4-17) | 12 (10-20) |
| **Day 18** | n = 6 | 0.00 (0.00-0.35) | 7.9 (0.00-13) | 8.0 (5.0-27) |
| **Day 21** | n = 5 | 0.58 (0.17-1.2) | 8.2 (2.4-25) | 11 (9.1-48) |

* Values are expressed as median (range)

In total, no significant changes in T cell content and the distribution of $CD4^+$ T cell subtypes have been detected during the longitudinal observation. Thus, there was no hint for a systemic T cell response following intra tracheal BLM application. To investigate the local effects of BLM treatment, BALF and lung tissue were analyzed in an analogous way.

### 5.3.2 **BALF**

#### 5.3.2.1 ***Cell count***

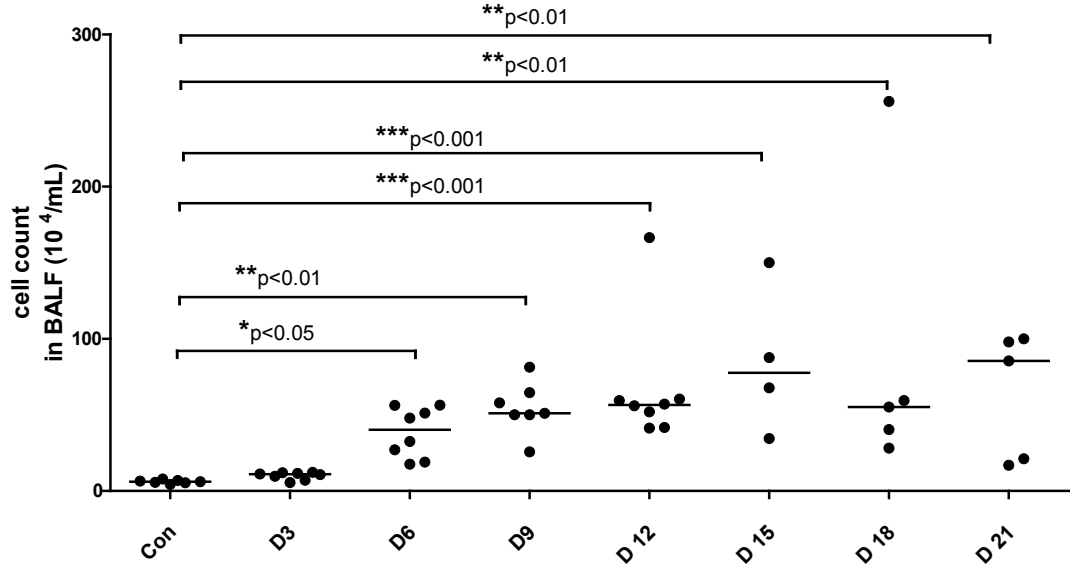



**Figure 15 Cell count of BAL during time course***; 1ml of sterile PBS was instilled, cell count is given as $10^4$/ml; indicated p-values obtained by Dunn Multiple Comparison test; Kruskal Wallis test: ***p<0.001*

BAL cells were analyzed to monitor the recruitment of inflammatory cells to the airways of BLM treated mice. BAL from untreated mice contains only few cells, which are predominantly alveolar macrophages, and nearly no lymphocytes. After BLM treatment, median cell counts increased up to 14 times at day 21 compared to saline treated mice. The most significant increase was detected at days 12 and 15. However, there was a wide range from 41.3 $10^4$/ml to 166.5 $10^4$/ml at day 12 and 34.5 $10^4$ to 150.0 $10^4$ at day 15. Notably, two animals showed high BAL cell counts, one at day 12 and the other one at day 21. The outlier at day 12 corresponds to an extreme loss of body weight of the respective animal, whereas the outlier at day 18 did not show an extreme loss of body weight or any other outstanding value within the parameters measured.

#### 5.3.2.2 ***$CD4^+$ and $CD8^+$ T cells***

As expected, there were nearly no lymphocytes detectable in control mice. The relative content of $CD4^+$ T cells was between 0 and 5 %, the relative content of $CD8^+$ T cells between 0 and 0.3 %.

In contrast, a significant increase of the percentage of $CD4^+$ T cells compared to the control group was found at days 9, 12, 15 and 21. The highest median percentage of $CD4^+$ T cells was

detected at day 15. However, there was a wide range, and due to the low number of samples analyzed in this group, the result is difficult to evaluate (Figure 16).

Percentages of $CD8^+$ T cells were increased similar to $CD4^+$ T cells. At the time points from day 6 to day 12, the percentage of $CD8^+$ T cells within living cells was significantly higher than in the control group (Figure 17).

An analysis of T cell subtypes in BAL was not possible due to the limited cell number in these samples.

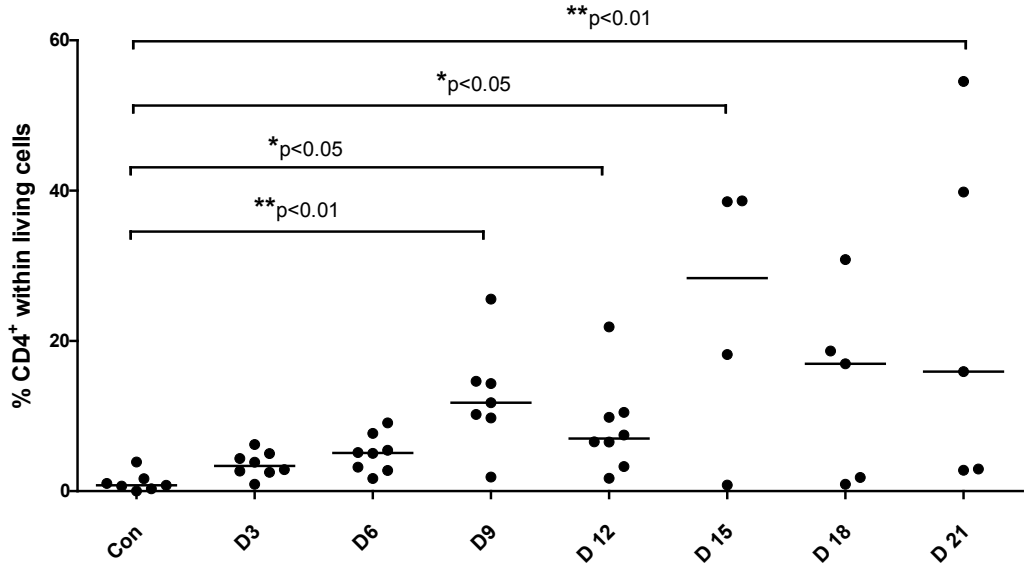



**Figure 16 Percentages of $CD4^+$ T cells within living BAL *cells***; *indicated p-values obtained by Dunn Multiple Comparison test; Kruskal Wallis test: **p<0.01*

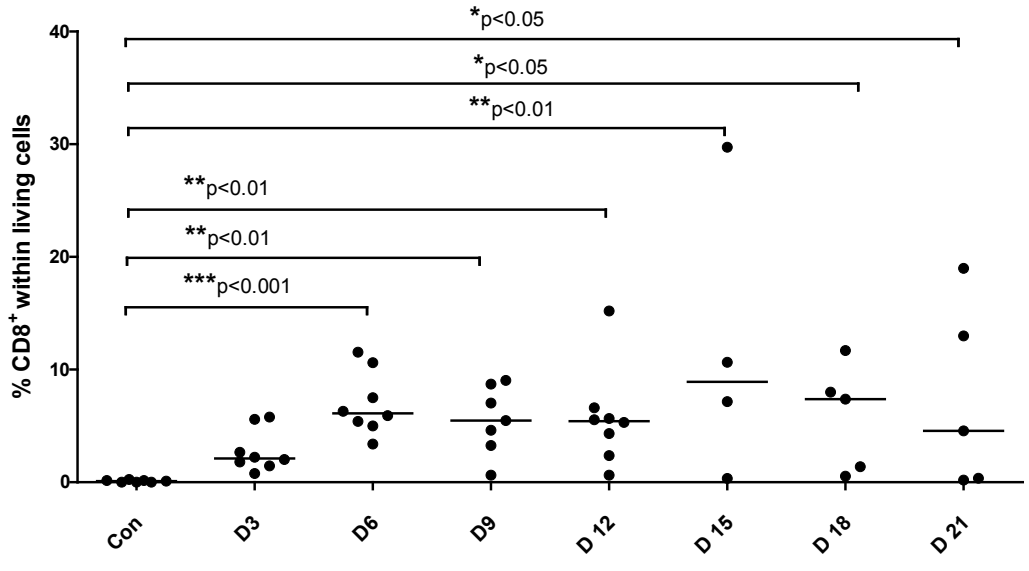



**Figure 17 Percentages of $CD8^+$ T-cells within living BAL cells**; *indicated p-values obtained by Dunn Multiple Comparison test; Kruskal Wallis test: **p<0.01*

### 5.3.3 **Lung**

#### 5.3.3.1 ***CD4$^+$ and CD8$^+$ T cells***

To further characterize the lymphocyte response to BLM induced lung injury, flow cytometric analysis of $CD4^+$ and $CD8^+$ T cells as well as $CD4^+$ T cell subtypes was performed in lung tissue.

Overall, there was a clear increase of the percentage of $CD4^+$ T cells over time. A significant difference from control mice, which showed a median percentage of $CD4^+$ T cells of 11% (8.7-16%), was detected at day 18 with a median 16% $CD4^+$ T cells (11-22%). Results of all time points are shown in Figure 18.

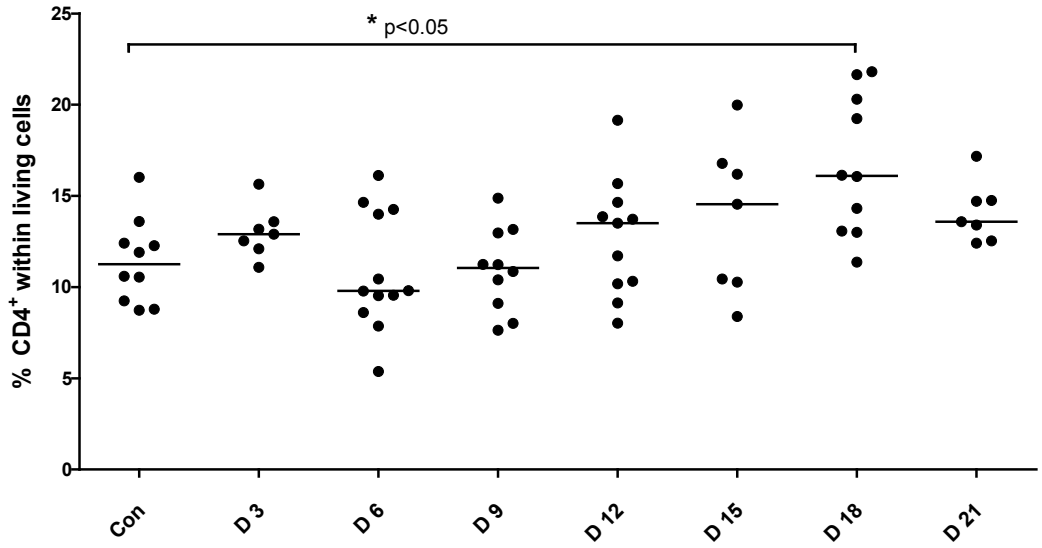



**Figure 18 Percentages of $CD4^+$ T cells within total living cells in lung samples during time course;** *indicated p-values obtained by Dunn Multiple Comparison test; Kruskal Wallis test: **p<0.01*

The longitudinal changes of the percentage of $CD8^+$ T cells differed from the changes of the $CD4^+$ T cell population (Figure 19). From day 9 to day 15, the percentage of $CD8^+$ T cells decreased significantly compared to the control group (median 7.4%; range 5.2-10%). At day 18 and day 21, it increased again. The minimum was detected at day 15 with a median $CD8^+$ population of 3.7% (2.4-5.2%) within living cells.

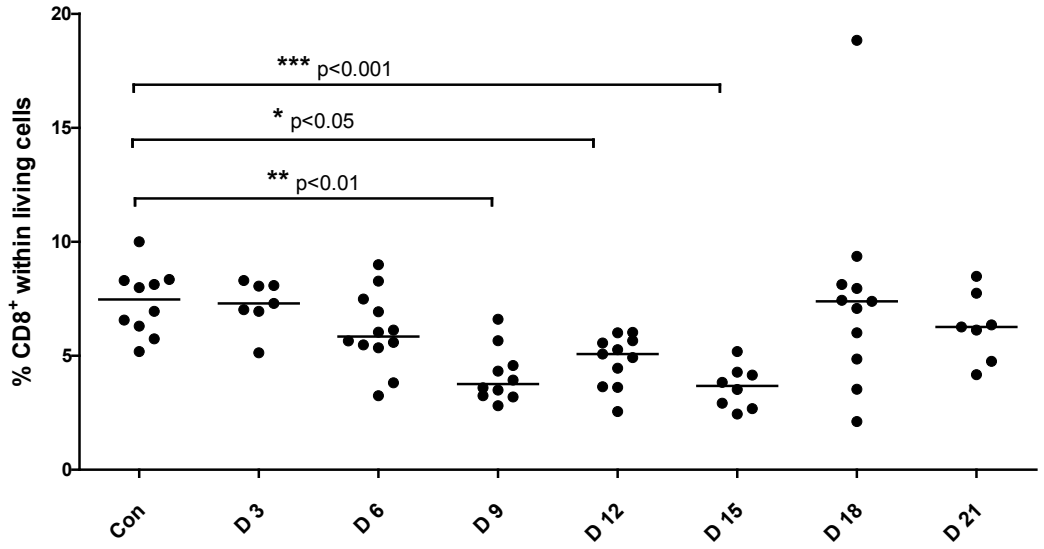



**Figure 19 Percentages of CD8$^+$ T cells within living cells in lung samples during time course***; indicated p-values obtained by Dunn Multiple Comparison test; Kruskal Wallis test: ***p<0.001*

### 5.3.3.2 *Naïve, central memory, effector memory T cells*

Naïve, central memory, and effector memory CD4$^+$ T cells in lung tissue were analyzed analogous to spleen samples. CD44$^{low}$CD62L$^{hi}$ naïve T cells built the largest group with 75% (58- 83%) of CD4$^+$ T cells in saline treated animals. The percentage of naïve CD4$^+$ T cells decreased following BLM treatment with a minimum at day 9 and day 12 (medians 52% and 58%) (Figure 20).

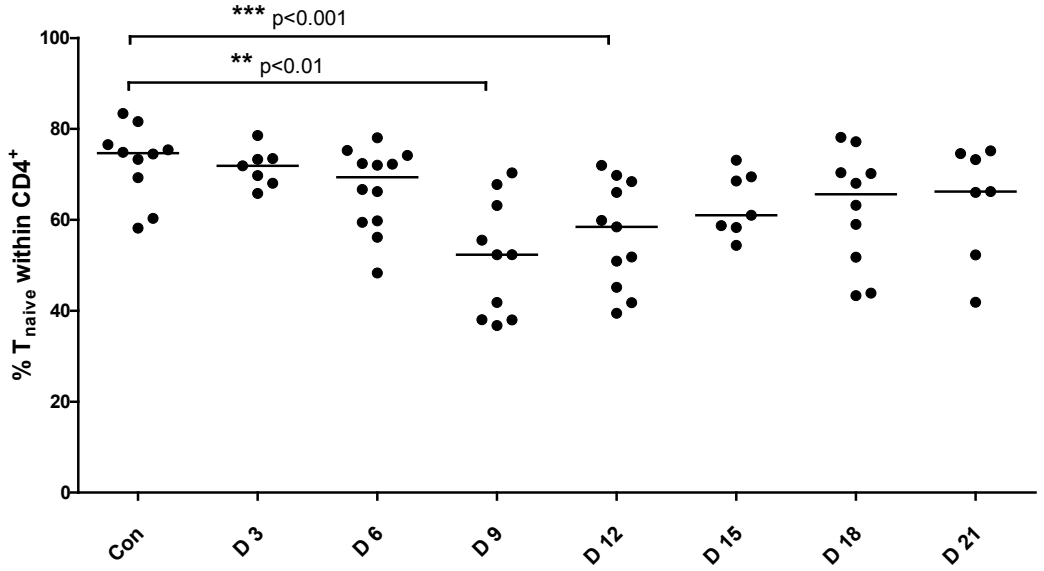



**Figure 20 Percentages of $T_{naive}$ CD4$^+$ cells within total CD4$^+$ T cells in lung samples during time course***; indicated p-values obtained by Dunn Multiple Comparison test; Kruskal Wallis test: **p<0.01*

$CD44^{hi}CD62L^{hi}$ central memory T cells were the smallest group of $CD4^+$ T cell subsets. There were no changes of the percentage of $T_{cm}$. The median portion of $T_{cm}$ within total $CD4^+$ T cells was between 2.8 % at day 12 and 4.2% in the control group (Figure 21).

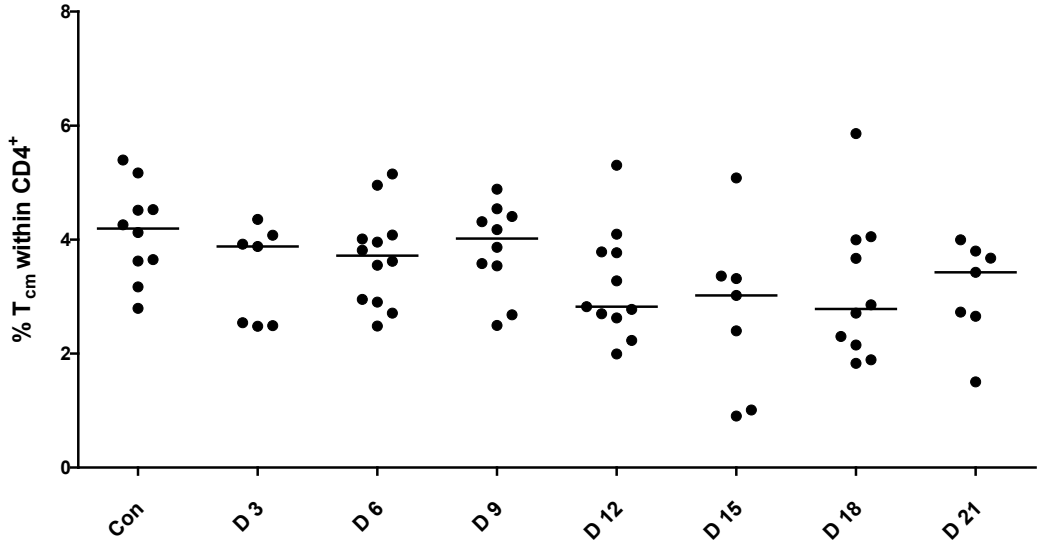



**Figure 21 Percentages of $T_{cm}$ $CD4^+$ cells content within total $CD4^+$ T cells in lung samples during time course***; indicated p-values obtained by Dunn Multiple Comparison test; Kruskal Wallis test: ns p=0.08*

Concurrently to the decrease of $T_{naive}$, $CD44^{hi}CD62L^{low}$ effector memory cells increased. Significantly higher values compared to controls, which showed a median fraction of $T_{em}$ of 16% (6.9-23%), were found on day 9 with 31% (17-50%) and day 12 with 27% (15-51%) (Figure 22).

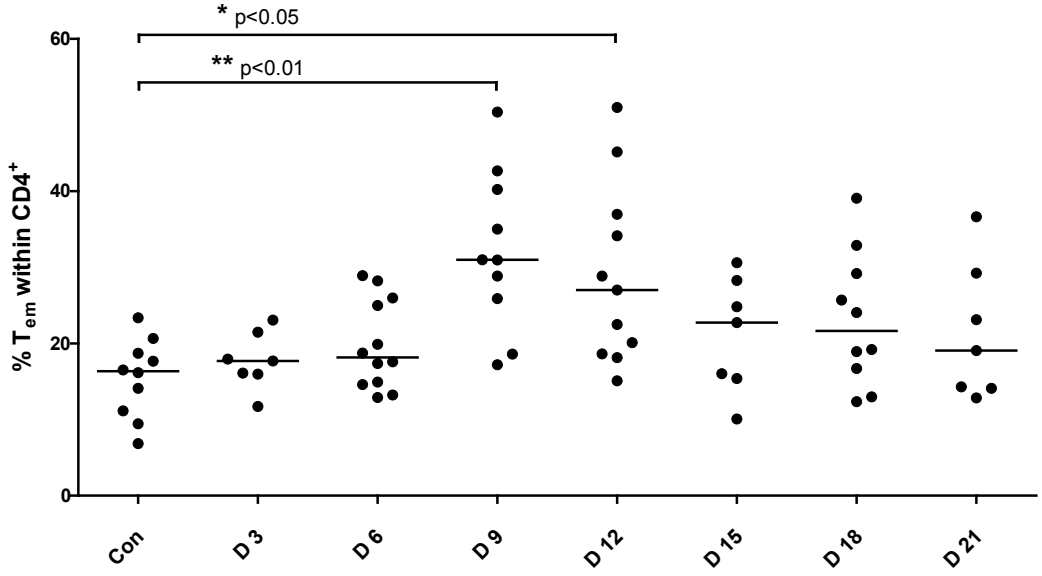



**Figure 22 Percentages of $T_{em}$ $CD4^+$ cells within total $CD4^+$ T cells in lung samples during time course***; indicated p-values obtained by Dunn Multiple Comparison test; Kruskal Wallis test: **p<0.01*

## 5.4 Maximal increase of the percentage of CCR2$^+$ T cells after bleomycin treatment

### 5.4.1 BALF

#### 5.4.1.1 *Percentage of CCR2 expressing BAL lymphocytes*

BAL samples of control mice did not contain enough lymphocytes to analyze the fraction of CCR2 expressing T cells. For this, values were set to zero for the control group, which also allowed statistic testing. Although the baseline percentage of CCR2$^+$ T cells could not be displayed, the results imply their increase in BAL following BLM treatment with a maximum between day 6 and day 12. After day 12 they decreased again (Figure 23).

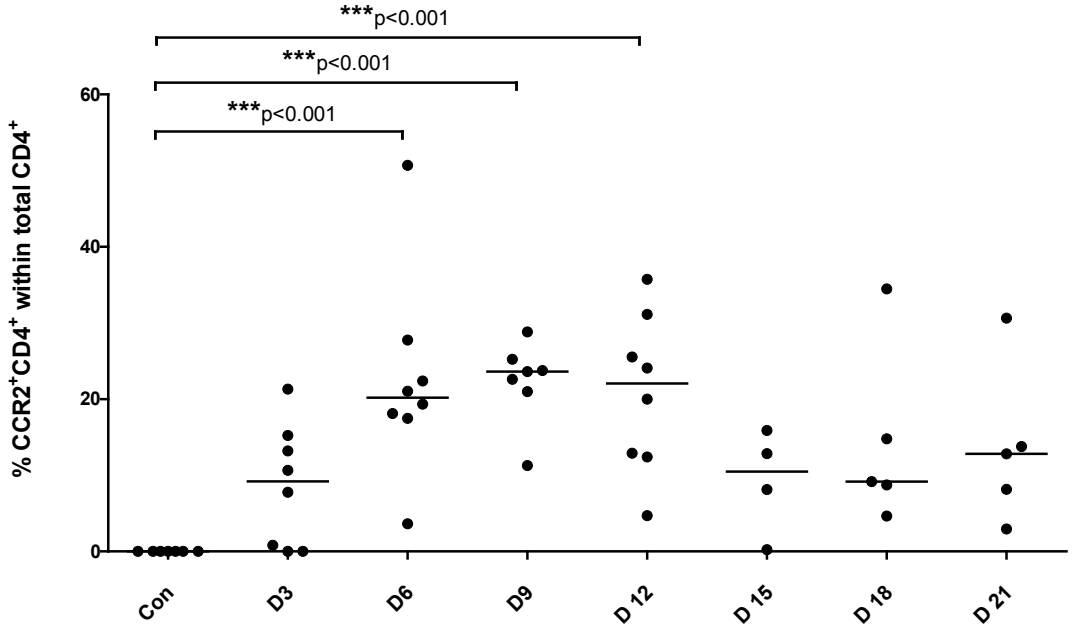



**Figure 23 Percentage of CCR2$^+$CD4$^+$ T cells within total CD4$^+$ T cells in BAL***; indicated p-values obtained by Dunn Multiple Comparison test; Kruskal Wallis test: ***p<0.001*

A similar kinetic of the percentage of CCR2$^+$ cells was found within the CD8$^+$ T cell population in BAL. The median amount of CCR2 expressing CD8$^+$ T cells was between 1.8% (0.58%-2.9%) at day 15 and 8.5 % (0.00-11%) at day 9 (Figure 24).

At day 6, one animal showed a very high percentage of CCR2$^+$ cells within CD4$^+$ T cells (51%) and CD8$^+$ T cells (22%) in BAL, but did not show any other extreme values within the parameters measured.

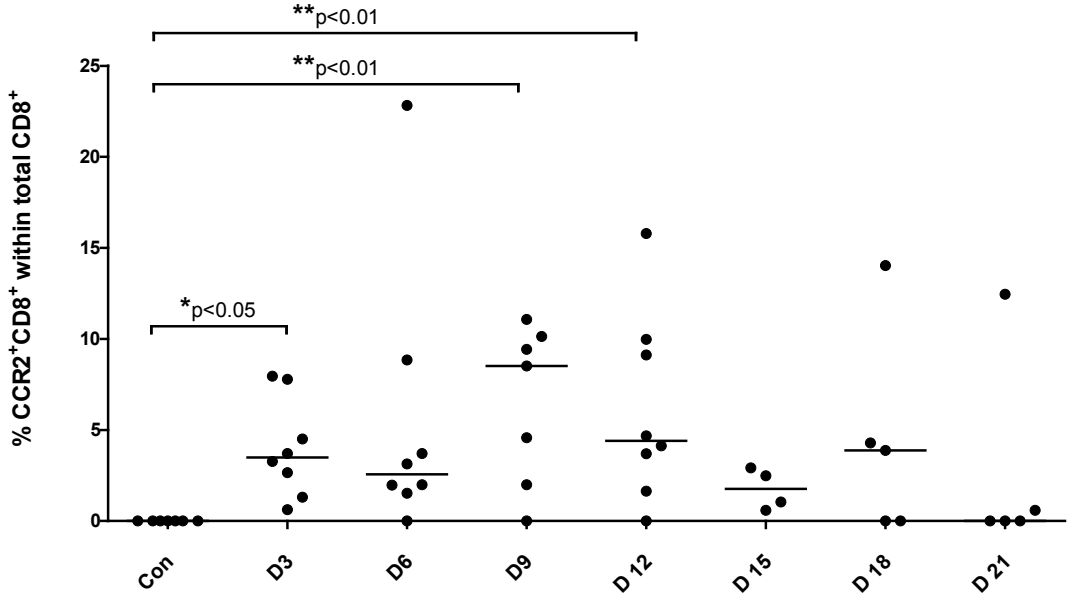



**Figure 24 Percentage of CCR2$^+$CD8$^+$ T cells within total CD8$^+$ T cells in BAL***; indicated p-values obtained by Dunn Multiple Comparison test; Kruskal Wallis test: *p<0.05*

### 5.4.2 **Lung**

#### 5.4.2.1 ***CCR2$^+$cells within total CD4$^+$ and CD8$^+$ T cells***

The percentage of CCR2 expressing CD4 T cells increased in lungs of treated mice with a maximal percentage at days 9 and 12, and then decreased again at day 18 and day 21. In control mice, CCR2 was expressed on 2.3% to 9.8% (median 4.2 %) of CD4$^+$ T cells. At day 9, the CCR2$^+$ population within total CD4$^+$ T cells peaked with a threefold increase (14.6%; range: 5.8-27%) (Figure 25).

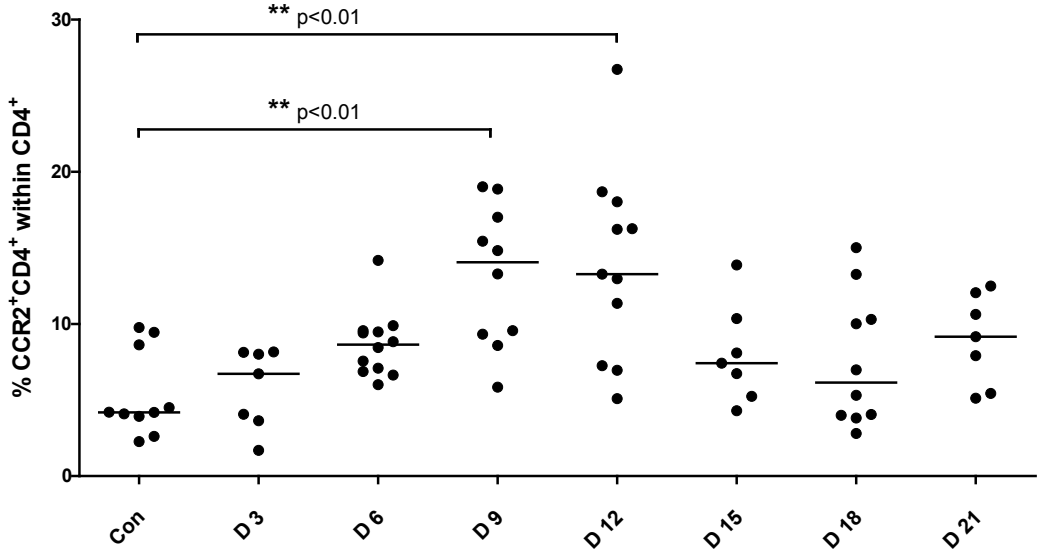



**Figure 25 Percentages of CCR2$^+$CD4$^+$ T cells within total CD4$^+$ T cells in lung samples***; indicated p-values obtained by Dunn Multiple Comparison test; Kruskal Wallis test: ***p<0.001*

Figure 26 shows the $CCR2^+$ CD4 T cell fraction calculated back to the total living cell population. $CCR2^+CD4^+$ T cells represented 0.54% (0.24% and 0.85%) of total living cells in the control group. Calculated like this, the peak increase was detected at day 12, when $CCR2^+CD4^+$ T cells constituted between 0.66 and 2.1% (median 1.6%). This was in consequence of the slightly higher total $CD4^+$ T cell frequency at this time point.

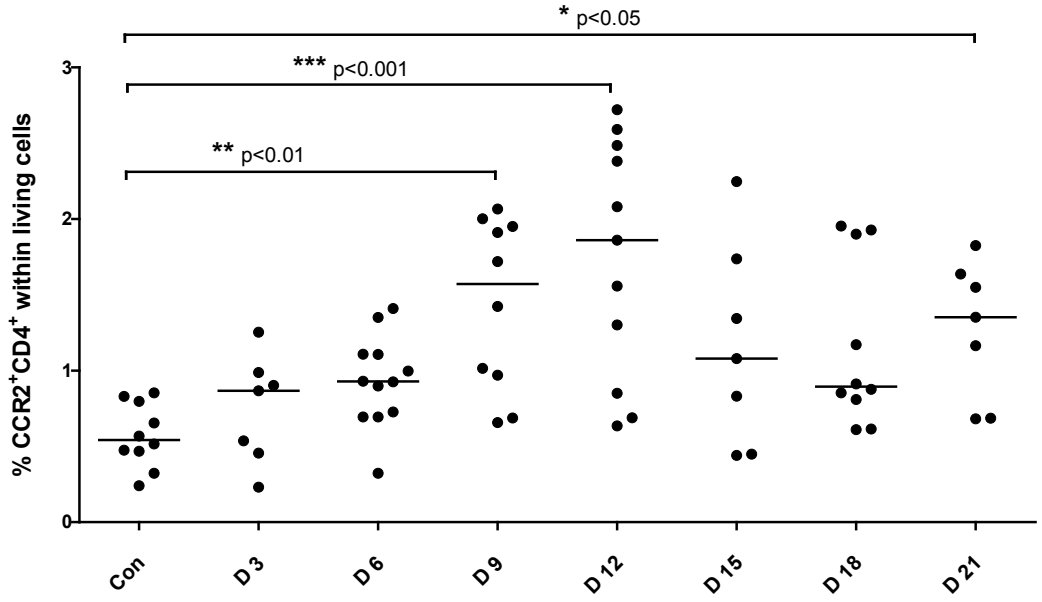



**Figure 26 Percentages of $CCR2^+CD4^+$ T cells within total living cells**; *indicated p-values obtained by Dunn Multiple Comparison test; Kruskal Wallis test: **p<0.01*

Within the $CD8^+$ T cell population CCR2 expressing cells were slightly rarer than within $CD4^+$ T cells. The percentage of CCR2 expressing $CD8^+$ T cells showed an increase with a peak at day 9 (median 9.1%) followed by a decrease at days 18 and 21 (medians 1.7% and 4.3%) (Figure 27).

Although the relative content of total $CD8^+$ T cells decreased in lung tissue following BLM treatment, $CCR2^+CD8^+$ T cells showed a significant increase compared to controls (median 0.12%) at day 6 (median 0.33%) and day 9 (median 0.28%), when calculated back to total living cells (Figure 28).

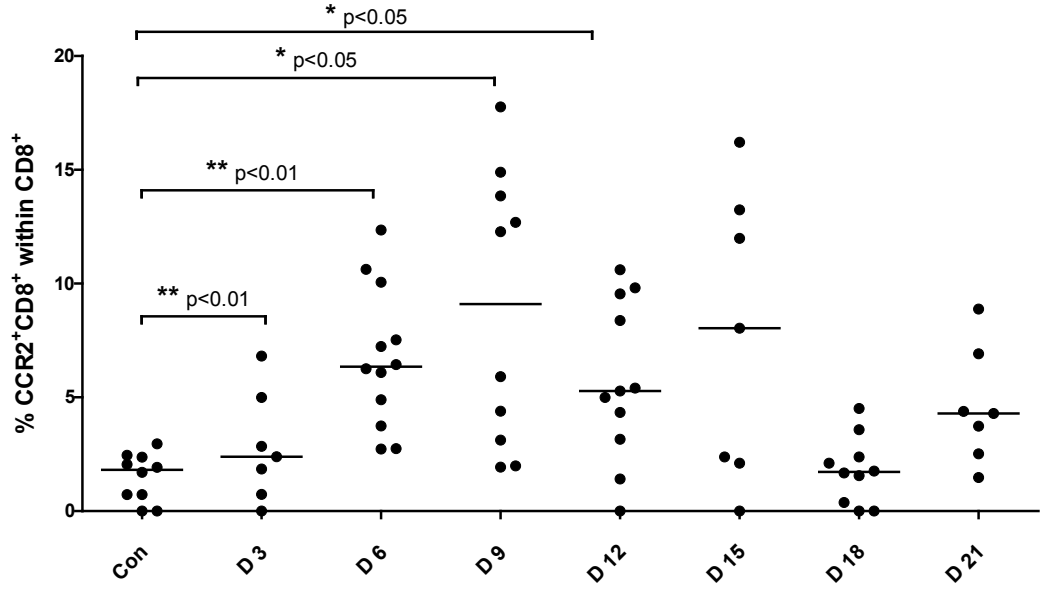



**Figure 27 Percentages of CCR2$^+$CD8$^+$ T cells of total CD8$^+$ T cells in lung samples during time course**; *indicated p-values obtained by Dunn Multiple Comparison test; Kruskal Wallis test: ***p<0.001*

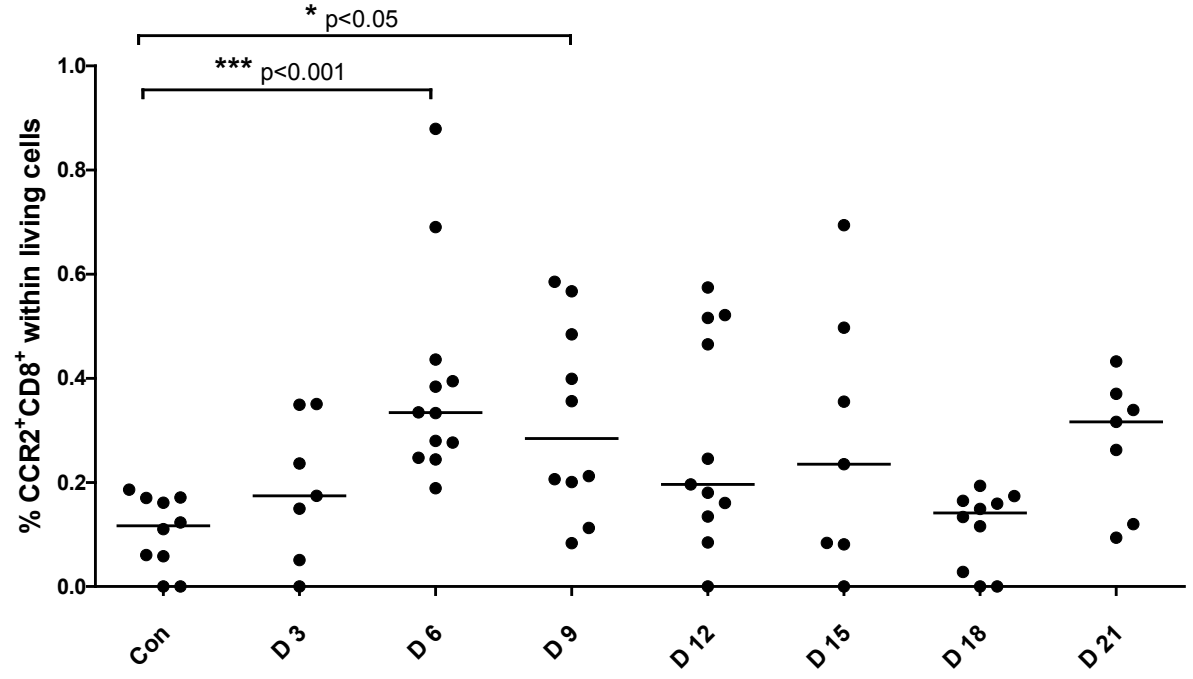



**Figure 28 Percentages of CCR2$^+$ CD4$^+$ T cells within total living cells during time course**; *indicated p-values obtained by Dunn Multiple Comparison test; Kruskal Wallis test: ***p<0.001*

### 5.4.2.2 *CCR2$^+$cells within CD4$^+$ T cell subtypes*

Like in spleen samples, the portion of CCR2$^+$ cells within the three CD4$^+$ T cell subtypes was also analyzed in the lung. Within naïve CD4$^+$ T cells, the frequency of CCR2$^+$ cells was

between 0% and 3.7%. It did not vary significantly among different time points following BLM treatment and the control group (Figure 29).

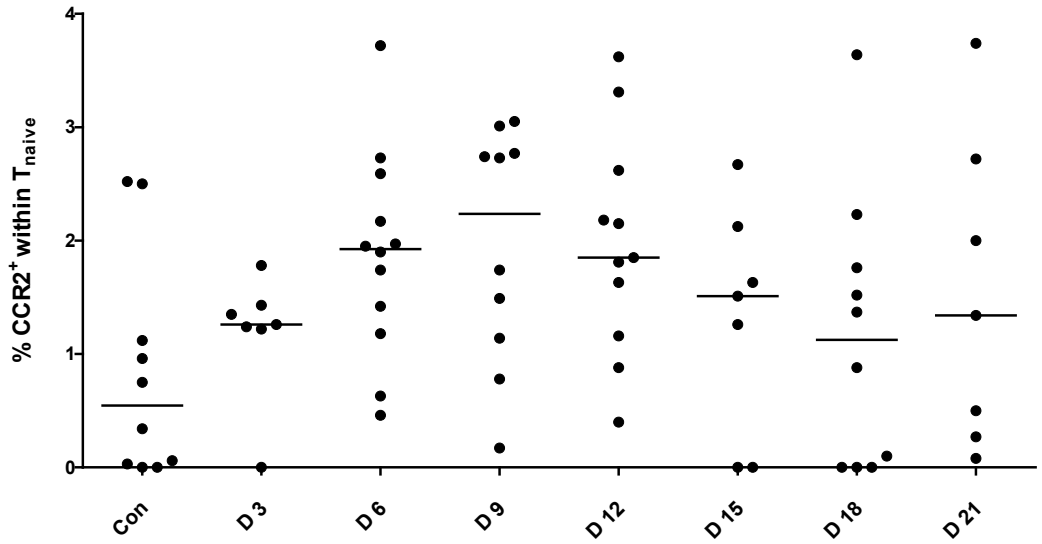



**Figure 29 Percentages of CCR2$^+$ $T_{naïve}$ within total $T_{naive}$ during time course**; *Kruskal Wallis test: ns p=0.08*

The CCR2$^+$ central memory population was too small to be analyzed adequately.

Similar to the result in spleen samples, CCR2 was predominantly expressed on effector memory T cells. In control mice, the median percentage of CCR2$^+$ cells within $T_{em}$ cells was 23% (14-31%). Following BLM treatment, the percentage was significantly increased at day 12 (median 34 %, range 20-48%). On the following time points it decreased again (Figure 30).

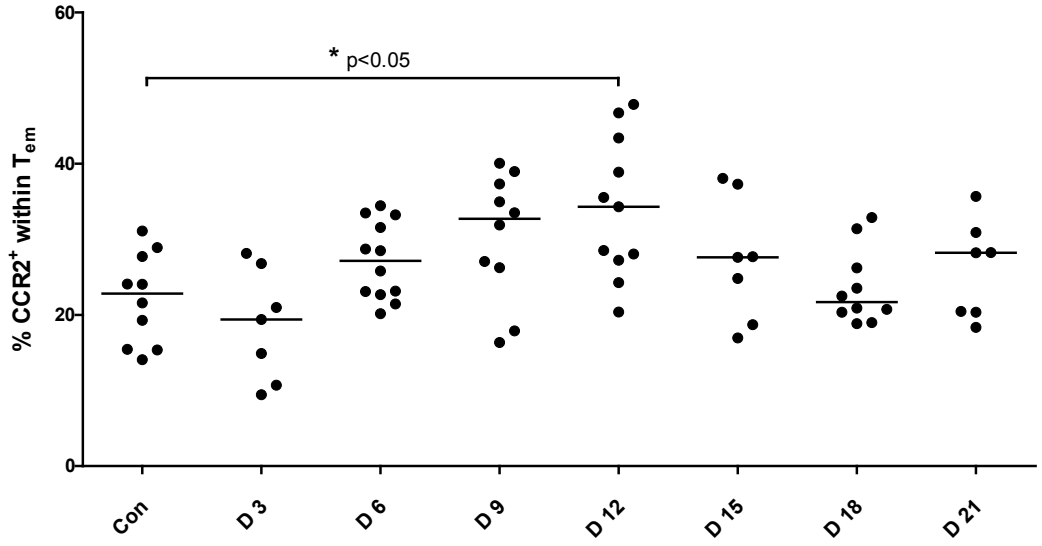



**Figure 30 Percentages of CCR2$^+$ $T_{em}$ within total $T_{em}$ during time course**, *indicated p-values obtained by Dunn Multiple Comparison test; Kruskal Wallis test: **p<0.01*

### 5.4.2.3 *Maximal content of CCR2$^+$ T cells*

To determine the peak of the relative content of CCR2$^+$ T cells, percentages of CCR2$^+$CD4$^+$ T cells and CCR2$^+$CD8$^+$ T cells within living cells were added up. With a median percentage of 2.1%, the frequency of CCR2$^+$ T lymphocytes reached the maximum at day 12. Thus, day 12 was chosen for the further characterization of CCR2$^+$ T cells.

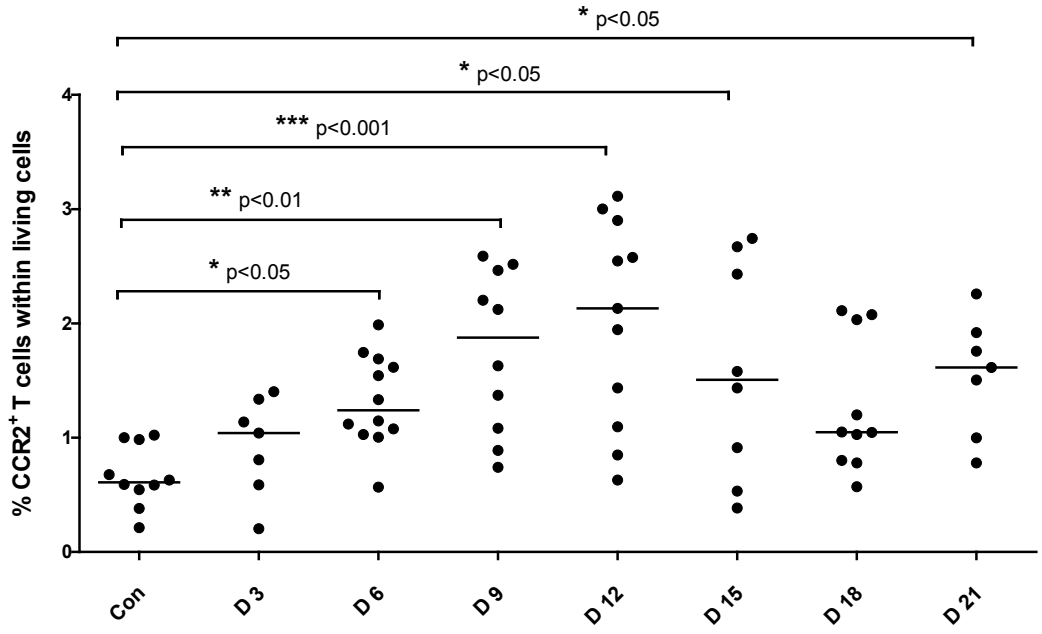



**Figure 31 Sums of the percentages of CCR2$^+$CD4$^+$ and CCR2$^+$CD8$^+$ T cells within total living lung cells***; indicated p-values obtained by Dunn Multiple Comparison test; Kruskal Wallis test: **p<0.01*

## 5.5 **Chemokine Receptor Co-expression**

To characterize $CCR2^+$ T lymphocytes in fibrotic lungs, the co-expression of other chemokine receptors with CCR2 on T cells was analysed. As mentioned above, $CCR2^+$ T cells were most frequent at day 12 after BLM treatment. For that reason, all following experiments were performed at this time point.

### 5.5.1 **CCR2**

The percentage of $CCR2^+$ T cells at day 12 after BLM treatment was analysed again. The median percentage of CCR2 expressing cells within $CD4^+$ T cells was 7.9% (4.9-11%) in lungs from saline treated mice and 18% (6.4-29%) in samples from BLM treated mice. Thus, CCR2 expression was slightly higher than on day 12 in the time course experiments.

The same was seen for $CD8^+$ T cells from control animals, which showed a CCR2 expression on 7.4% (3.9-9.2%) of the cells. In samples from BLM treated mice, $CCR2^+$ cells represented 22% (6.2-34%) of CD8 T cells (Figure 32).

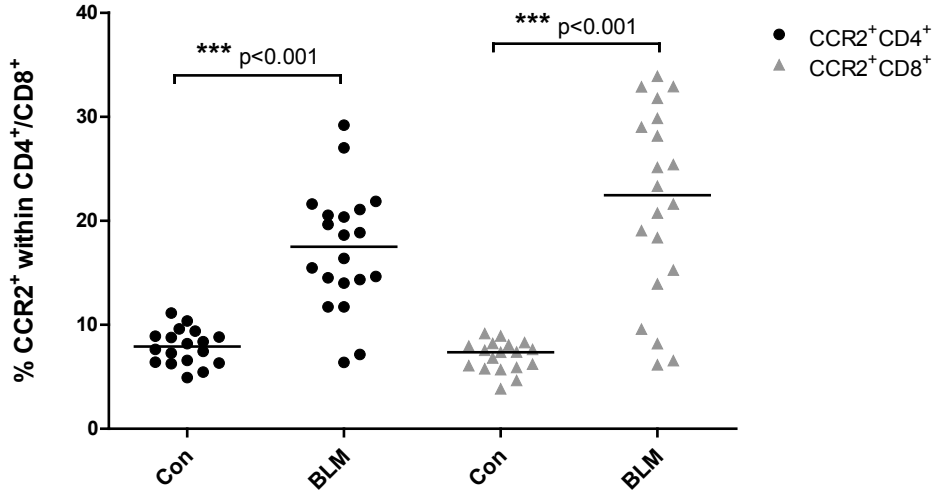



**Figure 32 $CCR2^+$ $CD4^+$ and $CCR2^+CD8^+$ T cells at day 12 from saline treated control mice and bleomycin treated mice***; indicated p values obtained by Mann Whitney U test*

### 5.5.2 **CCR3**

In control lungs, CCR3 was expressed on 2.0% (0.00-2.9%) of $CD4^+$ T cells. In BLM treated mice, this number was doubled to 4.1% (1.9-5.7%). $CCR3^+CD8^+$ T cells were only detected in two of 6 samples of control mice (0.9% and 1.3%). In BLM treated animals, CCR3 was expressed on 0.9% (0.00-2.5%) pulmonary $CD8^+$ T cells. However, the difference to control animals was not significant (Figure 33a).

While $CCR3^+CCR2^+CD4^+$ T cells were almost absent in control mice (median 0.25%), they increased to 2% (0.4-3.5%) of $CD4^+$ T cells after BLM treatment. Among $CD8^+$ T cells of treated mice, $CCR2^+CCR3^+$ cells represented 0.8% of $CD8^+$ T cells (range 0.00-1.7) (Figure 33b).

At day 12 after BLM treatment, 11% (2.0-16.2%) of $CCR2^+CD4^+$ T cells were $CCR3^+$, significantly more than in the saline treated group (4.0%; range 0.0-82%).

CCR3 was not expressed on pulmonary $CCR2^+CD8^+$ T cells from control mice. CCR3 expression amounted to 3.2% (0.0-6.8%) of $CCR2^+CD8^+$ T cells in lungs from BLM treated mice (Figure 33c).

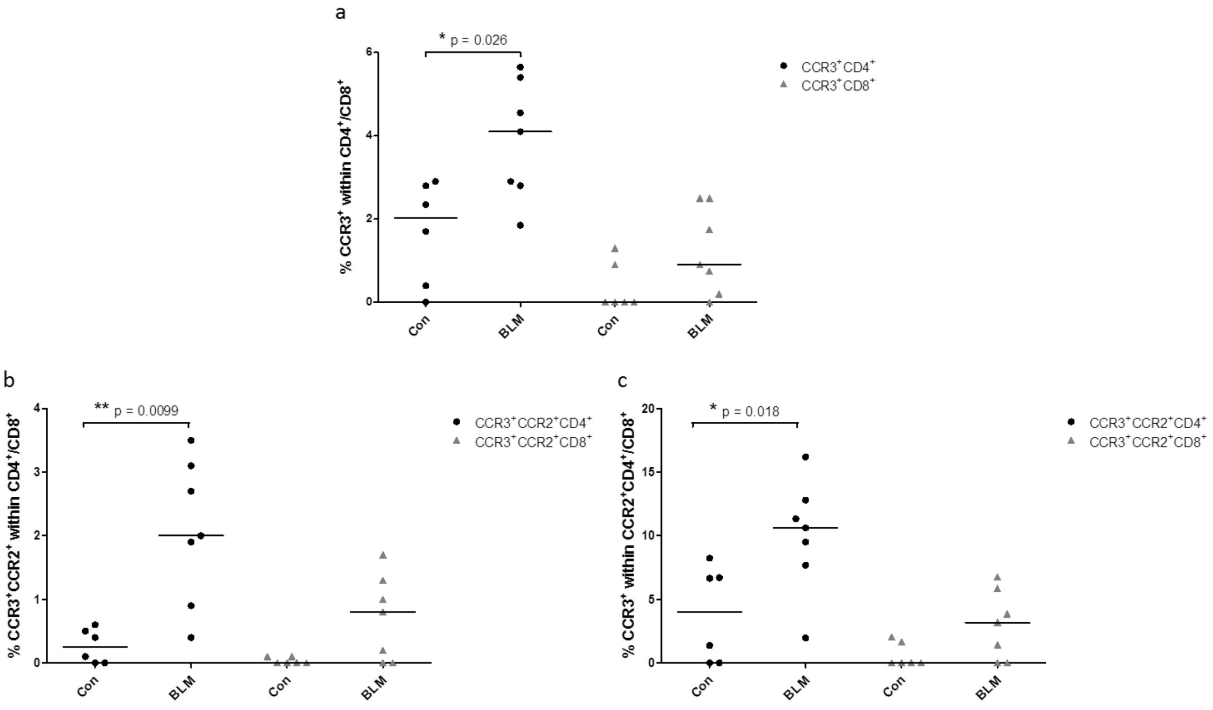



**Figure 33 $CCR3^+$ T cells at day 12 after BLM *treatment*** *a) $CCR3^+$ T cells within total $CD4^+$ or $CD8^+$ T cells; b) $CCR3^+CCR2^+$ T cells within total $CD4^+$ or $CD8^+$ T cells; c) $CCR3^+CCR2^+$ T cells within total $CCR2^+$ $CD4^+$ or $CD8^+$ T cells; indicated p values obtained by Mann Whitney U test*

### 5.5.3 **CCR4**

1.2% of $CD4^+$ T cells showed expression of CCR4 under control conditions (range 0.00-3.7%). Following BLM treatment, the percentage increased to 3.7% (0.35-8.5%). On $CD8^+$ T cells, the percentage of CCR4 expressing cells did not differ among control and treated mice. Only in two of the control samples, an expression of CCR4 could be detected (0.6% and 2.4%). In BLM samples, CCR4 was expressed on a median percentage of 0.22% (0.00-3.8%) of $CD8^+$ T cells (Figure 34a).

A co-expression of CCR4 and CCR2 was only found on $CD4^+$ T cells from bleomycin treated mice with a median of 0.5% (0.00-3.7%) of $CD4^+$ T cells (Figure 34b). Related to the $CCR2^+$ $CD4^+$ T cell population, $CCR4^+CCR2^+$ cells amounted to 7.0% (0.00-19%) of $CCR2^+CD4^+$ T cells. However, statistically the difference between control and BLM group was not significant (p=0.052) (Figure 34c).

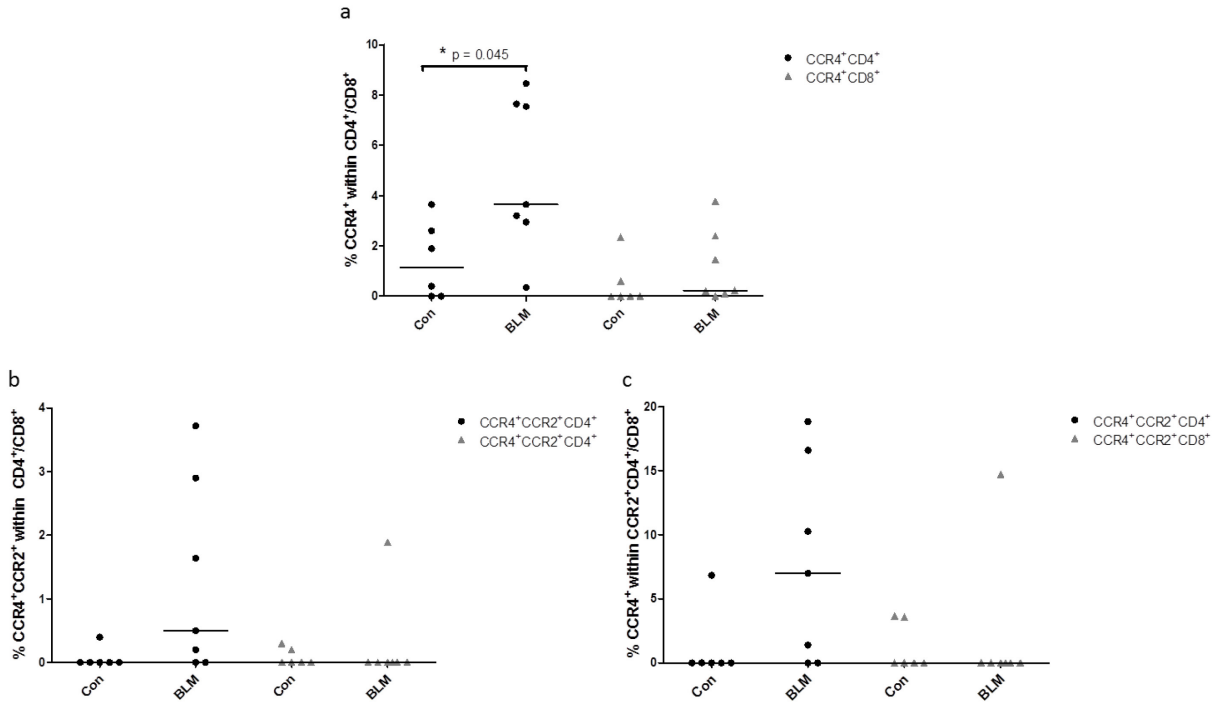



**Figure 34 $CCR4^+$ T cells at day 12 after BLM treatment**; *a) $CCR4^+$T cells within $CD4^+$ or $CD8^+$ T cells; b) $CCR4^+CCR2^+$T cells within $CD4^+$ or $CD8^+$ T cells; c) $CCR4^+CCR2^+$ T cells within total $CCR2^+CD4^+$ or $CD8^+$ T cells; indicated p values obtained by Mann Whitney U test*

### 5.5.4 **CCR5**

CCR5 was expressed only in single samples on pulmonary $CD4^+$ T cells of saline and bleomycin treated animals, as well as on $CD8^+$ T cells from saline treated animals. In contrast, 4% (2.5-14.5%) of pulmonary $CD8^+$ T cells from BLM treated mice expressed CCR5 (Figure 35a). 2.2% (1.3-8.9%) of $CD8^+$ T cells in this group were $CCR2^+CCR5^+$ cells (Figure 35b). This corresponds to 11% (5.1-34.6%) of $CCR5^+$ cells within $CCR2^+CD8^+$ T cells (Figure 35c).

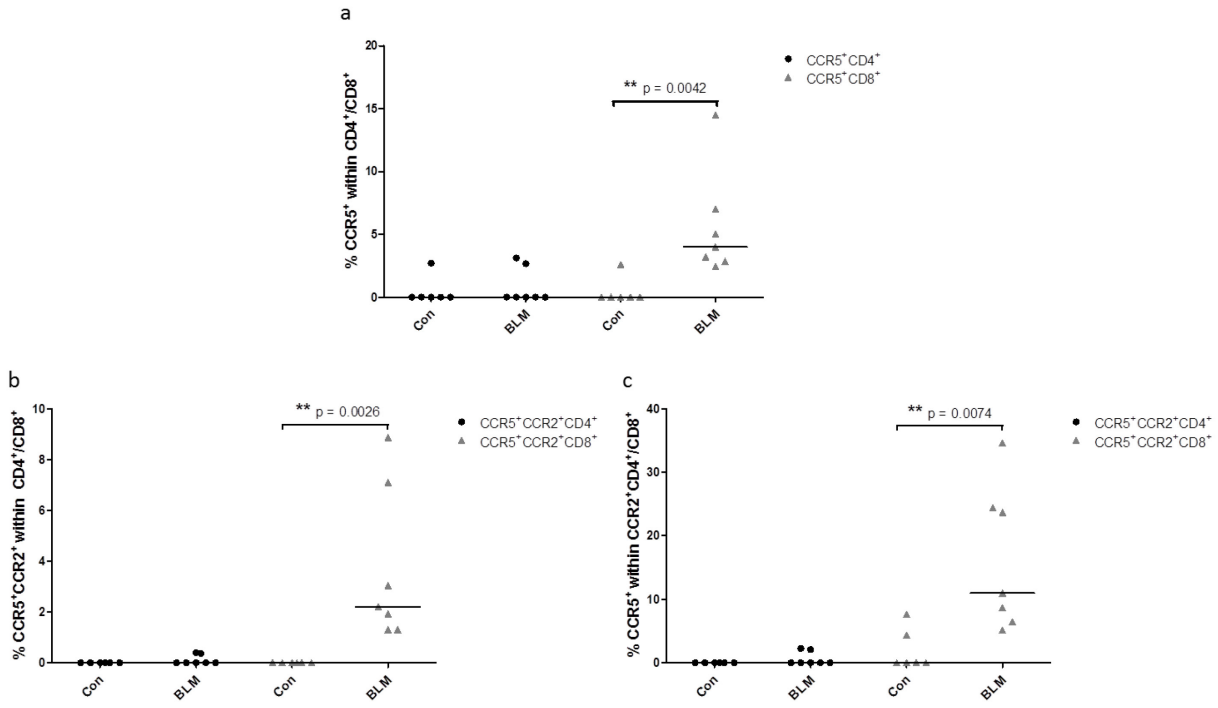



**Figure 35 CCR5$^+$ T cells at day 12 after BLM treatment**; *a) CCR5$^+$T cells within CD4$^+$ or CD8$^+$ T cells; b) CCR5$^+$CCR2$^+$ T cells within CD4$^+$ or CD8$^+$ T cells; c) CCR5$^+$CCR2$^+$ T cells within total CCR2$^+$ CD4 or CD8 T cells; indicated p values obtained by Mann Whitney U test*

### 5.5.5 **CCR6**

CCR6$^+$ cell populations increased significantly after BLM treatment. CCR6 was expressed on lung lymphocytes from 3 of 6 control animals on both, CD4$^+$ and CD8$^+$ T cells. The other control animals showed no CCR6 expression. In BLM treated mice, CCR6 was expressed on 13.5% (0.00-23%) of CD4$^+$ T cells and on 11% (0.00-23%) of CD8$^+$ T cells. In one animal no CCR6 signal could be detected (Figure 36a).

Generally, CCR6 was not co-expressed with CCR2 in control mice besides one sample which showed 0.9% double positive cells within CD4$^+$ and CD8$^+$ T cells and one sample which showed only 0.4% double positive CD8$^+$ T cells. In contrast to the control group, pulmonary T cells from BLM treated animals clearly contained a population of CCR2$^+$CCR6$^+$ cells. They represented 5.3% (0.0-7.4%) of CD4$^+$ T cells and 4.8% (0.0-10.9%) of CD8$^+$ T cells (Figure 36b). Thus, CCR6 was expressed on 34% (0.0-39%) of CCR2$^+$CD4$^+$ cells and on 20% (0.0-45%) of CD8$^+$ cells (Figure 36c).

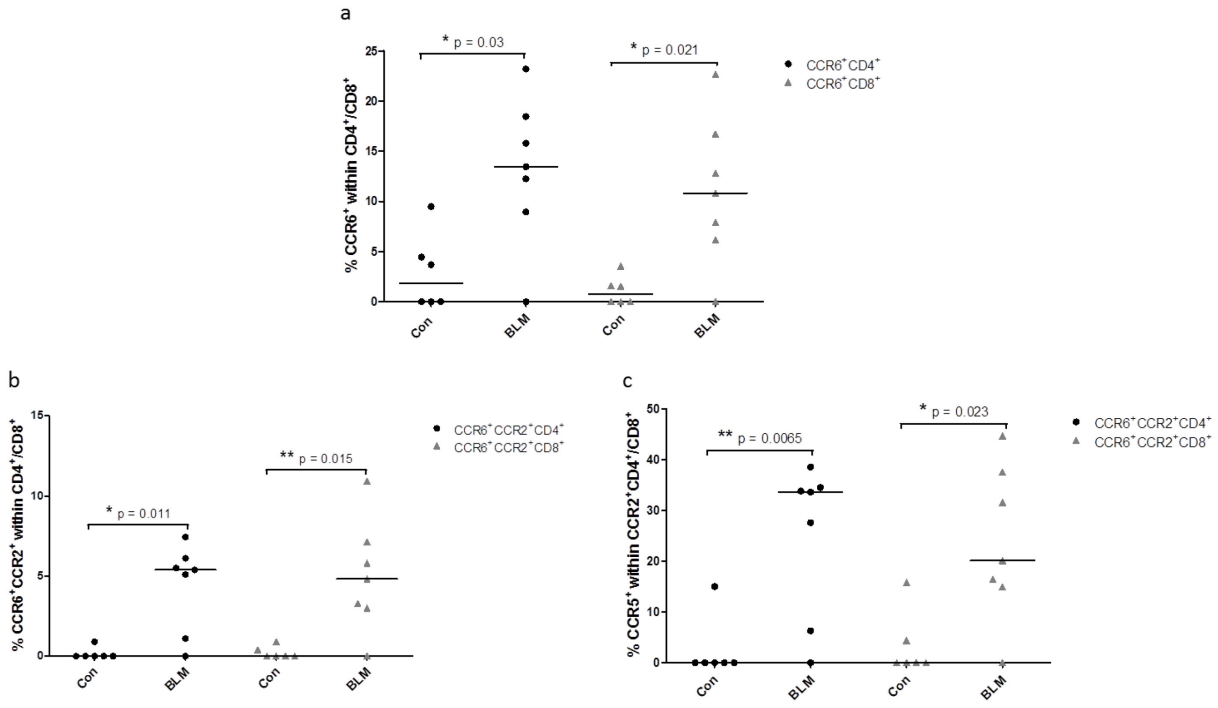



**Figure 36 CCR6+ T cells at day 12 after BLM treatment**; *a) CCR6$^+$T cells within CD4$^+$ or CD8$^+$ T cells; b) CCR6$^+$CCR2$^+$ T cells within CD4$^+$ or CD8$^+$ T cells; c) CCR6$^+$CCR2$^+$ T cells within total CCR2$^+$CD4$^+$ or CD8$^+$ T cells; indicated p values obtained by Mann Whitney U test*

### 5.5.6 **CCR7**

CCR7 was the most expressed chemokine receptor on both, CD4$^+$ and CD8$^+$ T cells. 39% (35-53%) of pulmonary CD4$^+$ T cells and 28% (5.6-36%) of CD8$^+$ T cells from saline treated animals expressed CCR7. In the BLM group 43% (30-47%) of CD4$^+$ T cells and 24% (12-37%) of CD8$^+$ T cells were CCR7$^+$. Thus, there was no significant difference regarding the frequency of CCR7$^+$ cells among the BLM group and controls (Figure 37a).

CCR2$^+$CCR7$^+$ cells amounted to 3.3% (1.0-5.9%) of CD4$^+$ T cells and 2.4% (0.00-4.8%) of CD8$^+$ T cells in control mice. These numbers increased to 5.3% (3.8-13%) of CD4$^+$ T cells and 6.5% (3.2-13.2%) of CD8$^+$ T cells in bleomycin treated mice. This significant increase was most likely due to the general increase of CCR2 expressing cells (Figure 37b), since the percentage of CCR7$^+$ cells within the CCR2$^+$CD4$^+$ and CD8$^+$ T cells did not differ among control and treated mice. The relative content of CCR7$^+$ cells in this population was comparable to the general percentage of CCR7$^+$ cells within total CD4$^+$ and CD8$^+$ T cells (Figure 37c). Thus, CCR2$^+$CCR7$^+$ T cells increased following BLM treatment, but the relation of CCR2$^+$CCR7$^+$ and CCR2$^+$CCR7$^-$ cells was stable.

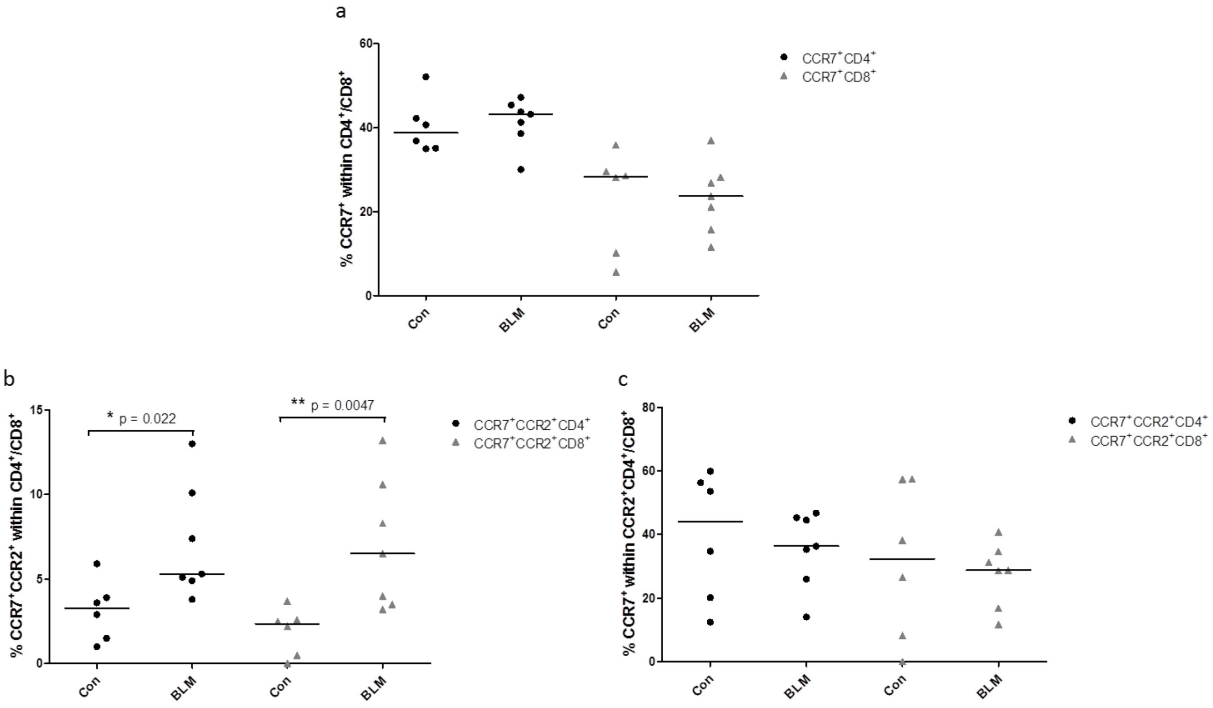



**Figure 37 CCR7$^+$ T cells at day 12 after BLM treatment***; a) CCR7$^+$ T cells within CD4$^+$ or CD8$^+$ T cells; b) CCR7$^+$CCR2$^+$ T cells within CD4$^+$ or CD8$^+$ T cells; c) CCR7$^+$CCR2$^+$ T cells within total CCR2$^+$ CD4$^+$ or CD8$^+$ T cells; indicated p values obtained by Mann Whitney U test*

### 5.5.7 **CCR9**

The expression of CCR9 varied among the animals within one group. On pulmonary CD4$^+$ T cells, half of the animals in the control group (between 3.0 and 5.6%) and two of the animals from the BLM group (3.7% and 5.7%) showed a positive signal for CCR9. For all others, no CCR9 signal was detected.

On CD8$^+$ T cells CCR9 expression could be detected in most of the control samples (median 4.3%, range 0.00-7.2%) and in 3 of the BLM samples (between 1.3% and 10%) (Figure 38a).

A co-expression with CCR2 was not seen in the majority of the samples in which CCR9 expression was observed (Figure 38b+c). Statistically, there was no difference in the relative content of CCR9$^+$ T cells in the BLM and the control group.

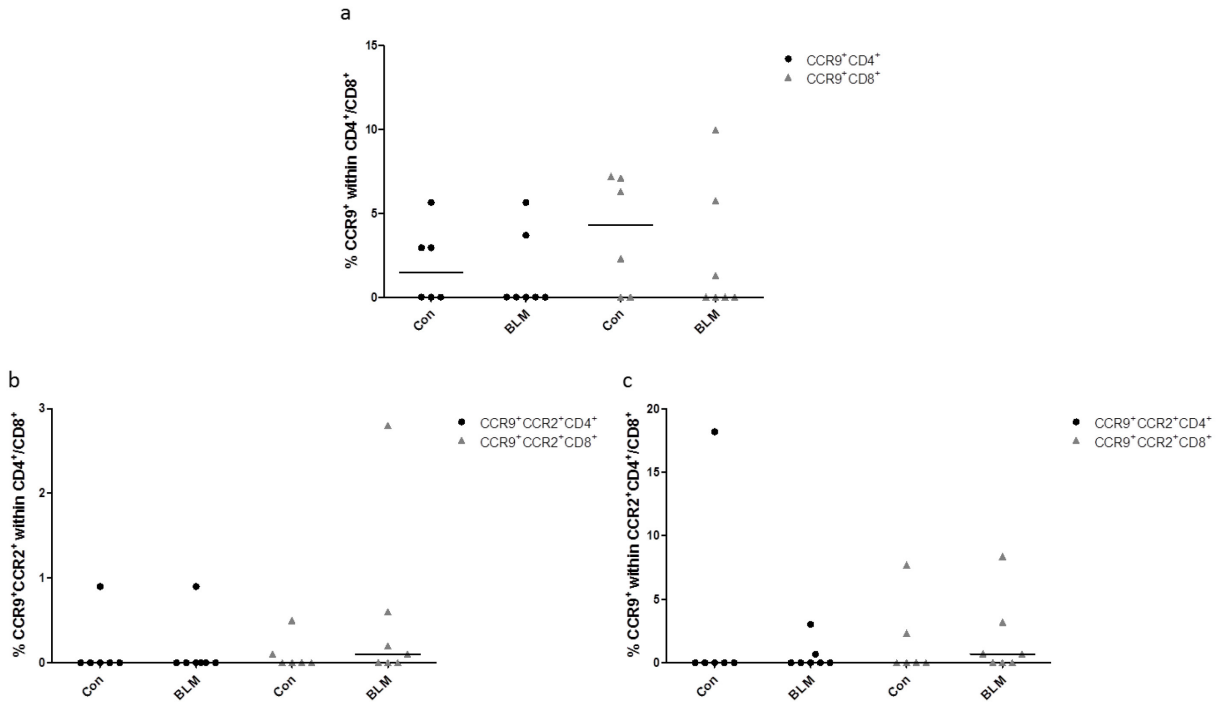



**Figure 38 CCR9$^+$ T cells at day 12 after BLM treatment**; *a) CCR9$^+$T cells within CD4$^+$ or CD8$^+$ T cells; b) CCR9$^+$CCR2$^+$T cells within CD4$^+$ or CD8$^+$ T cells; c) CCR9$^+$CCR2$^+$ T cells within total CCR2$^+$ CD4$^+$ or CD8$^+$ T cells; indicated p values obtained by Mann Whitney U test*

### 5.5.8 **CCR10**

CCR10 was only expressed on CD4$^+$ T cells from control lungs with 1.3% (0.0-2%), but was not co-expressed with CCR2. For all other groups no CCR10 signal was obtained.

### 5.5.9 **CXCR3**

CXCR3 was expressed on 5.0% (2.8-9.7%) of CD4$^+$ T cells from control lungs and on 7.7% (3.8-11%) of CD4$^+$ T cells. However, this increase was not statistically significant. CXCR3$^+$CD8$^+$ T cells represented 1.1% (0.00-4.2%) of pulmonary CD8$^+$ T cells from control animals. In BLM mice, they amounted to 8.4% (0.00-15 %). The difference was also not statistically significant (p=0.07) (Figure 39a).

In control mice, CXCR3 was not co-expressed with CCR2. Only in one sample double positive cells were found for both, CD4$^+$ and CD8$^+$ T cells (1.7% and 0.5%). Another sample showed some co-expression of CXCR3 and CCR2 only on CD4$^+$ T cells (0.7%). In samples from BLM treated animals, the percentage of CXCR3$^+$CCR2$^+$ T cells was higher. 1.3% (0.30-2.2%) of CD4$^+$ T cells were double positive. However, the difference to the control group was not significant (p =0.06). Within CD8$^+$ T cells a co-expression between 0.7% and 2.8% was seen in 4 of 7 samples (Figure 39b).

Calculated to $CCR2^+CD4^+$ T cells, 7.6% (1.9-14.7%) of cells expressed CXCR3, to $CCR2^+CD8^+$ cells this were 3.5% (0.00-11%) (Figure 39c).

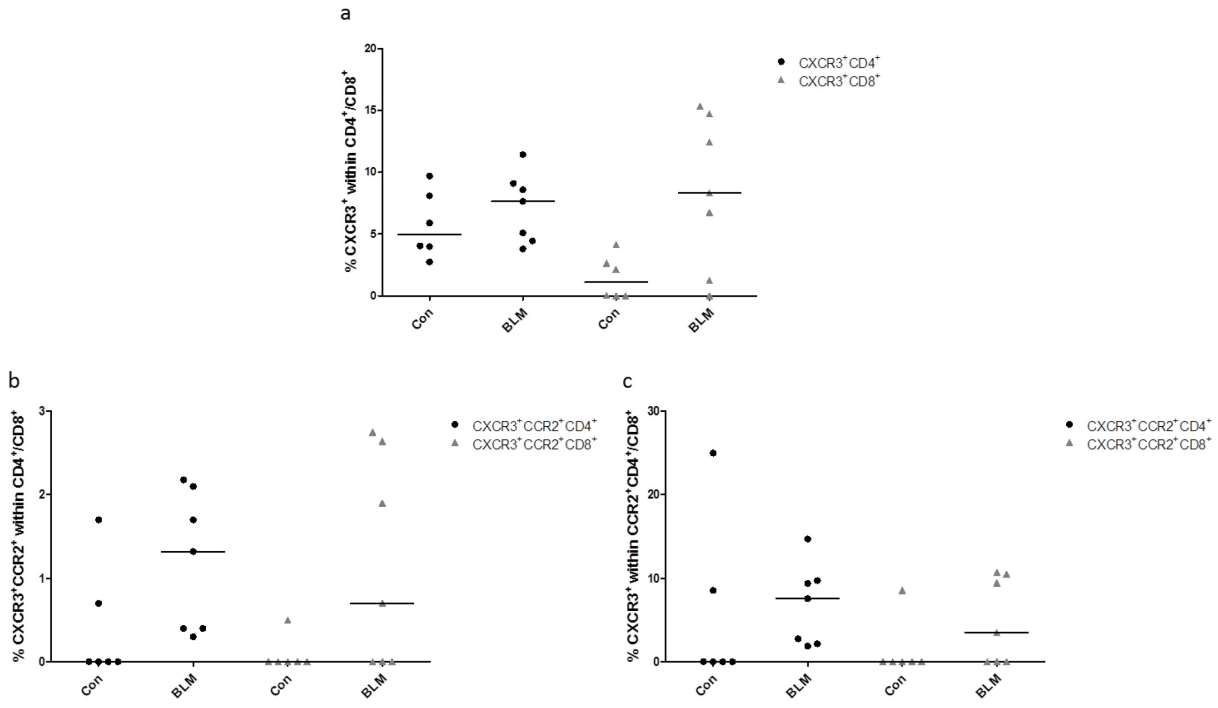



**Figure 39 $CXCR3^+$ T cells at day 12 after BLM treatment**; *a) $CXCR3^+$T cells within $CD4^+$ or $CD8^+$ T cells; b) $CXCR3^+CCR2^+$ T cells within $CD4^+$ or $CD8^+$ T cells; c) $CXCR3^+CCR2^+$ T cells within total $CCR2^+CD4^+$ or $CD8^+$ T cells; indicated p values obtained by Mann Whitney U test*

### 5.5.10 **CXCR4**

4.1% (0.00-8.3%) of $CD4^+$ T cells and 3.7% (0.80-5.4%) of $CD8^+$ T cells from lungs of saline treated animals expressed CXCR4. Within $CD4^+$ T cells from bleomycin treated mice, the fraction of $CXCR4^+$ cells increased significantly to 7.2% (5.5-27%). Within $CD8^+$ T cells from bleomycin treated mice 10% (0.15-16%) of the cells were $CXCR4^+$, but the difference was not significant compared to control mice (Figure 40a).

The co-expression with CCR2 was only weak. No $CXCR4^+CD4^+$ T cells were detected within pulmonary $CD4^+$ T cells from control mice. Within $CD4^+$ T cells from treated animals, double positive cells amounted to 0.7% (0.00-9%). Regarding the $CCR2^+CD4^+$ T cell population, 4.8% (0.00-45%) of the cells expressed CXCR4. Double positive cells represented 0.15% (0.00-1.5%) of $CD8^+$ T cells in control mice and 1.1% (0.00-7.2%) in BLM treated mice. Differences among control group and BLM group were not significant for both cell types (Figure 40b+c).

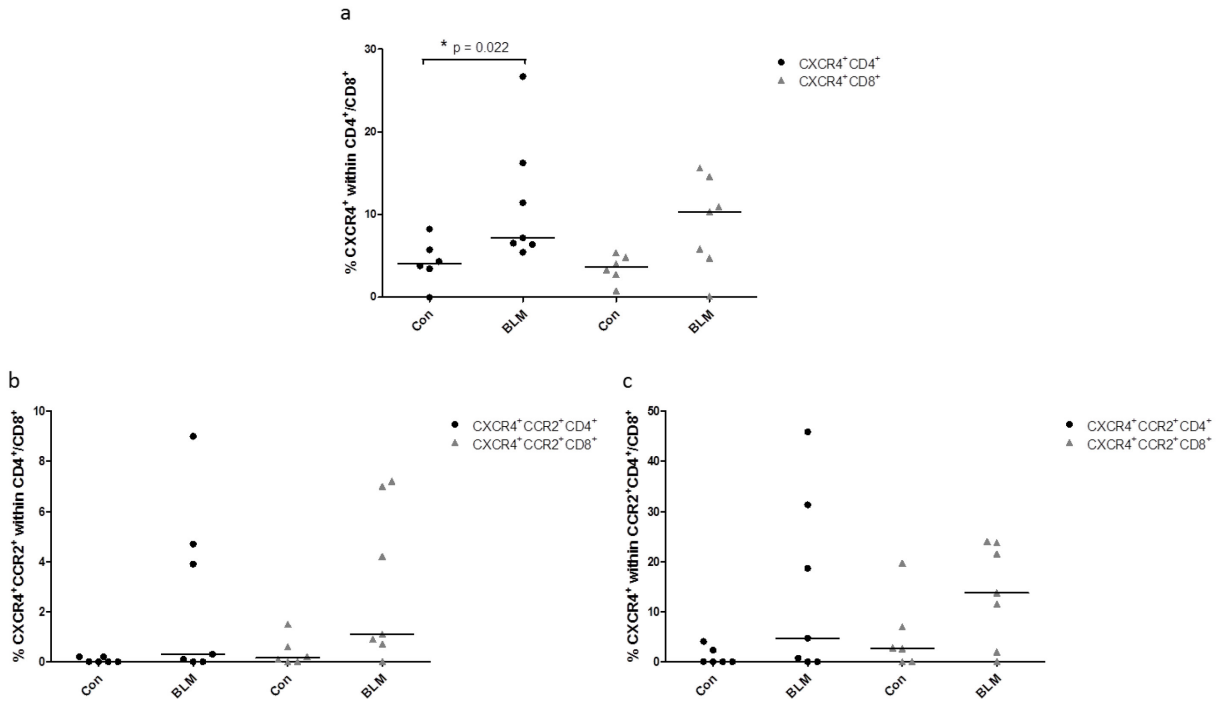



**Figure 40 CXCR4$^+$ T cells at day 12 after BLM treatment**; *a) CXCR4$^+$ T cells within CD4$^+$ or CD8$^+$ T cells; b) CXCR4$^+$CCR2$^+$ T cells within CD4$^+$ or CD8$^+$ T cells; c) CXCR4$^+$CCR2$^+$ T cells within total CCR2$^+$ CD4 or CD8 T cells; indicated p values obtained by Mann Whitney U test*

### 5.5.11 **CXCR5**

CXCR5 was only rarely expressed on cells from control mice. On 0.30% (0.00-1.7%) of CD4$^+$ T cells CXCR5 expression was detected. Within CD8$^+$ T cells 0.70% (0.00-1.6%) expressed CXCR5. In lungs from BLM treated mice, this percentage increased significantly to 6.8% (0.00-10%) within CD4$^+$ T cells and to 11% (2.3-17%) within CD8$^+$ T cells (Figure 41a).

In accordance with the general low expression, a co-expression with CCR2 was not found in control samples. In contrast, double positive cells amounted to 3.2% (0.00-5.7%) of CD4$^+$ T cells and 6.0% (1.0-12%) of CD8$^+$ T cells in samples from BLM treated animals (Figure 41b). Related to CCR2$^+$CD4$^+$ or CCR2$^+$CD8$^+$ T cells, CXCR5$^+$CCR2$^+$ cells represented 12% (0.00-19%) and 20% (7.2-36%) respectively (Figure 41c).

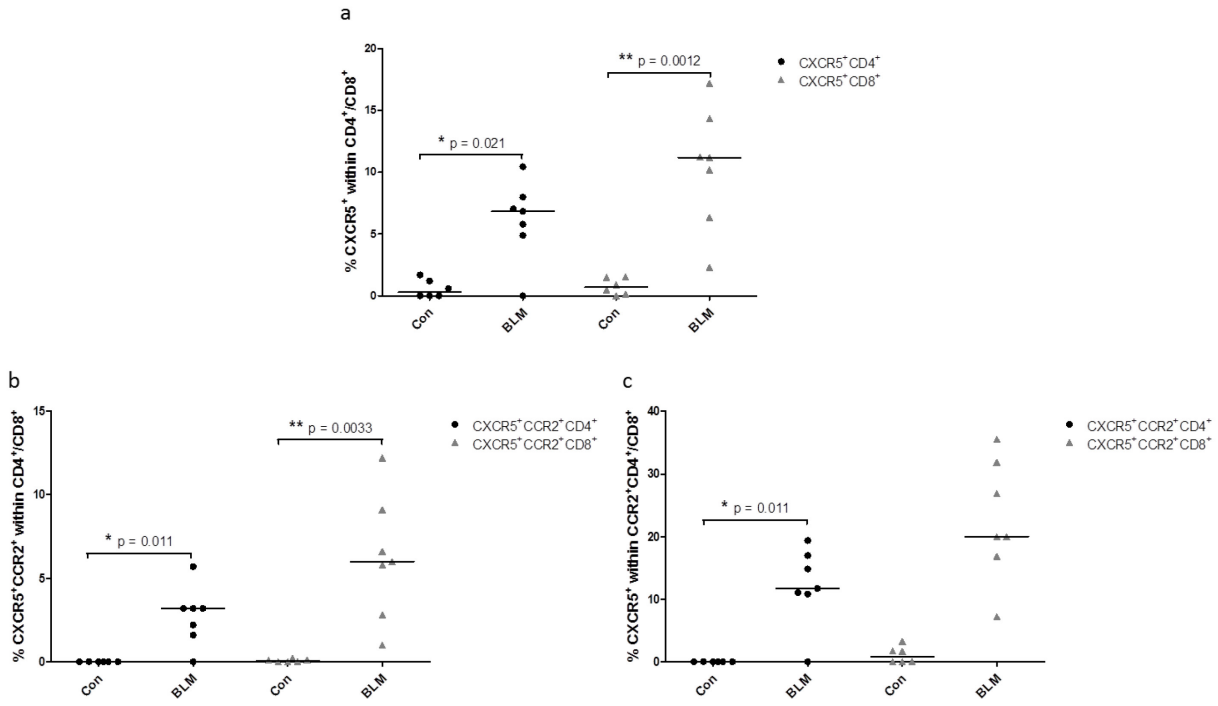



**Figure 41 CXCR5$^+$ T cells at day 12 after BLM treatment**; *a) CXCR5$^+$ T cells within CD4$^+$ or CD8$^+$ T cells; b) CXCR5$^+$CCR2$^+$T cells within CD4$^+$ or CD8$^+$ T cells; c) CXCR5$^+$CCR2$^+$ T cells within total CCR2$^+$ CD4$^+$ or CD8$^+$ T cells; indicated p values obtained by Mann Whitney U test*

### 5.5.12 **CXCR6**

The fraction of CXCR6$^+$ T cells did not differ significantly among the control group and the bleomycin treated group. CXCR6 was expressed on 2.4% (0.00-3.1%) of CD4$^+$ T cells in control samples and on 2.9% (0.25-15%) in samples from the BLM group. On CD8$^+$ T cells it amounted to 1.5 (0.00-1.9%) and 4.9% (0.00-11%) (Figure 42a).

In control samples, no CCR2$^+$CXCR6$^+$ T cells could be detected, besides in one sample which showed 1% of double positive CD8$^+$ T cells. In 3 BLM samples, double positive cells were between 2.2% and 5.9% of CD4$^+$ T cells and between 1.9% and 4.9% of CD8$^+$ T cells (Figure 42b). This amounted to 15 to 31% CCR2$^+$CXCR6$^+$ cells of total CCR2$^+$CD4$^+$ T cells and 11 to 15% of CCR2$^+$ CD8$^+$ T cells, respectively. One sample showed only double positive CD8$^+$ T cells (0.4%), which relates to 4.2% of CCR2$^+$CD8$^+$ T cells. For the other 3 samples no CXCR6$^+$CCR2$^+$ cells were detected (Figure 42c).

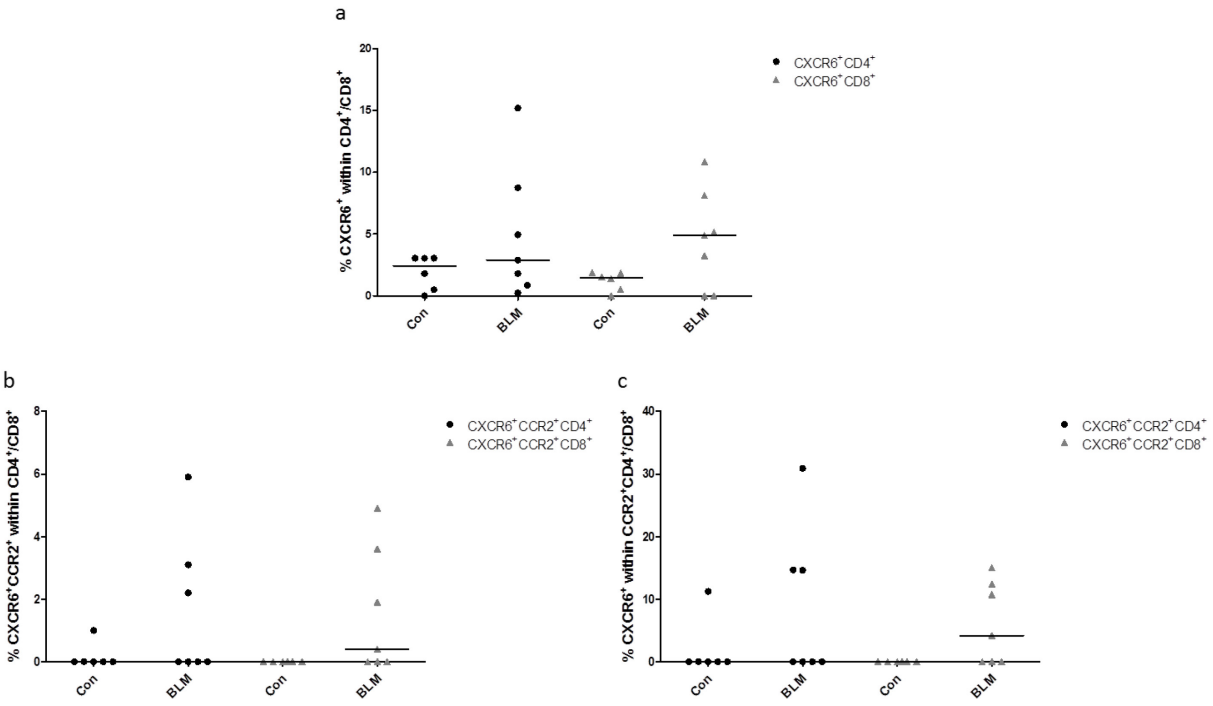



**Figure 42 CXCR6$^+$ T cells at day 12 after BLM treatment**, *a) CXCR6$^+$ T cells within CD4$^+$ or CD8$^+$ T cells; b) CXCR6$^+$CCR2$^+$T cells within CD4$^+$ or CD8$^+$ T cells; c) CXCR6$^+$CC2R$^+$T cells within total CCR2$^+$ CD4$^+$ or CD8$^+$ T cells; indicated p values obtained by Mann Whitney U test*

# 6 Discussion

The pulmonary and systemic T cell responses following intratracheal bleomycin administration were analyzed using flow cytometry. On time points between 3 and 21 days after treatment the frequency of different T cell subtypes and CCR2 expression were investigated in spleen and lung of C57BL/6 mice. While there were no significant changes of the composition of the analysed T cell subtypes in the spleen after bleomycin treatment, the percentages of $T_{em}$, as well as of $CCR2^+$ T cells increased in the lung. The maximum of $CCR2^+CD4^+$ T cell frequency was detected on day 12 after BLM treatment. At this time point co-expression of other chemokine receptors was examined.

## 6.1 Mouse model

For this work, a model of single intratracheal administration of 5U/kg bleomycin to C57BL/6 mice was used.

Bleomycin is not a single substance but a mixture of glycopeptide antibiotics produced by *Streptomyces verticillus,* first described in 1966 (70). It belongs to the group of antineoplastic antibiotics and is used for the therapy of different types of malignancies such as testicular cancer (71) and lymphoma (72). Bleomycin causes DNA single and double strand breaks which stops cell proliferation and results in cell death (73, 74). It shows distinct tissue specificity depending on the content of the so called bleomycin hydrolase, a cytosolic aminopeptidase within the tissue (75). This specificity might be responsible for the major advantage of BLM compared to most other anti-neoplastic drugs: the lack of myelosuppression and thus of immunodeficiency following BLM treatment. On the other hand, this results in BLM accumulation in tissues having a relative lack of bleomycin hydrolase, such as squamous epithelium and the lungs (76). This explains the tropism of the specific adverse effects of bleomycin like cutaneous and mucosal side effects and the development of diffuse interstitial pneumonitis, which occurs in approximately 10% of patients and is the dose limiting factor of bleomycin therapy (77). This pulmonary toxicity was used for induction of pulmonary fibrosis in animals for the investigation of mechanisms leading to interstitial lung diseases (78).

The bleomycin model is a well characterized mouse model for ILD and the most commonly used one. It offers several advantages compared to other models for pulmonary fibrosis: the time for development of the fibrotic response, at least if the bleomycin is applied

intratracheally, is shorter than in most other models like silica or irradiation induced fibrosis. It is easy to perform and does not need special equipment in contrast to irradiation or transgenic models. Another widely used model is the induction of the fibrotic reaction with the flourescent agent FITC. (79, 80)

The FITC model was not suitable for this study since the agent can provide background staining. This would have limited the use of fluorocrome bound antibodies for FACS experiments used in the present study.

However, the bleomycin model, like most animal models, is only partially able to simulate the pathological mechanisms of IPF. Although it represents some main histologic features of UIP, such as a mixed appearance of the lung tissue with fibrotic areas next to others with histological normal tissue and to a limited extend the histologic honeycombing, other typical patterns do not appear. The main histologic difference to the human disease is the location of fibrosis within the lung, which is mostly basal and subpleural in IPF but more peribronchial in the mouse model. Another important discrepancy is the lack of typically organized fibroblast foci in bleomycin induced pulmonary fibrosis. Furthermore, the bleomycin model initially shows a strong inflammatory reaction followed by the initiation of the fibrotic response which is not described for human IPF. (79, 80)

The main point of criticism on the BLM mouse model is that it does not reflect the relentless progression seen in IPF. In contrast, the BLM induced fibrosis resolves 6 week after treatment (81). A clear disadvantage of this model is the considerable mortality during bleomycin treatment.

Susceptibility to bleomycin induced fibrosis is different among mouse straines. BALB/c mice are not susceptible as they express bleomycin hydrolase. For this reason, we decided to use C57BL/6 mice which were previously found to be most susceptible to lung injury through BLM (82, 83).

There is no standard protocol for the performance of this model. The bleomycin can be applied by intravenous, intraperitoneal, subcutanous or intratracheal injection and in different doses. The different aplication routes result in different localizations of the pulmonary lesions and a different timecourse for the development of fibrosis. Frequently used doses for intratracheal administration of bleomycin in mouse models differ between 1 and 5 U/kg body weight (64, 84, 85). In the present study, a dose of 5 U/kg body weight bleomycin was chosen, as published previously (86).

### 6.1.1 Mice with fibrotic disease show body weight loss but no systemic immune response

A loss of body weight is often seen in severe and systemic diseases. It is the result of an increased requirement for energy, especially in diseases with a high proliferation rate of distinct cell types like malignancies or inflammatory diseases.

In accordance with previous publications, a body weight loss was detected in BLM treated mice (84, 87, 88). It showed a maximum at days 6 and 9.

The change in T cell populations in the spleen as secondary lymphoid organ was examined as an indicator of an extra-pulmonary T cell response following intra tracheal BLM instillation. Neither the percentages of total $CD4^+$ and $CD8^+$ T cells nor in the composition of naïve $CD4^+$ T cells, $T_{em,}$ and $T_{cm}$ changed during development of pulmonary fibrosis. About 2.1 % of $CD4^+$ T cells and 1.2 % of $CD8^+$ T cells in the spleen expressed CCR2. This percentage did not change significantly at any time point after bleomycin treatment. Thus, we did not find indications for a systemic T cell response following intra tracheal bleomycin administration.

## 6.2 T-cell kinetics in BAL and lung tissue during time course

### 6.2.1 $CD4^+$ and $CD8^+$ T cells

The analysis of BAL is the standard method to evaluate cell and cytokine alterations in human pulmonary diseases (89, 90). The method is also frequently used in animal models for lung disorders, since this offers the possibility to compare the results with those in human disease in the same medium.

Under physiologic conditions, human BALF contains about 85% alveolar macrophages and 10% lymphocytes (91). As expected, very few lymphocytes were detected in saline treated control mice. Following treatment with bleomycin, the relative content of T cells increased, as well as total cell numbers. This is in accordance with previous publications, which found increased numbers of total cells and lymphocytes to a comparable extend by differential count of BAL cells (88, 92, 93).

Of note, in BALF from BLM treated mice, levels of both, $CD4^+$ and $CD8^+$ T cells, were elevated, but in lung tissue the percentage of $CD4^+$ T cells showed only a slight increase and the percentage of $CD8^+$ T cells even decreased compared to control mice up to day 15.

A previous study found a stronger increase of $CD4^+$ T cells and also an increase of $CD8^+$ T cells at days 3; 7 and 14 compared to control mice, although the percentage of $CD8^+$ T cells on day 14 also tended to be decreased compared to day 3 or 7 (94). However, the results are

not fully comparable, as they calculated T cell percentages from total cells of a lung single cell suspension, whereas in the present study dead cells were excluded from the analysis. Furthermore, another report found stable percentages of $CD4^+$ T cells in lungs of BLM treated mice during the disease course (95).

Taken together, the results confirm an inflammatory reaction following BLM treatment. The somewhat contrary T cell kinetics in BAL and lung tissue might be due to a T cell migration to the airways or differential recruitment of T cells to the airways and the interstitial space. However, further studies are necessary to confirm and to explain this phenomenon.

### 6.2.2 **Increase of effector memory T cells following bleomycin treatment in lung tissue**

More important than the percentage of total T cells might be the content of different lymphocyte subtypes, as the kinetic of their composition during the time course allows drawing conclusions about the activation status, and thus indirectly about the role of the cells.

Following the recognition of an antigen, naïve T cells expand and differentiate into effector T cells. Within one week, the majority of these effector cells will undergo apoptosis but a minor population will get further differentiated into memory cells. The memory T cell pool contains at least two subtypes; the central memory T cells ($T_{cm}$) and the effector memory T cells. $T_{cm}$ are mostly found in secondary lymphoid organs. $T_{em}$ emigrate to peripheral tissues for rapid response following recognition of a known antigen. During this development, T cells change the expression pattern of their surface molecules. (96-98)

Naïve T cells express peripheral lymph node homing receptors like CD62L and CCR7, but do not express activation markers like CD44 or CD45RO. Following activation through an antigen, naïve T cells down regulate CD62L and up regulate CD44 (99). Expression of CD44, which is considered as memory or activation marker, can be used to separate naïve T cells from memory cells (100, 101). In addition, central memory T cells express CD62L and CCR7 also found on naïve T cells (102). Effector memory T cells lack CD62L and CCR7, but gain expression of tissue specific homing receptors like CCR5 (103).

In the present study, the kinetics of these CD4 T cell subtypes were examined as defined by the expression of the adhesion molecules CD62L and CD44.

The main cell type in lung and spleen of control mice were $CD62L^{hi}$ $CD44^{low}$ $CD4^+$ T cells, and thus considered as naïve T cells. With a median of 75% versus 81% the percentage of naïve T

cells was slightly lower in lung than in spleen of saline treated controls. Following bleomycin treatment $CD62L^{hi}CD44^{low}CD4^{+}$ $T_{naïve}$ cells decreased while $CD62L^{low}CD44^{hi}$ $T_{em}$ cells increased from 16% to a maximum of 31%. This might indicate either an activation of resident lung T cells or a recruitment of activated cells from the circulation to the lung as a response to the bleomycin induced lung injury.

Similar results for $CD62L^{hi}CD4^{+}$ T cells and $CD44^{hi}$ $CD4^{+}$ T cells in normal lung tissue were found in a study looking for migration of naïve T cells into various organs under steady state conditions in BALB/c mice (104). Another publication reported a population of about 70% $CD3^{+}CD44^{+}$ T cells in lungs of bleomycin treated animals, which did not change significantly between day 3 and 14 following BLM treatment. However, in controls the $CD3^{+}CD44^{+}$ T cell population was only 40% (94). Further, it is difficult to compare this study with the present results as there it is referred to total $CD3^{+}$ cells, not to $CD4^{+}$ T cells.

Nevertheless, these results indicate that pulmonary T lymphocytes are activated after BLM application. This suggests that T cells might contribute to the initial pathogenesis of BLM induced pulmonary fibrosis.

### 6.2.3 **$CCR2^{+}CD4^{+}$ T cells are increased and show $CD62L^{low}CD44^{hi}$ phenotype**

The percentage of $CCR2^{+}$ $CD4^{+}$ and $CD8^{+}$ T cells clearly increased during the first two weeks following BLM treatment with a maximum at day 12 and decreased again at the later time points paralleling the kinetic of the $T_{em}$ subpopulation.

Increased $CCR2^{+}$ T cells were also found in BAL from paediatric ILD patients (68). In contrast, in BAL of Sarcoidosis patients, the CCR2 expressing population among $CD4^{+}$ T cells was decreased (105). Furthermore, CCL2, the major ligand of CCR2, was increased in BAL of patients with different ILD, with BAL from IPF patients showing the highest levels (106-108).

One study found that mice with artificial pulmonary overexpression of CCL2 were protected from mortality of bleomycin induced lung injury, while CCR2 deficiency abolished this protective effect. Surprisingly, they found increased numbers of lymphocytes and mononuclear cells in BAL of transgenic mice compared to WT mice (65).

This observation contrasts previous publications, which claimed that CCR2 deficiency attenuates pulmonary fibrosis (64, 66, 67).

In murine peripheral blood, CCR2 expression was found on the $CD44^{+}$ T cell subpopulation but was nearly absent from $CD44^{-}$ T cells (62). Similar observations were made in human

peripheral blood, where CCR2 was predominantly expressed on CD45 $RO^+$ effector memory cells (109).

This differential expression pattern was also observed in the present study. The majority of the $CCR2^+CD4^+$ T cells exhibited $CD62L^{low}CD44^{hi}$ phenotype, thus belonged to the $T_{em}$ subtype. With a percentage of 23% in control mice and 34% at day 12, $CCR2^+$ cells represented a considerable fraction of pulmonary $T_{em}$ cells. In spleen, the $T_{em}$ subpopulation contained only 10 to 15% $CCR2^+$ cells. In contrast CCR2 was expressed only in a minor population of $CD62L^{hi}CD44^{low}$ $T_{naive}$ cells.

The increase of $CCR2^+$ $CD4^+$ T cells and their affiliation to the $T_{em}$ subtype indicates that they are a distinct population of activated cells. Although further investigation is needed to evaluate the specific role of these cells, it is likely that they play a role in the pulmonary immune response and the initiation of fibrogenesis in BLM induced pulmonary fibrosis in mice.

## 6.3 **Chemokine receptors**

To obtain insight in the potential migratory capacity of the T cells we performed a comprehensive analysis of their chemokine receptor expression. For some chemokine receptors, antibodies for the flow cytometric analysis were not commercially available at the time point of this investigation. Therefore, some chemokine receptors like CCR1 and CXCR2, which were previously shown to play a role in pulmonary fibrosis, could not be taken into consideration (110, 111).

### 6.3.1 **CCR6**

The highest co-expression with CCR2 was observed for CCR7 and CCR6, whereas CCR7 was expressed on a similar percentage of T cells in control and BLM treated mice CCR6 was nearly absent on $CCR2^+$ T cells of control animals but expressed on a median of 34 % $CCR2^+CD4^+$ T cells and of 20% $CCR2^+CD8^+$ T cells from treated mice. This was about two times higher than the percentage of T cells expressing CCR6 within total $CD4^+$ and $CD8^+$ T cells.

CCR6 is frequently expressed on Th17 T cells (112, 113), an effector T cell subset that was shown to play a role in autoimmune diseases like rheumatoid arthritis or hashimoto's thyreoiditis (114, 115). Furthermore, CCR6 expression was also found on a $CD25^+CD4^+$ T cell subpopulation. However, it was not restricted to these regulatory T cells. These $CCR6^+CD4^+$ cells expressed the memory marker CD44 and most of them presented a $CD62L^{low}$ phenotype (116). Thus, like $CCR2^+$ $CD4^+$ T cells, they present a $T_{em}$ phenotype.

Unlike most other chemokine receptors, only one chemokine, CCL20, is known to bind to CCR6 (117). CCL20 was found to be produced by human pulmonary epithelial cells *in vitro* (118). It mediated migration of $CD4^+$ T cells (119), as well as of blood derived dendritic cells *in vitro* (118). There are several reports about specific functions of $CCR6^+$ T cells in the lung. $CCR6^+$ T cells were highly enriched in BAL of asthmatic patients compared to peripheral blood (120).

One study investigated the CCR6 expression on T cells from atopic patients with active allergic rhinitis and non-atopic healthy controls. $CCR6^+$ T cells were enriched among T cells derived from nasal mucosa, lung, skin and BAL compared to peripheral blood derived T cells. There was no difference between atopic patients and the control group. Therefore, they suggested a role of CCR6 in the recruitment of T cells to the airways under steady state conditions. (121)

In a COPD mouse model, $CCR6^+$ lymphocytes and levels of other CCR6 expressing cells were increased following cigarette smoke exposure for four weeks. In turn, CCR6 deficient mice showed less increase of dendritic cells, neutrophils and lymphocytes in BAL compared to wild type mice (122).

In human sarcoidosis, CCR6 expression on $CD4^+$ T cells was increased in BAL from patients with active disease, whereas $CD8^+$ T cells were $CCR6^-$ (119). Another study investigated chemokine production and chemokine receptor expression on lymphocytes from blood of patients suffering from systemic sclerosis. The frequency of $CCR6^+CCR10^-CD4^+$ T cells correlated with IL-17 and IL-22 producing T cells. Patients with associated ILD presented higher IL17 and IL-22 producing cells compared to patients without ILD, which gives evidence for a role of these cells in scleroderma associated pulmonary fibrosis (123).

An immunohistological study found higher CCR6 in lungs of IPF patients compared to control lungs. However, it was seen on epithelial sites but not on lymphocytes, this might indicate a role of CCR6 in idiopathic pulmonary fibrosis (124).

As described above, there is evidence for a role of the CCR6/CCL20 axis in the lymphocyte recruitment to the airways in different diseases as well as under physiological conditions.

CCR6 was clearly expressed on a higher percentage of $CCR2^+$ T cells than on total $CD4^+$ or $CD8^+$ T cells. This could indicate a preferential recruitment of $CCR2^+$ T cells to the lung in bleomycin induced fibrosis. The high co-expression of CCR6 and CCR2 might also be a hint towards an enhanced Th17 polarization of $CCR2^+CD4^+$ T cells. The presence of CCR6 on $CD25^+$ regulatory T cells, mentioned above, is also in accordance with the hypothesis of regulatory functions of $CCR2^+$ T cells. However, this observation needs further functional investigation of these cell populations such as the analysis of their cytokine production.

### 6.3.2 **CCR7**

CCR7 is expressed on different subsets of lymphocytes and mature dendritic cells. It is necessary for leukocytes migration to secondary lymphoid organs through high endothelial venules. Thus, its ligands CCL19 and CCL21 are preferentially expressed in lymphoid tissue, but also on gastrointestinal sites, kidneys and lungs (125).

CCR7 deficient mice accumulated T cells in the periphery; in consequence they were reduced in the secondary lymphoid tissues. Further, CCR7 deficiency caused impaired lymph node

architecture, whereas formation of tertiary lymphoid tissue in the intestinal tract and the airways was still possible (126).

In human blood CCR7 was expressed on nearly all $CD62L^+CD27^+CD4^+$ T cells, representing the naïve and the central memory T cell population. However, CCR7 expression itself does not define a distinct subset as it is also expressed to a lower extend on cell populations lacking CD62L, CD27 or both of them. On $CD8^+$ T cells, CCR7 was found to be expressed on all naïve cells defined by the expression of CD45RA and CD27, to a lower amount on memory cells ($CD45RA^-CD27^+$) and nearly absent from effector cells ($CD45RA^+CD27^-$) (127).

Th1 and Th2 cell lines up regulated CCR7 following in vitro stimulation with CD3 (103), whereas $CD25^+CD4^+$ $T_{reg}$ cells from human peripheral blood down regulated CCR7 and up regulated CCR4 upon allergen stimulation (128).

There are some reports about an involvement of CCR7 in the context of pulmonary fibrosis. CCR7 was overexpressed in fibrotic regions of lung biopsies from patients with UIP compared to NSIP and RBILD. However, CCR7 expression determined by immunohistology was found in all three groups, but not in normal tissue from cancer patients. CCR7 was partly co-localized with CD45, thus expressed on leukocytes and not with aSMA, indicating no CCR7 expression on fibroblasts. (129)

Bleomycin induced fibrosis was attenuated in CCR7 deficient mice. These mice showed organized formation of BALT, which was absent in wild type mice, and a specific accumulation of $CD4^+CD25^{hi}FoxP3^+$ $T_{reg}$ cells. (95)

The proportion of $CCR7^+$ T cells did not change following BLM treatment, neither to total $CD4^+$ or $CD8^+$ T cells, nor to $CCR2^+CD4^+$ or $CCR2^+CD8^+$ T cells. Clearly, in this study CCR7 expression was not restricted to the $T_{naive}$ subpopulation, as it was expressed on a high percentage of $CCR2^+CD4^+$ T cells which exhibited predominantly $T_{em}$ phenotype.

When taking CCR7 as surrogate parameter for the lymph node homing capacity, it suggests that a considerable population of pulmonary T cells keep the capability to enter the lymph node even if they change the phenotype towards $T_{em}$ cells following BLM treatment. This might also demonstrate that the borders between the different T cell subsets are not completely fixed, but there exist overlapping phenotypes.

### 6.3.3 **CCR3 and CCR4**

CCR3 was found mainly on eosinophils as well as on basophils and T cells. It has several ligands, the most well-known being eotaxin 1-3 (CCL11, 24, 26) but also others like MCP 2-4 (CCL7, 8, 13) and RANTES (CCL5) (130).

CCR4 is expressed on T cells, NK cells and basophils. Several chemokines bind to CCR4 like TARC, MDC and MIP-1β. CCR3 and CCR4 are considered to be preferentially expressed on Th2 lymphocytes (131, 132).

In the lung, CCR3 and CCR4 were mainly investigated in the context of the classical Th2 associated disease asthma. They were both predominately, but not exclusively, expressed on IL-4 producing cells in BAL and blood from asthmatic patients, as well as from healthy controls (133). CCR4, but not CCR3 was expressed on T cells from transbronchial biopsies of asthmatic patients, and allergen challenged asthmatics had significantly higher $CCR4^+$ $CD4^+$ T cells (134).

Furthermore, CCR3 might play a role in the pulmonary response to chronic exposure to irritants, since $CCR3^+CD8^+$ T cells as well as total $CCR3^+$ T cell population was increased in BAL of COPD patients and smokers compared to non-smokers (135).

There are several reports about an involvement of CCR3, CCR4 and their ligands in extra-pulmonary and pulmonary fibrotic diseases. CCR3 ligands, CCL11 and CCL5 were increased in patients with idiopathic retroperitoneal fibrosis and various CCR3 expressing cell types including lymphocytes were found in the fibrotic lesions (136). In a study with patients suffering from sarcoidosis or exogen allergic alveolitis (EAA), CCR3 expression on BAL $CD4^+$ T cells correlated with HRCT score and reduced $TL_{co}$ in the EAA group which showed partly histological UIP pattern (137). $CCR4^+CD4^+$ T cells were increased in BAL of children with ILD compared to the control group (68). Furthermore, IPF patients showed higher $CCR4^+CD4^+$ T cells in BAL compared to patients with other ILD and healthy controls. In these patients the proportion of $CCR4^+CD4^+$ T cells was higher in BAL than in blood (138). The mRNA levels of the CCR4 ligands CCL17 and CCL22 were increased in lung tissue from bleomycin treated mice at time points up to 20 days following treatment. Neutralization of CCL17 attenuated the fibrotic response (139). Hence, especially CCR4 seems to have an active role in experimental as well as in human pulmonary fibrosis.

Our results showed a significant increase of CCR3 and CCR4 expressing T cells within total $CD4^+$ T cells as well as within the $CCR2^+CD4^+$ T cell subpopulation on day 12 after BLM

treatment. This observation might indicate an enhanced Th2 polarization of $CD4^+$ T cells in bleomycin induced pulmonary fibrosis. Of note, CCR4 expression was absent on pulmonary $CCR2^+$ T cells from saline treated mice, but was found following bleomycin treatment. Thus, $CCR2^+$ T cells seem to selectively express CCR4 upon activation through the BLM induced lung injury. Notably, in BLM treated mice, the percentage of CCR3 and CCR4 expressing cells was higher within the population of $CCR2^+CD4^+$ T cells than within total $CD4^+$ T cells. This preferential expression of the Th2 associated markers on $CCR2^+$ T cells might be an indication for specific functions of these cells in the T cell response to bleomycin treatment. However, the Th2 phenotype of these cells still needs to be confirmed by assessment of their cytokine production.

### 6.3.4 **CXCR5**

$CXCR5^+CD4^+$ T cells were suggested to define a distinct subset of B helper T cells which are found in the B cell zone of lymphoid tissue germinal centres, called follicular helper T cells ($T_{FH}$) (140, 141). This T cell subset was recently described, and their categorization within the different T cell populations is not fully clarified yet (142).

The main function attributed to $CXCR5^+$ T cells is an evident role for the migration of T cells to the B cell zone and in the regulation of the antibody production by B cells (143, 144). So called circulating $T_{FH}$ cells were found in human chronic hepatitis virus B and C infection (145, 146). $CXCR5^+CD4^+$ T cells were also increased in liver and spleen of HBV transgenic mice (145). These cells co-expressed CCR7 and CD62L in contrast to their relatives in lymphoid tissue and induced Ig production from B cells (144, 147). A study using CXCR5 deficient mice showed that CXCR5 was needed for the formation of tertiary lymphoid tissue (tLT) during *H. pylori* infection and CXCR5 deficiency resulted in impaired antibody response to *H pylori* (148).

These circulating $T_{FH}$ cells were also shown to be increased in peripheral blood of patients with distinct autoimmune diseases like severe systemic lupus erythematodes (149) and primary Sjögren's Syndrome (150). In patients with primary Sjögren's Syndrome, a subpopulation of CCR6 expressing Th17 like $T_{FH}$ cells was increased (150). However, in the present study co-expression of CCR6 and CXCR5 was not assessed, expression of both receptors increased after BLM treatment. Furthermore, both receptors were expressed on pulmonary $CCR2^+$ T cells from BLM treated mice, but not from control mice.

In human lung tissue samples of patients suffering from idiopathic pulmonary hypertension, $CXCR5^+CD4^+$ T cells were found in peri-arterial tLT, and the level of $CXCR5^+CD4^+$ T cells was decreased in peripheral blood of these patients (151). Thus, there are hints for a role of these cells in pulmonary diseases which offer approaches for further investigation of their functions.

Within pulmonary $CD8^+$ T cells of BLM treated mice, CXCR5 expressing cells were even more frequent as within $CD4^+$ T cells. $CXCR5^+CD8^+$ T cells are not very well described, yet. These cells were found in the B cells zone of tonsil lymphoid tissue and, to a lower extend in peripheral blood of patients undergoing routine tonsillectomy. They expressed activation markers like CD45RO and did not express CCR7. Consequently, they were classified as effector memory cells. Furthermore, tonsil $CXCR5^+CD8^+$ T cells co-expressed CCR5 (152, 153). On the other hand, CXCR5 and CCR7 were upregulated in cell lines following TCR stimulation in vitro (103).

### 6.3.5 **CCR5**

CCR5 is commonly considered as a Th1 related chemokine receptor together with CXCR3 (132). However, there is growing evidence that the expression of these chemokine receptors is not strictly limited to Th1 or Th2 cells *in vivo* (154).

In humans, CCR2 is strongly co-expressed with CCR5 (109), and the two receptors were shown to form heterodimers upon activation (155). CCR5 expression on peripheral blood T cells was shown to be similar in mice and humans. However, its expression differed on other cell types. It was more expressed on $CD8^+$ T cells than on $CD4^+$ T cells in peripheral blood (56).

CCR5 is well known for its role in HIV infection (156-158), but it also played a role in several inflammatory diseases such as multiple sclerosis (61). CCR5 expression on $CD8^+$ T cells from resected human lung tissue was shown to correlate with disease severity of COPD (159).

CCR5 expressing $CD4^+$ and $CD8^+$ T cells were highly enriched in BAL of asthmatic patients compared to peripheral blood (120). In a mouse model of ovalbumin induced asthma, CCR5 deficiency attenuated airway hyper responsiveness and goblet cell metaplasia (160). In a mouse model of viral challenge, $CCR5^+CD8^+$ T cells were rapidly recruited to the lung airways (161). Mice deficient for CCR5 or CCL3, a ligand for CCR5, showed attenuated pulmonary

fibrosis trough impairment of fibrocyte accumulation and macrophage migration (162). However, this effect could not be shown in another publication (66).

CCR5 expression was virtually absent from pulmonary $CD4^+$ T cells from control mice and bleomycin treated ones. On $CD8^+$ T cells CCR5 expression was also not detected in control lungs but increased after bleomycin instillation. On $CD8^+$ T cells CCR5 showed also a co-expression with CCR2 to a variable extend. The lack of CCR5 expression on pulmonary $CD4^+$ T cells from treated mice might vote against a Th1 response to the bleomycin treatment.

### 6.3.6 **CXCR4**

On human T cells, CXCR4 is expressed on naïve populations (132, 163). In mice, no preferential expression on subtypes was found and expression on peripheral blood lymphocytes was evidently lower than in humans. CXCR4 on murine cells increased following stimulation with phytohaemagglutinin. On human cells, it decreased first, and then increased from day 2 on. CXCR4 expression on $CD8^+$ T cells but not on $CD4^+$ T cells increased in secondary lymphoid tissue following antigen challenge. (164)

CXCR4, like CCR5, was shown to act as co-receptor of HIV-1 entrance to lymphocytes (165).

A high number of CXCR4 expressing T cells was found in human renal allograft rejection (166). This implicates a possible role in non-infectious inflammatory diseases.

The level of CXCR4 ligand CXCL12 (SDF-1) was increased in murine lungs following BLM administration during the first week after treatment whereas CXCR4 expression was increased from day 3 to 21. Blockade of CXCR4 resulted in lower collagen deposition in the lungs of bleomycin treated mice (167, 168). However, this effect was mainly attributed to the impairment of the recruitment of bone marrow derived mesenchymal stem cells (BMDMSC), so called fibrocytes, which express CXCR4 and are attracted to the lung following BLM treatment and may differentiate into fibroblasts (35, 169).

CXCL12 gene expression was upregulated in lungs of patients suffering from IIP. However, CXCR4 gene expression did not differ significantly among diseased and healthy patients. Immunohistological studies suggested macrophages as the main source of CXCL12 in IIP. Furthermore, in $CXCR4^{+/-}$ mice collagen content was decreased, although these mice showed higher contents of lymphocyte in BAL (170).

About the role of T cells expressing CXCR4 in the context of chronic lung diseases, there is not much known. In fact, the levels of $CXCR4^+CD4^+$ T cells were increased in BAL of patients

with chronic hypersensitivity pneumonitis when comparing patients with subacute hypersensitivity pneumonitis and healthy controls. (171).

The percentage of $CXCR4^+$ cells increased within $CD4^+$ T cells following BLM treatment. Within $CD8^+$ T cells, the increase was not statistical significant. Co expression with CCR2 was stronger on $CD8^+$ T cells. However, some samples also showed very high co-expression on $CD4^+$ T cells. The significance of this increase is difficult to evaluate as there is not much known about the function of $CXCR4^+$ T cells and, as mentioned above, evident differences exist among the species.

### 6.3.7 **CCR9 and CCR10**

CCR9 was only expressed on a minor population of T cells and was not co-expressed with CCR2. Furthermore, no difference in CCR9 percentages could be observed between BLM treated mice and control mice. These findings are in line with the attributed function of CCR9 as a specific homing receptor to intestinal sites playing a role for example in inflammatory bowel diseases (172-174). CCR9 was found to be important for the migration of $T_{reg}$ to the intestine in mice under healthy conditions (175). Furthermore, it played a role in T-cell development in the thymus (176).

In the lung, no expression was observed on human lung homogenates from non-asthmatic and asthmatic donors (177).

In contrast, CCR10 plays a role in migration of distinct lymphocytes to the skin (178), and through this, it is involved in contact hypersensitivity (179).

In a study investigating the role of regulator of g protein signalling 16 (RGS16) in T cells trafficking, CCR10 expressing T cells were found in the lungs of $Rgs16^{-/-}$ mice following challenge with *S. mansoni*, but only to a minor extend in wild type mice (180). This finding might suggest a specific role of CCR10 in lymphocyte recruitment to the lung during infection.

However, in the present study, CCR10 was nearly absent on lung lymphocytes from saline and BLM treated mice, voting against a specific role of $CCR10^+$ T cells in bleomycin induced pulmonary fibrosis.

### 6.3.8 **CXCR6**

CXCR6 was described as chemokine receptor responsible for lymphocytes homing to the lung as well as their retention in the lung. It was preferentially expressed on Th1 effector/memory T cells (181). Its ligand CXCL16 was constitutively expressed on human bronchial epithelial cells (182).

Antigen specific $CD8^+$ or $CD4^+$ T cells expressing CXCR6 increased in BAL and lung of mice immunized intranasally with recombinant tuberculosis antigen expressing adenovirus, or recombinant antigen respectively, but not in mice immunized subcutaneously. Mice receiving antigen and CXCL16 before infection with *M. tuberculosis*, and thus presenting higher $CXCR6^+CD8^+$ T cell numbers, could significantly decrease the pathogen burden. (183)

CXCR6 expression on $CD8^+$ T cells from lung tissue of COPD patients correlated with the disease severity. However, levels of CXCL16 were equally high in the different stages (159).

$CXCR6^+$ T cells were enriched in human BAL from patients with sarcoidosis compared to peripheral blood. Furthermore, the count of $CXCR6^+$ T cells in BAL was higher in ILD and Sarcoidosis patients than in healthy control patients and asthmatic patients (184). In lung filtrates CXCR6 was highly expressed on a T-cell subset expressing CD103, a late activation marker, but not on early activated $CD69^-$ T cells (185). This indicated an involvement of $CXCR6^+$ T cells in different interstitial lung diseases.

Despite these reports about specific functions of $CXCR6^+$ T cells in the lung the current results did not show significant differences in the percentage of pulmonary CXCR6 expressing T cells among saline and BLM treated mice. However, especially among the samples of treated mice the proportion of $CXCR6^+CD4^+$ T cells was not homogenous. In some samples $CXCR6^+$ T cells represented a considerable population; in others no CXCR6 expression could be detected. In the samples which showed CXCR6 expression, it was also frequently co-expressed with CCR2. For a valid statement about these changes a higher number of samples would probably be necessary, but the differences in the CXCR6 expression among the samples could be an indicator of the different capability of the animals to react to the BLM induced lung injury.

### 6.3.9 **CXCR3**

CXCR3 was found to be preferentially expressed on Th1 polarized T cells (132, 181).

On murine $CD8^+$ T cells, it was expressed on most activated cells (186). In one study on murine *B. bronchiseptica* infection, concentrations of CXCR3 ligands I-TAG (CXCL11), MIC (CXCL9), and IP-10 (CXCL10) were increased and resulted in leucocyte migration to the lung (187). A study examining chemokine receptor expression in BAL and peripheral blood of asthmatic patients found higher CXCR3 expression on BAL cells than on cells from peripheral blood. The concentration of CXCR3 ligands increased following segmental allergen challenge, while CXCR3 surface expression decreased most likely through receptor internalization (120). CXCR3 deficient mice showed increased mortality and more severe fibrotic reaction following BLM treatment. In the same study, lower lymphocyte numbers were detected in CXCR3 deficient animals 7 days after BLM treatment, but no difference for other inflammatory cells (85). This also gives hints to a role of CXCR3 in lymphocyte recruitment to the lung airways.

However, in BAL of patients with IPF, lower expression of CXCR3 on $CD4^+$ T cells was found compared to non-IPF, sarcoidosis, and control patients and higher CXCR3 expression on $CD4^+$ T cells in peripheral blood. Notably, they found higher CXCR3 expression on BAL lymphocytes when patients were treated with glucocorticoids. Lower CXCR3 expression correlated with a decrease of total lung capacity and vital capacity as well as an increase of in alveolar-arterial $pO_2$ difference 6 to 12 months later. (138)

For CXCR3 no difference among control and BLM group could be detected. However, within $CD8^+$ T cells, there was a trend towards a higher percentage of $CXCR3^+$ cells but did not reach statistical significance. Together with the lack of CCR5 expression on $CD4^+$ T cells the stable CXCR3 expression votes against a Th1 polarization following BLM treatment.

## 6.4 **Conclusion**

This project aimed a phenotypic characterization of $CCR2^+$ T cells in an animal model of bleomycin induced pulmonary fibrosis as basis for further functional analysis of these cells.

First of all, the percentages of $CCR2^+$ T cell were increased in murine lungs following BLM treatment. This leads to the question if these cells have a specific role in the disease course in this model. Although no functional assessment was performed here, the predominant affiliation of $CCR2^+$ to the $T_{em}$ suggests an active participation of T cells in BLM induced pulmonary fibrosis. The peak of the relative content of $CCR2^+$ T cells was at day 12, thus in the beginning of the fibrotic phase of bleomycin induced fibrosis. This could lead to two different speculations: $CCR2^+$ T cells could play a role in the initiation of the fibrotic response; or $CCR2^+$ T cells could be a reaction of the immune system in order to limit the fibrotic response.

However, the differences in chemokine receptor co-expression among control group and BLM treated mice suggests that $CCR2^+$ T cells are not a static population with a defined phenotype, but can regulate the surface expression of these receptors in response to alterations of the (patho-) physiological conditions.

Taking chemokine receptor expression as indicator for the assignment to different $CD4^+$ T cell subsets, $CCR2^+CD4^+$ T cells from lungs of BLM treated mice showed increased proportions of three different subpopulations. The increased percentage of $CCR3^+$ and $CCR4^+$ cells indicated a subpopulation of Th2-like cells within the $CCR2^+$ $CD4^+$ T cell population. Whereas, the markedly increased amount of $CCR6^+$ cells suggests a Th17 phenotype of a large group of $CD4^+$ T cells. The third subset was the $T_{FH}$ population, defined by the expression of CXCR5, which was perhaps the most surprising finding.

Further studies are necessary to reveal the functional potential of these cells. To prove the polarization of the different subsets, it will be necessary to test the production of the respective cytokines. Furthermore, the regulatory function needs to be proven by the assessment of classical $T_{reg}$ marker like CD25 and FoxP3 as well as in functional assays. The relevance of these findings for the human disease needs to get investigated in analogous studies in human samples.

Nevertheless, the results of this study strengthen the hypothesis that there is a specific role of $CCR2^+$ T cells in murine BLM induced pulmonary fibrosis. The understanding of this role

might give further insight into the pathogenic processes of ILD and provide new targets for therapeutic approaches.

# 7 Summary

Interstitial lung diseases (ILD) are severe chronic lung diseases characterized by an increased deposition of extracellular matrix in the lung interstitial space, leading to a thickening of the alveolar walls and impairment of the gas exchange. One of the most common entities in this category is idiopathic pulmonary fibrosis (IPF) with a mean survival time of 2 to 3 years from diagnosis. Until now, there is no curative therapy available and the symptomatic anti-inflammatory treatment and oxygen supplementation cannot prevent the development of the end stage pulmonary fibrosis.

The chemokine receptor CCR2 is important for leukocyte recruitment to inflamed tissues through interaction with CCL2 (MCP-1). The blockade of the CCR2/CCL2 pathway attenuated the development of pulmonary fibrosis in mouse models. However, $CCR2^+$ T-lymphocytes acquired regulatory functions in experimental arthritis during the course of disease. Therefore, it is unknown whether $CCR2^+$ T cells are involved in the pathogenesis of IPF or, on the contrary, represent an unsuccessful effort of the immune system to limit the disease.

Observations in paediatric patients with different forms of ILDs suggested a role for $CCR2^+$ T cells in pulmonary fibrosis.

To characterize these T cells, flow cytometric studies were performed using the bleomycin mouse model of pulmonary fibrosis. The kinetic of $CCR2^+$ T cells in BALF, lung tissue, and spleen following intratracheal administration of bleomycin (BLM) was assessed at time points between day 3 and day 21. To determine, if the constellation of naïve, central memory and effector memory T cells changes after BLM treatment, and to which of these subtypes $CCR2^+$ T cells belong to, the cells were additionally stained for CD62L and CD44. For further characterization of $CCR2^+$ T cells, chemokine receptor co-expression with CCR2 was investigated at the time point of the maximal presence of $CCR2^+$ T cells.

Total T cell numbers increased in BAL and lung tissue but not in spleen. Percentages of $CD62L^{low}CD44^{hi}$ effector memory T cells increased in lung tissue in the early phase of BLM induced fibrosis, while the $CD62L^{hi}CD44^{low}$ naïve T cell population decreased.

The percentage of $CCR2^+$ T cells increased following BLM treatment with a maximum on day 12. The majority of $CCR2^+CD4^+$ T cells showed a $T_{em}$ phenotype.

CCR3, CCR4, CCR6, CXCR4, and CXCR5 expressing cells increased within the pulmonary $CD4^+$ T cell population following bleomycin treatment. Among $CD8^+$ T cells from treated mice,

CCR5, CCR6, and CXCR5 positive cells were increased. CCR7 was highly co-expressed with CCR2 in saline and bleomycin treated mice, whereas co-expression of CCR3, CCR4, CCR6 and CXCR5 increased significantly in treated mice.

The results indicate an activation of pulmonary T cell populations following bleomycin treatment. $CCR2^{+}CD4^{+}$ T cells probably take part on this T cell response as they exhibit an effector memory phenotype and increase following BLM treatment. In contrast, the stable percentages of the different T cell subtypes in spleens gave no hint for a systemic T cell reaction.

The pattern of chemokine receptor expression argues against a Th1 polarization and towards a Th2, Th17 or $T_{FH}$ polarization of $CCR2^{+}$ T cells.

# 8 Zusammenfassung

Interstitielle Lungenerkrankungen (ILD) bilden eine Gruppe schwerer chronisch progredienter Lungenerkrankungen. Sie sind gekennzeichnet durch die vermehrte Bildung extrazellularer Matrix im Interstitium der Lunge, welche zu einer Verdickung der Alveolarwände und damit einer Gasaustauschstörung führt. Die häufigste Erkrankung dieser Gruppe ist die Idiopathische pulmonale Fibrose (IPF). Die mittlere Überlebenszeit von IPF Patienten liegt bei etwa 2 bis 3 Jahren nach Diagnosestellung. Bis heute gibt es keine kurative Therapie und die symptomatische Therapie mit anti-inflammatorischen Medikamenten und Sauerstoff kann das Fortschreiten der Erkrankung nicht verhindern.

Der Chemokinrezeptor CCR2 spielt eine wichtige Rolle bei der Migration von Leukozyten in entzündete Gewebe, durch Interaktion mit dessen Liganden CCL2 (MCP-1)

Die Blockade der CCR2/CCL2 Achse konnte im Mausmodell die Entwicklung einer Lungenfibrose verringern. Andererseits wurde in einem Mausmodell für Rheumatoide Arthritis gezeigt, dass $CCR2^+$ T-Zellen regulatorische Funktionen zeigen können. Somit ist unklar, ob $CCR2^+$ T-Zellen an der Pathogenese der Lungenfibrose beteiligt sind, oder einen erfolglosen Versuch des Immunsystems darstellen, die Krankheit einzudämmen.

Beobachtungen bei Kindern mit verschiedenen Formen interstitieller Lungenerkrankungen legen eine Funktion von $CCR2^+$ T-Zellen bei Lungenfibrose nahe.

Um diese Zellen näher zu charakterisieren wurden durchflusszytometrische Untersuchungen am Bleomycin Mausmodel für Lungenfibrose durchgeführt.

Die Veränderungen des prozentualen Anteiles von $CCR2^+$ T Zellen in BAL, Lungengewebe und Milz wurden an Zeitpunkten zwischen Tag 3 und Tag 21 nach der Behandlung mit Bleomycin untersucht. Zusätzlich wurde die Expression von CD62L und CD44 bestimmt, um zu untersuchen, ob sich das Verhältnis von naiven, effector memory, und central memory T-Zellen nach der Behandlung mit Bleomycin ändert und zu welchen der Subtypen die $CCR2^+$ T-Zellen gehören. Zur weiteren Charakterisierung wurde die gleichzeitige Expression anderer Chemokinrezeptoren zu dem Zeitpunkt bestimmt, an dem der höchste Anteil an $CCR2^+$ T-Zellen gemessen wurde.

In der BAL und im Lungengewebe stieg der Anteil von T-Zellen an, während sich in der Milz keine Veränderungen zeigten. In der Lunge stiegen die $CD62L^{low}CD44^{hi}$ effector memory T-

Zellen in der frühen Phase der BLM induzierten Fibrose an, während die $CD62L^{hi}CD44^{low}$ naiven T-Zellen absanken. Die Milz zeigte auch hier keine Veränderungen.

Auch die $CCR2^+$ T-Zellen stiegen nach der Behandlung mit BLM an und zeigten ein Maximum an Tag 12. Die Mehrzahl der $CCR2^+CD4^+$ Zellen gehörten zu den effector memory T-Zellen.

Im Vergleich zur Kontrollgruppe fanden sich in der Lunge von Bleomycin behandelten Mäusen vermehrt $CD4^+$ T-Zellen, die die Chemokinrezeptoren CCR3, CCR4, CCR6, CXCR4 und CXCR5 exprimierten. Innerhalb der $CD8^+$ Zellpopulation waren CCR5, CCR6 und CXCR5 häufiger exprimiert. CCR7 war sowohl in der Kontrollgruppe, als auch bei behandelten Mäusen am häufigsten gleichzeitig mit CCR2 exprimiert. Der Anteil an CCR3, CCR4, CCR6 und CXCR5 exprimierenden $CCR2^+$ Zellen stieg nach Behandlung mit Bleomycin signifikant an.

Die Ergebnisse legen nahe, dass pulmonale T-Zellen in Folge der Bleomycinbehandlung aktiviert werden. Da $CCR2^+$ T-Zellen einen erheblichen Anteil dieser aktivierten Zellen ausmachen, scheint es wahrscheinlich, dass diese eine wichtige Rolle im Rahmen der T-Zellreaktion spielen. Im Gegensatz dazu fanden sich keine Hinweise auf eine systemische Reaktion des T-Zellsystems in den Proben aus der Milz.

Die Konstellation der exprimierten Chemokinrezeptoren spricht gegen eine Th1 Polarisierung der $CCR2^+$ T-Zellen. Vielmehr zeigten sich Hinweise für eine Th2, Th17 oder $T_{FH}$ Differenzierung.

# 9 Appendix

## 9.1 References

1. American Thoracic Society/European Respiratory Society International Multidisciplinary Consensus Classification of the Idiopathic Interstitial Pneumonias. This joint statement of the American Thoracic Society (ATS), and the European Respiratory Society (ERS) was adopted by the ATS board of directors, June 2001 and by the ERS Executive Committee, June 2001. American Journal of Respiratory and Critical Care Medicine. 2002;165(2):277-304.

2. Loscalzo J. Interstitielle Lungenerkrankungen. In: Welte T, editor. Harrisons Lungenheilkunde und intensivmedizinische Betreuung. 1 ed. Berlin: ABW Wissenschaftsverlag GmbH; 2011.

3. Raghu G, Collard HR, Egan JJ, Martinez FJ, Behr J, Brown KK, et al. An official ATS/ERS/JRS/ALAT statement: idiopathic pulmonary fibrosis: evidence-based guidelines for diagnosis and management. American Journal of Respiratory and Critical Care Medicine. 2011;183(6):788-824.

4. Bjoraker JA, Ryu JH, Edwin MK, Myers JL, Tazelaar HD, Schroeder DR, et al. Prognostic significance of histopathologic subsets in idiopathic pulmonary fibrosis. American Journal of Respiratory and Critical Care Medicine. 1998;157(1):199-203.

5. Flaherty KR, Toews GB, Travis WD, Colby TV, Kazerooni EA, Gross BH, et al. Clinical significance of histological classification of idiopathic interstitial pneumonia. The European Respiratory Journal : official journal of the European Society for Clinical Respiratory Physiology. 2002;19(2):275-83.

6. Raghu G, Weycker D, Edelsberg J, Bradford WZ, Oster G. Incidence and prevalence of idiopathic pulmonary fibrosis. American Journal of Respiratory and Critical Care Medicine. 2006;174(7):810-6.

7. Gribbin J, Hubbard RB, Le Jeune I, Smith CJ, West J, Tata LJ. Incidence and mortality of idiopathic pulmonary fibrosis and sarcoidosis in the UK. Thorax. 2006;61(11):980-5.

8. Martinez FJ, Safrin S, Weycker D, Starko KM, Bradford WZ, King TE, Jr., et al. The clinical course of patients with idiopathic pulmonary fibrosis. Annals of Internal Medicine. 2005;142(12 Pt 1):963-7.

9. Ley B, Collard HR, King TE. Clinical Course and Prediction of Survival in Idiopathic Pulmonary Fibrosis. American Journal of Respiratory and Critical Care Medicine. 2011;183(4):431-40.

10. Lynch DA, Godwin JD, Safrin S, Starko KM, Hormel P, Brown KK, et al. High-Resolution Computed Tomography in Idiopathic Pulmonary Fibrosis. American Journal of Respiratory and Critical Care Medicine. 2005;172(4):488-93.

11. Bessis L, Callard P, Gotheil C, Biaggi A, Grenier P. High-resolution CT of parenchymal lung disease: precise correlation with histologic findings. Cancer. 1992;12(1):45-58.

12. Visscher DW, Myers JL. Histologic spectrum of idiopathic interstitial pneumonias. Proceedings of the American Thoracic Society. 2006;3(4):322-9.

13. Morawiec E, Tillie-Leblond I, Pansini V, Salleron J, Remy-Jardin M, Wallaert B. Exacerbations of idiopathic pulmonary fibrosis treated with corticosteroids and cyclophosphamide pulses. European Respiratory Journal. 2011;38(6):1487-9.

14. Raghu G, Anstrom KJ, King Jr TE, Lasky JA, Martinez FJ. Prednisone, Azathioprine, and N-Acetylcysteine for Pulmonary Fibrosis. New England Journal of Medicine. 2012;366(21):1968-77.

15. Thabut G, Mal H, Castier Y, Groussard O, Brugière O, Marrash-Chahla R, et al. Survival benefit of lung transplantation for patients with idiopathic pulmonary fibrosis. The Journal of Thoracic and Cardiovascular Surgery. 2003;126(2):469-75.

16. Noble PW, Albera C, Bradford WZ, Costabel U, Glassberg MK, Kardatzke D, et al. Pirfenidone in patients with idiopathic pulmonary fibrosis (CAPACITY): two randomised trials. The Lancet.377(9779):1760-9.

17. Wuyts WA, Thomeer M, Demedts MG. Newer modes of treating interstitial lung disease. Current Opinion in Pulmonary Medicine. 2011;17(5):332-6.

18. Kondoh Y, Taniguchi H, Yokoi T, Nishiyama O, Ohishi T, Kato T, et al. Cyclophosphamide and low-dose prednisolone in idiopathic pulmonary fibrosis and fibrosing nonspecific interstitial pneumonia. European Respiratory Journal. 2005;25(3):528-33.

19. Baumgartner KB, Samet JM, Stidley CA, Colby TV, Waldron JA. Cigarette smoking: a risk factor for idiopathic pulmonary fibrosis. American Journal of Respiratory and Critical Care Medicine. 1997;155(1):242-8.

20. Baumgartner KB, Samet JM, Coultas DB, Stidley CA, Hunt WC, Colby TV, et al. Occupational and environmental risk factors for idiopathic pulmonary fibrosis: a multicenter case-control study. Collaborating Centers. American Journal of Epidemiology. 2000;152(4):307-15.

21. Yonemaru M, Kasuga I, Kusumoto H, Kunisawa A, Kiyokawa H, Kuwabara S, et al. Elevation of antibodies to cytomegalovirus and other herpes viruses in pulmonary fibrosis. The European Respiratory Journal : official journal of the European Society for Clinical Respiratory Physiology. 1997;10(9):2040-5.

22. Hershcovici T, Jha LK, Johnson T, Gerson L, Stave C, Malo J, et al. Systematic review: the relationship between interstitial lung diseases and gastro-oesophageal reflux disease. Alimentary Pharmacology & Therapeutics. 2011;34(11-12):1295-305.

23. Coward WR, Saini G, Jenkins G. The pathogenesis of idiopathic pulmonary fibrosis. Therapeutic Advances in Respiratory Disease. 2010;4(6):367-88.

24. Lawson WE, Grant SW, Ambrosini V, Womble KE, Dawson EP, Lane KB, et al. Genetic mutations in surfactant protein C are a rare cause of sporadic cases of IPF. Thorax. 2004;59(11):977-80.

25. Wolters PJ, Collard HR, Jones KD. Pathogenesis of Idiopathic Pulmonary Fibrosis. Annual Review of Pathology. 2013.

26. Alder JK, Chen JJ, Lancaster L, Danoff S, Su SC, Cogan JD, et al. Short telomeres are a risk factor for idiopathic pulmonary fibrosis. Proceedings of the National Academy of Sciences of the United States of America. 2008;105(35):13051-6.

27. Cronkhite JT, Xing C, Raghu G, Chin KM, Torres F, Rosenblatt RL, et al. Telomere shortening in familial and sporadic pulmonary fibrosis. American Journal of Respiratory and Critical Care Medicine. 2008;178(7):729-37.

28. Suga M, Iyonaga K, Okamoto T, Gushima Y, Miyakawa H, Akaike T, et al. Characteristic elevation of matrix metalloproteinase activity in idiopathic interstitial pneumonias. American Journal of Respiratory and Critical Care Medicine. 2000;162(5):1949-56.

29. Zuo F, Kaminski N, Eugui E, Allard J, Yakhini Z, Ben-Dor A, et al. Gene expression analysis reveals matrilysin as a key regulator of pulmonary fibrosis in mice and humans. Proceedings of the National Academy of Sciences of the United States of America. 2002;99(9):6292-7.

30. Hagimoto N, Kuwano K, Inoshima I, Yoshimi M, Nakamura N, Fujita M, et al. TGF-beta 1 as an enhancer of Fas-mediated apoptosis of lung epithelial cells. Journal of Immunology 2002;168(12):6470-8.

31. Jain R, Shaul PW, Borok Z, Willis BC. Endothelin-1 Induces Alveolar Epithelial–Mesenchymal Transition through Endothelin Type A Receptor–Mediated Production of TGF-β1. American Journal of Respiratory Cell and Molecular Biology. 2007;37(1):38-47.

32. Zhang M, Zhang Z, Pan HY, Wang DX, Deng ZT, Ye XL. TGF-beta1 induces human bronchial epithelial cell-to-mesenchymal transition in vitro. Lung. 2009;187(3):187-94.

33. Ramirez AM, Shen Z, Ritzenthaler JD, Roman J. Myofibroblast transdifferentiation in obliterative bronchiolitis: tgf-beta signaling through smad3-dependent and -independent pathways. American Journal of Transplantation : official journal of the American Society of Transplantation and the American Society of Transplant Surgeons. 2006;6(9):2080-8.

34. Kim KK, Kugler MC, Wolters PJ, Robillard L, Galvez MG, Brumwell AN, et al. Alveolar epithelial cell mesenchymal transition develops in vivo during pulmonary fibrosis and is regulated by the extracellular matrix. Proceedings of the National Academy of Sciences. 2006;103(35):13180-5.

35. Phillips RJ, Burdick MD, Hong K, Lutz MA, Murray LA, Xue YY, et al. Circulating fibrocytes traffic to the lungs in response to CXCL12 and mediate fibrosis. The Journal of Clinical Investigation. 2004;114(3):438-46.

36. Wynn TA. Fibrotic disease and the T(H)1/T(H)2 paradigm. Nature Reviews Immunology 2004;4(8):583-94.

37. Wilson MS, Madala SK, Ramalingam TR, Gochuico BR, Rosas IO, Cheever AW, et al. Bleomycin and IL-1beta-mediated pulmonary fibrosis is IL-17A dependent. The Journal of Experimental Medicine. 2010;207(3):535-52.

38. Zhu Z, Homer RJ, Wang Z, Chen Q, Geba GP, Wang J, et al. Pulmonary expression of interleukin-13 causes inflammation, mucus hypersecretion, subepithelial fibrosis, physiologic abnormalities, and eotaxin production. The Journal of Clinical Investigation. 1999;103(6):779-88.

39. Blease K, Jakubzick C, Westwick J, Lukacs N, Kunkel SL, Hogaboam CM. Therapeutic Effect of IL-13 Immunoneutralization During Chronic Experimental Fungal Asthma. The Journal of Immunology. 2001;166(8):5219-24.

40. Belperio JA, Dy M, Burdick MD, Xue YY, Li K, Elias JA, et al. Interaction of IL-13 and C10 in the Pathogenesis of Bleomycin-Induced Pulmonary Fibrosis. American Journal of Respiratory Cell and Molecular Biology. 2002;27(4):419-27.

41. Lee CG, Homer RJ, Zhu Z, Lanone S, Wang X, Koteliansky V, et al. Interleukin-13 induces tissue fibrosis by selectively stimulating and activating transforming growth factor beta(1). The Journal of Experimental Medicine. 2001;194(6):809-21.

42. Wallace WA, Ramage EA, Lamb D, Howie SE. A type 2 (Th2-like) pattern of immune response predominates in the pulmonary interstitium of patients with cryptogenic fibrosing alveolitis (CFA). Clinical and Experimental Immunology. 1995;101(3):436-41.

43. Sumida A, Hasegawa Y, Okamoto M, Hashimoto N, Imaizumi K, Yatsuya H, et al. TH1/TH2 immune response in lung fibroblasts in interstitial lung disease. Archives of Medical Research. 2008;39(5):503-10.

44. Oldroyd SD, Thomas GL, Gabbiani G, El Nahas AM. Interferon-gamma inhibits experimental renal fibrosis. Kidney International. 1999;56(6):2116-27.

45. Gurujeyalakshmi G, Giri SN. Molecular mechanisms of antifibrotic effect of interferon gamma in bleomycin-mouse model of lung fibrosis: downregulation of TGF-beta and procollagen I and III gene expression. Experimental Lung Research. 1995;21(5):791-808.

46. Arai T, Abe KY, Matsuoka H, Yoshida M, Mori M, Goya S, et al. Introduction of the interleukin-10 gene into mice inhibited bleomycin-induced lung injury in vivo. American Journal of Physiology - Lung Cellular and Molecular Physiology. 2000;278(5):L914-L22.

47. Nakagome K, Dohi M, Okunishi K, Tanaka R, Miyazaki J, Yamamoto K. In vivo IL-10 gene delivery attenuates bleomycin induced pulmonary fibrosis by inhibiting the production and activation of TGF-β in the lung. Thorax. 2006;61(10):886-94.

48. Whittington HA, Freeburn RW, Godinho SI, Egan J, Haider Y, Millar AB. Analysis of an IL-10 polymorphism in idiopathic pulmonary fibrosis. Genes and Immunity. 2003;4(4):258-64.

49. Frade JM, Mellado M, del Real G, Gutierrez-Ramos JC, Lind P, Martinez AC. Characterization of the CCR2 chemokine receptor: functional CCR2 receptor expression in B cells. The Journal of Immunology 1997;159(11):5576-84.

50. Moore BB, Kolodsick JE, Thannickal VJ, Cooke K, Moore TA, Hogaboam C, et al. CCR2-Mediated Recruitment of Fibrocytes to the Alveolar Space after Fibrotic Injury. The American Journal of Pathology. 2005;166(3):675-84.

51. Ekert JE, Murray LA, Das AM, Sheng H, Giles-Komar J, Rycyzyn MA. Chemokine (C-C motif) ligand 2 mediates direct and indirect fibrotic responses in human and murine cultured fibrocytes. Fibrogenesis & Tissue repair. 2011;4(1):23.

52. Zlotnik A, Yoshie O, Nomiyama H. The chemokine and chemokine receptor superfamilies and their molecular evolution. Genome Biology. 2006;7(12):243.

53. Standiford TJ, Kunkel SL, Phan SH, Rollins BJ, Strieter RM. Alveolar macrophage-derived cytokines induce monocyte chemoattractant protein-1 expression from human pulmonary type II-like epithelial cells. Journal of Biological Chemistry. 1991;266(15):9912-8.

54. Cushing SD, Berliner JA, Valente AJ, Territo MC, Navab M, Parhami F, et al. Minimally modified low density lipoprotein induces monocyte chemotactic protein 1 in human endothelial cells and smooth muscle cells. Proceedings of the National Academy of Sciences. 1990;87(13):5134-8.

55. Rolfe MW, Kunkel SL, Standiford TJ, Orringer MB, Phan SH, Evanoff HL, et al. Expression and regulation of human pulmonary fibroblast-derived monocyte chemotactic peptide-1. The American Journal of Physiology. 1992;263(5 Pt 1):L536-45.

56. Mack M, Cihak J, Simonis C, Luckow B, Proudfoot AE, Plachy J, et al. Expression and characterization of the chemokine receptors CCR2 and CCR5 in mice. The Journal of Immunology 2001;166(7):4697-704.

57. Traynor TR, Kuziel WA, Toews GB, Huffnagle GB. CCR2 expression determines T1 versus T2 polarization during pulmonary Cryptococcus neoformans infection. The Journal of Immunology 2000;164(4):2021-7.

58. Gu L, Tseng S, Horner RM, Tam C, Loda M, Rollins BJ. Control of TH2 polarization by the chemokine monocyte chemoattractant protein-1. Nature. 2000;404(6776):407-11.

59. Connor SJ, Paraskevopoulos N, Newman R, Cuan N, Hampartzoumian T, Lloyd AR, et al. CCR2 expressing CD4+ T lymphocytes are preferentially recruited to the ileum in Crohn's disease. Gut. 2004;53(9):1287-94.

60. Ellingsen T, Hornung N, Moller BK, Poulsen JH, Stengaard-Pedersen K. Differential effect of methotrexate on the increased CCR2 density on circulating CD4 T lymphocytes and monocytes in active chronic rheumatoid arthritis, with a down regulation only on monocytes in responders. Annals of the Rheumatic Diseases. 2007;66(2):151-7.

61. Sato W, Tomita A, Ichikawa D, Lin Y, Kishida H, Miyake S, et al. CCR2+CCR5+ T Cells Produce Matrix Metalloproteinase-9 and Osteopontin in the Pathogenesis of Multiple Sclerosis. The Journal of Immunology 2012;189(10):5057-65.

62. Bruhl H, Cihak J, Schneider MA, Plachy J, Rupp T, Wenzel I, et al. Dual role of CCR2 during initiation and progression of collagen-induced arthritis: evidence for regulatory activity of CCR2+ T cells. The Journal of Immunology 2004;172(2):890-8.

63. Gharaee-Kermani M, Denholm EM, Phan SH. Costimulation of Fibroblast Collagen and Transforming Growth Factor β1 Gene Expression by Monocyte Chemoattractant Protein-1 via Specific Receptors. Journal of Biological Chemistry. 1996;271(30):17779-84.

64. Gharaee-Kermani M, McCullumsmith RE, Charo IF, Kunkel SL, Phan SH. CC-chemokine receptor 2 required for bleomycin-induced pulmonary fibrosis. Cytokine. 2003;24(6):266-76.

65. Liang J, Jung Y, Tighe RM, Xie T, Liu N, Leonard M, et al. A macrophage subpopulation recruited by CC chemokine ligand-2 clears apoptotic cells in noninfectious lung injury. American Journal of Physiology Lung Cellular and Molecular Physiology. 2012;302(9):L933-40.

66. Moore BB, Paine R, 3rd, Christensen PJ, Moore TA, Sitterding S, Ngan R, et al. Protection from pulmonary fibrosis in the absence of CCR2 signaling.The Journal of Immunology 2001;167(8):4368-77.

67. Okuma T, Terasaki Y, Kaikita K, Kobayashi H, Kuziel WA, Kawasuji M, et al. C-C chemokine receptor 2 (CCR2) deficiency improves bleomycin-induced pulmonary fibrosis by attenuation of both macrophage infiltration and production of macrophage-derived matrix metalloproteinases. The Journal of Pathology. 2004;204(5):594-604.

68. Hartl D, Griese M, Nicolai T, Zissel G, Prell C, Reinhardt D, et al. A role for MCP-1/CCR2 in interstitial lung disease in children. Respiratory Research. 2005;6:93.

69. Roederer M. Compensation in flow cytometry. Current protocols in cytometry / editorial board, J Paul Robinson, managing editor [et al]. 2002;Chapter 1:Unit 1 14.

70. Umezawa H, Maeda K, Takeuchi T, Okami Y. New antibiotics, bleomycin A and B. The Journal of Antibiotics. 1966;19(5):200-9.

71. Albers P, Albrecht W, Algaba F, Bokemeyer C, Cohn-Cedermark G, Fizazi K, et al. EAU Guidelines on Testicular Cancer: 2011 Update. European Urology. 2011;60(2):304-19.

72. Hoppe RT, Advani RH, Ai WZ, Ambinder RF, Bello CM, Bierman PJ, et al. Hodgkin Lymphoma. Journal of the National Comprehensive Cancer Network. 2011;9(9):1020-58.

73. Trush MA, Mimnaugh EG, Ginsburg E, Gram TE. Studies on the interaction of bleomycin A2 with rat lung microsomes. I. Characterization of factors which influence bleomycin-mediated DNA chain breakage. Journal of Pharmacology and Experimental Therapeutics. 1982;221(1):152-8.

74. Tounekti O, Pron G, Belehradek J, Mir LM. Bleomycin, an Apoptosis-mimetic Drug That Induces Two Types of Cell Death Depending on the Number of Molecules Internalized. Cancer Research. 1993;53(22):5462-9.

75. Takeda A, Higuchi D, Yamamoko T, Nakamura Y, Masuda Y, Hirabayashi T, et al. Purification and Characterization of Bleomycin Hydrolase, Which Represents a New Family of Cysteine Proteases, from Rat Skin. Journal of Biochemistry. 1996;119(1):29-36.

76. Adamson IY. Pulmonary toxicity of bleomycin. Environmental health Perspectives. 1976;16:119-26.

77. Blum RH, Carter SK, Agre K. A clinical review of bleomycin—a new antineoplastic agent. Cancer. 1973;31(4):903-14.

78. Lazo JS, Hoyt DG, Sebti SM, Pitt BR. Bleomycin: a pharmacologic tool in the study of the pathogenesis of interstitial pulmonary fibrosis. Pharmacology & therapeutics. 1990;47(3):347-58.

79. Mouratis MA, Aidinis V. Modeling pulmonary fibrosis with bleomycin. Current Opinion in Pulmonary Medicine. 2011;17(5):355-61.

80. Moore BB, Hogaboam CM. Murine models of pulmonary fibrosis. American Journal of Physiology Lung Cellular and Molecular Physiology. 2008;294(2):L152-60.

81. Chung MP, Monick MM, Hamzeh NY, Butler NS, Powers LS, Hunninghake GW. Role of repeated lung injury and genetic background in bleomycin-induced fibrosis. American Journal of Respiratory Cell and Molecular Biology. 2003;29(3 Pt 1):375-80.

82. Phan SH, Armstrong G, Sulavik MC, Schrier D, Johnson KJ, Ward PA. A comparative study of pulmonary fibrosis induced by bleomycin and an O2 metabolite producing enzyme system. Chest. 1983;83(5 Suppl):44S-5S.

83. Schrier DJ, Kunkel RG, Phan SH. The role of strain variation in murine bleomycin-induced pulmonary fibrosis. The American Review of Respiratory Disease. 1983;127(1):63-6.

84. Pociask DA, Chen K, Mi Choi S, Oury TD, Steele C, Kolls JK. [gamma][delta] T Cells Attenuate Bleomycin-Induced Fibrosis through the Production of CXCL10. The American Journal of Pathology. 2011;178(3):1167-76.

85. Jiang D, Liang J, Hodge J, Lu B, Zhu Z, Yu S, et al. Regulation of pulmonary fibrosis by chemokine receptor CXCR3. The Journal of Clinical Investigation. 2004;114(2):291-9.

86. Konigshoff M, Kramer M, Balsara N, Wilhelm J, Amarie OV, Jahn A, et al. WNT1-inducible signaling protein-1 mediates pulmonary fibrosis in mice and is upregulated in humans with idiopathic pulmonary fibrosis. The Journal of Clinical Investigation. 2009;119(4):772-87.

87. Xu PB, Mao YF, Meng HB, Tian YP, Deng XM. STY39, a novel alpha-melanocyte-stimulating hormone analogue, attenuates bleomycin-induced pulmonary inflammation and fibrosis in mice. Shock (Augusta, Ga). 2011;35(3):308-14.

88. Yamauchi K, Kasuya Y, Kuroda F, Tanaka K, Tsuyusaki J, Ishizaki S, et al. Attenuation of lung inflammation and fibrosis in CD69-deficient mice after intratracheal bleomycin. Respiratory Research. 2011;12:131.

89. Martin WR, Padrid PA, Cross CE. Bronchoalveolar lavage. Clinical Reviews in Allergy. 1990;8(2-3):305-32.

90. Reynolds HY. Bronchoalveolar lavage and other methods to define the human respiratory tract milieu in health and disease. Lung. 2011;189(2):87-99.

91. Cells in Bronchoalveolar Lavage Fluid. American Review of Respiratory Disease. 1990;141(5_pt_2):S175-S8.

92. Janick-Buckner D, Ranges GE, Hacker MP. Alteration of bronchoalveolar lavage cell populations following bleomycin treatment in mice. Toxicology and Applied Pharmacology. 1989;100(3):465-73.

93. Jiang D, Liang J, Campanella GS, Guo R, Yu S, Xie T, et al. Inhibition of pulmonary fibrosis in mice by CXCL10 requires glycosaminoglycan binding and syndecan-4. The Journal of Clinical Investigation. 2010;120(6):2049-57.

94. Bantsimba-Malanda C, Marchal-Somme J, Goven D, Freynet O, Michel L, Crestani B, et al. A role for dendritic cells in bleomycin-induced pulmonary fibrosis in mice? American Journal of Respiratory and Critical Care Medicine. 2010;182(3):385-95.

95. Trujillo G, Hartigan AJ, Hogaboam CM. T regulatory cells and attenuated bleomycin-induced fibrosis in lungs of CCR7-/- mice. Fibrogenesis & Tissue repair. 2010;3:18.

96. Pepper M, Jenkins MK. Origins of CD4(+) effector and central memory T cells. Nature Immunology. 2011;12(6):467-71.

97. Swain SL, Croft M, Dubey C, Haynes L, Rogers P, Zhang X, et al. From naive to memory T cells. Immunological Reviews. 1996;150:143-67.

98. Picker LJ, Treer JR, Ferguson-Darnell B, Collins PA, Buck D, Terstappen LW. Control of lymphocyte recirculation in man. I. Differential regulation of the peripheral lymph node homing receptor L-selectin on T cells during the virgin to memory cell transition. The Journal of Immunology 1993;150(3):1105-21.

99. McHeyzer-Williams MG, Davis MM. Antigen-specific development of primary and memory T cells in vivo. Science. 1995;268(5207):106-11.

100. Rothman BL, Blue ML, Kelley KA, Wunderlich D, Mierz DV, Aune TM. Human T cell activation by OKT3 is inhibited by a monoclonal antibody to CD44. The Journal of Immunology 1991;147(8):2493-9.

101. Gerberick GF, Cruse LW, Miller CM, Sikorski EE, Ridder GM. Selective modulation of T cell memory markers CD62L and CD44 on murine draining lymph node cells following allergen and irritant treatment. Toxicology and Applied Pharmacology. 1997;146(1):1-10.

102. Sallusto F, Lenig D, Forster R, Lipp M, Lanzavecchia A. Two subsets of memory T lymphocytes with distinct homing potentials and effector functions. Nature. 1999;401(6754):708-12.

103. Sallusto F, Kremmer E, Palermo B, Hoy A, Ponath P, Qin S, et al. Switch in chemokine receptor expression upon TCR stimulation reveals novel homing potential for recently activated T cells. European Journal of Immunology. 1999;29(6):2037-45.

104. Cose S, Brammer C, Khanna KM, Masopust D, Lefrançois L. Evidence that a significant number of naive T cells enter non-lymphoid organs as part of a normal migratory pathway. European Journal of Immunology. 2006;36(6):1423-33.

105. Idali F, Wahlstrom J, Muller-Suur C, Eklund A, Grunewald J. Analysis of regulatory T cell associated forkhead box P3 expression in the lungs of patients with sarcoidosis. Clinical and Experimental Immunology. 2008;152(1):127-37.

106. Meloni F, Caporali R, Marone Bianco A, Paschetto E, Morosini M, Fietta AM, et al. BAL cytokine profile in different interstitial lung diseases: a focus on systemic sclerosis. Sarcoidosis, Vasculitis, and Diffuse Lung Diseases : official journal of WASOG / World Association of Sarcoidosis and Other Granulomatous Disorders. 2004;21(2):111-8.

107. Mercer PF, Johns RH, Scotton CJ, Krupiczojc MA, Königshoff M, Howell DCJ, et al. Pulmonary Epithelium Is a Prominent Source of Proteinase-activated Receptor-1–inducible CCL2 in Pulmonary Fibrosis. American Journal of Respiratory and Critical Care Medicine. 2009;179(5):414-25.

108. Suga M, Iyonaga K, Ichiyasu H, Saita N, Yamasaki H, Ando M. Clinical significance of MCP-1 levels in BALF and serum in patients with interstitial lung diseases. European Respiratory Journal. 1999;14(2):376-82.

109. Zhang HH, Song K, Rabin RL, Hill BJ, Perfetto SP, Roederer M, et al. CCR2 identifies a stable population of human effector memory CD4+ T cells equipped for rapid recall response. The Journal of Immunology. 2010;185(11):6646-63.

110. Tokuda A, Itakura M, Onai N, Kimura H, Kuriyama T, Matsushima K. Pivotal role of CCR1-positive leukocytes in bleomycin-induced lung fibrosis in mice. The Journal of Immunology. 2000;164(5):2745-51.

111. Russo RC, Guabiraba R, Garcia CC, Barcelos LS, Roffe E, Souza AL, et al. Role of the chemokine receptor CXCR2 in bleomycin-induced pulmonary inflammation and fibrosis. American Journal of Respiratory Cell and Molecular Biology. 2009;40(4):410-21.

112. Annunziato F, Cosmi L, Santarlasci V, Maggi L, Liotta F, Mazzinghi B, et al. Phenotypic and functional features of human Th17 cells. The Journal of Experimental Medicine. 2007;204(8):1849-61.

113. Singh SP, Zhang HH, Foley JF, Hedrick MN, Farber JM. Human T cells that are able to produce IL-17 express the chemokine receptor CCR6. The Journal of Immunology. 2008;180(1):214-21.

114. Hirota K, Yoshitomi H, Hashimoto M, Maeda S, Teradaira S, Sugimoto N, et al. Preferential recruitment of CCR6-expressing Th17 cells to inflamed joints via CCL20 in rheumatoid arthritis and its animal model. The Journal of Experimental Medicine. 2007;204(12):2803-12.

115. Li D, Cai W, Gu R, Zhang Y, Zhang H, Tang K, et al. Th17 cell plays a role in the pathogenesis of Hashimoto's thyroiditis in patients. Clinical Immunology (Orlando, Fla). 2013;149(3pb):411-20.

116. Kleinewietfeld M, Puentes F, Borsellino G, Battistini L, Rotzschke O, Falk K. CCR6 expression defines regulatory effector/memory-like cells within the CD25(+)CD4+ T-cell subset. Blood. 2005;105(7):2877-86.

117. Power CA, Church DJ, Meyer A, Alouani S, Proudfoot AE, Clark-Lewis I, et al. Cloning and characterization of a specific receptor for the novel CC chemokine MIP-3alpha from lung dendritic cells. The Journal of Experimental Medicine. 1997;186(6):825-35.

118. Thorley AJ, Goldstraw P, Young A, Tetley TD. Primary human alveolar type II epithelial cell CCL20 (macrophage inflammatory protein-3alpha)-induced dendritic cell migration. American Journal of Respiratory Cell and Molecular Biology. 2005;32(4):262-7.

119. Facco M, Baesso I, Miorin M, Bortoli M, Cabrelle A, Boscaro E, et al. Expression and role of CCR6/CCL20 chemokine axis in pulmonary sarcoidosis. Journal of Leukocyte Biology. 2007;82(4):946-55.

120. Thomas SY, Banerji A, Medoff BD, Lilly CM, Luster AD. Multiple chemokine receptors, including CCR6 and CXCR3, regulate antigen-induced T cell homing to the human asthmatic airway. The Journal of Immunology 2007;179(3):1901-12.

121. Francis JN, Sabroe I, Lloyd CM, Durham SR, Till SJ. Elevated CCR6+ CD4+ T lymphocytes in tissue compared with blood and induction of CCL20 during the asthmatic late response. Clinical and Experimental Immunology. 2008;152(3):440-7.

122. Bracke KR, D'hulst AI, Maes T, Moerloose KB, Demedts IK, Lebecque S, et al. Cigarette Smoke-Induced Pulmonary Inflammation and Emphysema Are Attenuated in CCR6-Deficient Mice. The Journal of Immunology. 2006;177(7):4350-9.

123. Truchetet ME, Brembilla NC, Montanari E, Allanore Y, Chizzolini C. Increased frequency of circulating Th22 in addition to Th17 and Th2 lymphocytes in systemic sclerosis: association with interstitial lung disease. Arthritis Research & Therapy. 2011;13(5):R166.

124. Nuovo GJ, Hagood JS, Magro CM, Chin N, Kapil R, Davis L, et al. The distribution of immunomodulatory cells in the lungs of patients with idiopathic pulmonary fibrosis. Modern Pathology : an official journal of the United States and Canadian Academy of Pathology, Inc. 2012;25(3):416-33.

125. Forster R, Davalos-Misslitz AC, Rot A. CCR7 and its ligands: balancing immunity and tolerance. Nature Reviews Immunology. 2008;8(5):362-71.

126. Forster R, Schubel A, Breitfeld D, Kremmer E, Renner-Muller I, Wolf E, et al. CCR7 coordinates the primary immune response by establishing functional microenvironments in secondary lymphoid organs. Cell. 1999;99(1):23-33.

127. Campbell JJ, Murphy KE, Kunkel EJ, Brightling CE, Soler D, Shen Z, et al. CCR7 expression and memory T cell diversity in humans. The Journal of Immunology 2001;166(2):877-84.

128. Ahern D, Lloyd CM, Robinson DS. Chemokine responsiveness of CD4+ CD25+ regulatory and CD4+ CD25- T cells from atopic and nonatopic donors. Allergy. 2009;64(8):1121-9.

129. Choi ES, Pierce EM, Jakubzick C, Carpenter KJ, Kunkel SL, Evanoff H, et al. Focal interstitial CC chemokine receptor 7 (CCR7) expression in idiopathic interstitial pneumonia. Journal of Clinical Pathology. 2006;59(1):28-39.

130. Moser B, Loetscher P. Lymphocyte traffic control by chemokines. Nature Immunology. 2001;2(2):123-8.

131. Sallusto F, Mackay CR, Lanzavecchia A. Selective expression of the eotaxin receptor CCR3 by human T helper 2 cells. Science. 1997;277(5334):2005-7.

132. Bonecchi R, Bianchi G, Bordignon PP, D'Ambrosio D, Lang R, Borsatti A, et al. Differential expression of chemokine receptors and chemotactic responsiveness of type 1 T helper cells (Th1s) and Th2s. The Journal of Experimental Medicine. 1998;187(1):129-34.

133. Morgan AJ, Symon FA, Berry MA, Pavord ID, Corrigan CJ, Wardlaw AJ. IL-4-expressing bronchoalveolar T cells from asthmatic and healthy subjects preferentially express CCR 3 and CCR 4. The Journal of Allergy and Clinical Immunology. 2005;116(3):594-600.

134. Panina-Bordignon P, Papi A, Mariani M, Di Lucia P, Casoni G, Bellettato C, et al. The C-C chemokine receptors CCR4 and CCR8 identify airway T cells of allergen-challenged atopic asthmatics. The Journal of Clinical Investigation. 2001;107(11):1357-64.

135. Smyth LJ, Starkey C, Gordon FS, Vestbo J, Singh D. CD8 chemokine receptors in chronic obstructive pulmonary disease. Clinical and Experimental Immunology. 2008;154(1):56-63.

136. Mangieri D, Corradi D, Martorana D, Malerba G, Palmisano A, Libri I, et al. Eotaxin/CCL11 in idiopathic retroperitoneal fibrosis. Nephrology Dialysis Transplantation. 2012;27(10):3875-84.

137. Sterclova M, Vasakova M, Pavlicek J, Metlicka M, Krasna E, Striz I. Chemokine receptors in a regulation of interstitial lung fibrosis and inflammation. Experimental Lung Research. 2009;35(6):514-23.

138. Pignatti P, Brunetti G, Moretto D, Yacoub MR, Fiori M, Balbi B, et al. Role of the chemokine receptors CXCR3 and CCR4 in human pulmonary fibrosis. American Journal of Respiratory and Critical Care Medicine. 2006;173(3):310-7.

139. Belperio JA, Dy M, Murray L, Burdick MD, Xue YY, Strieter RM, et al. The role of the Th2 CC chemokine ligand CCL17 in pulmonary fibrosis. The Journal of Immunology. 2004;173(7):4692-8.

140. Rasheed A-U, Rahn H-P, Sallusto F, Lipp M, Müller G. Follicular B helper T cell activity is confined to CXCR5hiICOShi CD4 T cells and is independent of CD57 expression. European Journal of Immunology. 2006;36(7):1892-903.

141. Ansel KM, McHeyzer-Williams LJ, Ngo VN, McHeyzer-Williams MG, Cyster JG. In vivo-activated CD4 T cells upregulate CXC chemokine receptor 5 and reprogram their response to lymphoid chemokines. The Journal of Experimental Medicine. 1999;190(8):1123-34.

142. Crotty S. Follicular Helper CD4 T Cells (TFH). Annual Review of Immunology. 2011;29(1):621-63.

143. Hardtke S, Ohl L, Forster R. Balanced expression of CXCR5 and CCR7 on follicular T helper cells determines their transient positioning to lymph node follicles and is essential for efficient B-cell help. Blood. 2005;106(6):1924-31.

144. Breitfeld D, Ohl L, Kremmer E, Ellwart J, Sallusto F, Lipp M, et al. Follicular B helper T cells express CXC chemokine receptor 5, localize to B cell follicles, and support immunoglobulin production. The Journal of Experimental Medicine. 2000;192(11):1545-52.

145. Feng J, Lu L, Hua C, Qin L, Zhao P, Wang J, et al. High Frequency of CD4+CXCR5+ TFH Cells in Patients with Immune-Active Chronic Hepatitis B. PloS one. 2011;6(7):e21698.

146. Feng J, Hu X, Guo H, Sun X, Wang J, Xu L, et al. Patients with chronic hepatitis C express a high percentage of CD4+CXCR5+ T follicular helper cells. The Journal of Gastroenterology 2012;47(9):1048-56.

147. Morita R, Schmitt N, Bentebibel S-E, Ranganathan R, Bourdery L, Zurawski G, et al. Human Blood CXCR5+CD4+ T Cells Are Counterparts of T Follicular Cells and Contain Specific Subsets that Differentially Support Antibody Secretion. Immunity. 2011;34(1):108-21.

148. Winter S, Loddenkemper C, Aebischer A, Räbel K, Hoffmann K, Meyer T, et al. The chemokine receptor CXCR5 is pivotal for ectopic mucosa-associated lymphoid tissue neogenesis in chronic Helicobacter pylori-induced inflammation. The Journal of Molecular Medicine 2010;88(11):1169-80.

149. Simpson N, Gatenby PA, Wilson A, Malik S, Fulcher DA, Tangye SG, et al. Expansion of circulating T cells resembling follicular helper T cells is a fixed phenotype that identifies a subset of severe systemic lupus erythematosus. Arthritis & Rheumatism. 2010;62(1):234-44.

150. Li X-y, Wu Z-b, Ding J, Zheng Z-h, Li X-y, Chen L-n, et al. Role of the frequency of blood CD4+ CXCR5+ CCR6+ T cells in autoimmunity in patients with Sjögren's syndrome. Biochemical and Biophysical Research Communications. 2012;422(2):238-44.

151. Perros F, Dorfmüller P, Montani D, Hammad H, Waelput W, Girerd B, et al. Pulmonary Lymphoid Neogenesis in Idiopathic Pulmonary Arterial Hypertension. American Journal of Respiratory and Critical Care Medicine. 2012;185(3):311-21.

152. Quigley MF, Gonzalez VD, Granath A, Andersson J, Sandberg JK. CXCR5+ CCR7- CD8 T cells are early effector memory cells that infiltrate tonsil B cell follicles. European Journal of Immunology. 2007;37(12):3352-62.

153. Forster R, Emrich T, Kremmer E, Lipp M. Expression of the G-protein--coupled receptor BLR1 defines mature, recirculating B cells and a subset of T-helper memory cells. Blood. 1994;84(3):830-40.

154. Andrew DP, Ruffing N, Kim CH, Miao W, Heath H, Li Y, et al. C-C chemokine receptor 4 expression defines a major subset of circulating nonintestinal memory T cells of both Th1 and Th2 potential. The Journal of Immunology 2001;166(1):103-11.

155. El-Asmar L, Springael JY, Ballet S, Andrieu EU, Vassart G, Parmentier M. Evidence for negative binding cooperativity within CCR5-CCR2b heterodimers. Molecular Pharmacology. 2005;67(2):460-9.

156. Bjorndal A, Deng H, Jansson M, Fiore JR, Colognesi C, Karlsson A, et al. Coreceptor usage of primary human immunodeficiency virus type 1 isolates varies according to biological phenotype. Journal of Virology. 1997;71(10):7478-87.

157. Simmons G, Wilkinson D, Reeves JD, Dittmar MT, Beddows S, Weber J, et al. Primary, syncytium-inducing human immunodeficiency virus type 1 isolates are dual-tropic and most can use either Lestr or CCR5 as coreceptors for virus entry. Journal of Virology. 1996;70(12):8355-60.

158. Deng H, Liu R, Ellmeier W, Choe S, Unutmaz D, Burkhart M, et al. Identification of a major co-receptor for primary isolates of HIV-1. Nature. 1996;381(6584):661-6.

159. Freeman CM, Curtis JL, Chensue SW. CC chemokine receptor 5 and CXC chemokine receptor 6 expression by lung CD8+ cells correlates with chronic obstructive pulmonary disease severity. The American Journal of Pathology. 2007;171(3):767-76.

160. Fuchimoto Y, Kanehiro A, Miyahara N, Koga H, Ikeda G, Waseda K, et al. Requirement for Chemokine Receptor 5 in the Development of Allergen-Induced Airway Hyperresponsiveness and Inflammation. American Journal of Respiratory Cell and Molecular Biology. 2011;45(6):1248-55.

161. Kohlmeier JE, Miller SC, Smith J, Lu B, Gerard C, Cookenham T, et al. The Chemokine Receptor CCR5 Plays a Key Role in the Early Memory CD8+ T Cell Response to Respiratory Virus Infections. Immunity. 2008;29(1):101-13.

162. Ishida Y, Kimura A, Kondo T, Hayashi T, Ueno M, Takakura N, et al. Essential roles of the CC chemokine ligand 3-CC chemokine receptor 5 axis in bleomycin-induced pulmonary fibrosis through regulation of macrophage and fibrocyte infiltration. The American Journal of Pathology. 2007;170(3):843-54.

163. Förster R, Kremmer E, Schubel A, Breitfeld D, Kleinschmidt A, Nerl C, et al. Intracellular and Surface Expression of the HIV-1 Coreceptor CXCR4/Fusin on Various Leukocyte Subsets: Rapid Internalization and Recycling Upon Activation. The Journal of Immunology. 1998;160(3):1522-31.

164. Schabath R, Müller G, Schubel A, Kremmer E, Lipp M, Förster R. The murine chemokine receptor CXCR4 is tightly regulated during T cell development and activation. Journal of Leukocyte Biology. 1999;66(6):996-1004.

165. Feng Y, Broder CC, Kennedy PE, Berger EA. HIV-1 entry cofactor: functional cDNA cloning of a seven-transmembrane, G protein-coupled receptor. Science. 1996;272(5263):872-7.

166. Eitner F, Cui Y, Hudkins KL, Alpers CE. Chemokine receptor (CXCR4) mRNA-expressing leukocytes are increased in human renal allograft rejection. Transplantation. 1998;66(11):1551-7.

167. Song JS, Kang CM, Kang HH, Yoon HK, Kim YK, Kim KH, et al. Inhibitory effect of CXC chemokine receptor 4 antagonist AMD3100 on bleomycin induced murine pulmonary fibrosis. Experimental & Molecular Medicine. 2010;42(6):465-72.

168. Xu J, Mora A, Shim H, Stecenko A, Brigham KL, Rojas M. Role of the SDF-1/CXCR4 axis in the pathogenesis of lung injury and fibrosis. American Journal of Respiratory Cell and Molecular Biology. 2007;37(3):291-9.

169. Andersson-Sjöland A, de Alba CG, Nihlberg K, Becerril C, Ramírez R, Pardo A, et al. Fibrocytes are a potential source of lung fibroblasts in idiopathic pulmonary fibrosis. The international Journal of Biochemistry & Cell Biology. 2008;40(10):2129-40.

170. Yang IV, Burch LH, Steele MP, Savov JD, Hollingsworth JW, McElvania-Tekippe E, et al. Gene Expression Profiling of Familial and Sporadic Interstitial Pneumonia. American Journal of Respiratory and Critical Care Medicine. 2007;175(1):45-54.

171. Barrera L, Mendoza F, Zuñiga J, Estrada A, Zamora AC, Melendro EI, et al. Functional Diversity of T-Cell Subpopulations in Subacute and Chronic Hypersensitivity Pneumonitis. American Journal of Respiratory and Critical Care Medicine. 2008;177(1):44-55.

172. Johansson-Lindbom B, Svensson M, Wurbel M-A, Malissen B, Márquez G, Agace W. Selective Generation of Gut Tropic T Cells in Gut-associated Lymphoid Tissue (GALT): Requirement for GALT Dendritic Cells and Adjuvant. The Journal of Experimental Medicine. 2003;198(6):963-9.

173. Wendland M, Czeloth N, Mach N, Malissen B, Kremmer E, Pabst O, et al. CCR9 is a homing receptor for plasmacytoid dendritic cells to the small intestine. Proceedings of the National Academy of Sciences of the United States of America. 2007;104(15):6347-52.

174. Hart AL, Ng SC, Mann E, Al-Hassi HO, Bernardo D, Knight SC. Homing of immune cells: Role in homeostasis and intestinal inflammation. Inflammatory Bowel Diseases. 2010;16(11):1969-77.

175. Wermers JD, McNamee EN, Wurbel MA, Jedlicka P, Rivera–Nieves J. The Chemokine Receptor CCR9 Is Required for the T-Cell–Mediated Regulation of Chronic Ileitis in Mice. Gastroenterology. 2011;140(5):1526-35.e3.

176. Svensson M, Marsal J, Uronen-Hansson H, Cheng M, Jenkinson W, Cilio C, et al. Involvement of CCR9 at multiple stages of adult T lymphopoiesis. Journal of Leukocyte Biology. 2008;83(1):156-64.

177. Campbell JJ, Brightling CE, Symon FA, Qin S, Murphy KE, Hodge M, et al. Expression of Chemokine Receptors by Lung T Cells from Normal and Asthmatic Subjects. The Journal of Immunology. 2001;166(4):2842-8.

178. Soler D, Humphreys TL, Spinola SM, Campbell JJ. CCR4 versus CCR10 in human cutaneous TH lymphocyte trafficking. Blood. 2003;101(5):1677-82.

179. Kagami S, Saeki H, Tsunemi Y, Nakamura K, Kuwano Y, Komine M, et al. CCL27-transgenic mice show enhanced contact hypers ensitivity to Th2, but not Th1 stimuli. European Journal of Immunology. 2008;38(3):647-57.

180. Shankar SP, Wilson MS, DiVietro JA, Mentink-Kane MM, Xie Z, Wynn TA, et al. RGS16 Attenuates Pulmonary Th2/Th17 Inflammatory Responses. The Journal of Immunology. 2012;188(12):6347-56.

181. Calabresi PA, Yun SH, Allie R, Whartenby KA. Chemokine receptor expression on MBP-reactive T cells: CXCR6 is a marker of IFNγ-producing effector cells. Journal of Neuroimmunology. 2002;127(1–2):96-105.

182. Day C, Patel R, Guillen C, Wardlaw AJ. The chemokine CXCL16 is highly and constitutively expressed by human bronchial epithelial cells. Experimental Lung Research. 2009;35(4):272-83.

183. Lee LN, Ronan EO, de Lara C, Franken KLMC, Ottenhoff THM, Tchilian EZ, et al. CXCR6 Is a Marker for Protective Antigen-Specific Cells in the Lungs after Intranasal Immunization against Mycobacterium tuberculosis. Infection and Immunity. 2011;79(8):3328-37.

184. Morgan AJ, Guillen C, Symon FA, Huynh TT, Berry MA, Entwisle JJ, et al. Expression of CXCR6 and its ligand CXCL16 in the lung in health and disease. Clinical & Experimental Allergy. 2005;35(12):1572-80.

185. Morgan AJ, Guillen C, Symon FA, Birring SS, Campbell JJ, Wardlaw AJ. CXCR6 identifies a putative population of retained human lung T cells characterised by co-expression of activation markers. Immunobiology. 2008;213(7):599-608.

186. Ferguson AR, Engelhard VH. CD8 T cells activated in distinct lymphoid organs differentially express adhesion proteins and coexpress multiple chemokine receptors. The Journal of Immunology 2010;184(8):4079-86.

187. Widney DP, Hu Y, Foreman-Wykert AK, Bui KC, Nguyen TT, Lu B, et al. CXCR3 and its ligands participate in the host response to Bordetella bronchiseptica infection of the mouse respiratory tract but are not required for clearance of bacteria from the lung. Infection and immunity. 2005;73(1):485-93.

## 9.2 Illustrations

Figure 1 Classification of ILD and relative frequency of subgroups ..... 8
Figure 2 Emission spectra of FITC and PE with respective filter bandpass ..... 22
Figure 3 First step in the analysis of FACS data; example of a lung sample ..... 26
Figure 4 Histogram showing living cells ..... 27
Figure 5 Histograms showing $CD3^+$ cells ..... 27
Figure 6: BAL sample; Dot plot showing $CD3^+$ cells ..... 28
Figure 7 Histograms showing $CD4^+$ cells ..... 28
Figure 8 Dot plot showing $CD4^+$ T cells, quadrants determining $CD4^+$ T cell subtypes ..... 29
Figure 9 Histograms showing T-cell subtypes, in lung samples ..... 30
Figure 10 Dot plot showing living cells ..... 31
Figure 11 Example for assessment of chemokine receptor co-expression with CCR2 ..... 31
Figure 12 Experimental outline of bleomycin induced Lung fibrosis ..... 34
Figure 13 Body weight change over time course ..... 36
Figure 14 Masson Goldner's Tricrom stain of histological sections of lung tissue from saline or BLM treated mice ..... 37
Figure 15 Cell count of BAL during time course ..... 40
Figure 16 Percentages of $CD4^+$ T cells within living BAL ..... 41
Figure 17 Percentages of $CD8^+$ T-cells within living BAL cells ..... 41
Figure 18 Percentages of $CD4^+$ T cells within total living cells in lung samples during time course; ..... 42
Figure 19 Percentages of $CD8^+$ T cells within living cells in lung samples during time course ..... 43
Figure 20 Percentages of $T_{naive}$ $CD4^+$ cells within total $CD4^+$ T cells in lung samples during time course ..... 43
Figure 21 Percentages of $T_{cm}$ $CD4^+$ cells content within total $CD4^+$ T cells in lung samples during time course ..... 44
Figure 22 Percentages of $T_{em}$ $CD4^+$ cells within total $CD4^+$ T cells in lung samples during time course ..... 44
Figure 23 Percentage of $CCR2^+CD4^+$ T cells within total $CD4^+$ T cells in BAL ..... 45
Figure 24 Percentage of $CCR2^+CD8^+$ T cells within total $CD8^+$ T cells in BAL ..... 46
Figure 25 Percentages of $CCR2^+CD4^+$ T cells within total $CD4^+$ T cells in lung samples ..... 46
Figure 26 Percentages of $CCR2^+CD4^+$ T cells within total living cells ..... 47
Figure 27 Percentages of $CCR2^+CD8^+$ T cells of total $CD8^+$ T cells in lung samples during time course ..... 48
Figure 28 Percentages of $CCR2^+$ $CD4^+$ T cells within total living cells during time course ..... 48
Figure 29 Percentages of $CCR2^+$ $T_{naïve}$ within total $T_{naive}$ during time course ..... 49
Figure 30 Percentages of $CCR2^+$ $T_{em}$ within total $T_{em}$ during time course ..... 49
Figure 31 Sums of the percentages of $CCR2^+CD4^+$ and $CCR2^+CD8^+$ T cells within total living lung cells ..... 50
Figure 32 $CCR2^+$ $CD4^+$ and $CCR2^+CD8^+$ T cells at day 12 from saline treated control mice and bleomycin treated mice ..... 51
Figure 33 $CCR3^+$ T cells at day 12 after BLM ..... 52
Figure 34 $CCR4^+$ T cells at day 12 after BLM treatment ..... 53
Figure 35 $CCR5^+$ T cells at day 12 after BLM treatment ..... 54
Figure 36 CCR6+ T cells at day 12 after BLM treatment ..... 55
Figure 37 $CCR7^+$ T cells at day 12 after BLM treatment ..... 56
Figure 38 $CCR9^+$ T cells at day 12 after BLM treatment ..... 57
Figure 39 $CXCR3^+$ T cells at day 12 after BLM treatment ..... 58
Figure 40 $CXCR4^+$ T cells at day 12 after BLM treatment ..... 59
Figure 41 $CXCR5^+$ T cells at day 12 after BLM treatment ..... 60
Figure 42 $CXCR6^+$ T cells at day 12 after BLM treatment ..... 61

## 9.3 **Tables**

Table 1 Antibodies and set-up used to compensate for spectral overlap of fluorochromes ..... 23
Table 2 Spectral overlap for spleen samples ..... 23
Table 3 Spectral overlap for lung samples ..... 24
Table 4 Antibodies used for BAL samples ..... 24
Table 5 Antibodies used for spleen and lung samples ..... 24
Table 6 Antibodies used for assessment of chemokine receptor expression ..... 25
Table 7 Number of animals for time course experiments ..... 35
Table 8 Body weight on D0 and the different time points ..... 35
Table 9 Percentages of $CD4^+$ and $CD8^+$ T cells within total living cell population in spleen samples ..... 38
Table 10 Percentages of $CD4^+$ T-cell subtypes within total $CD4^+$ T cells in spleen ..... 38
Table 11 Percentages of CCR2 expressing $CD4^+$ or $CD8^+$ cells within total $CD4^+$ and $CD8^+$ cells in spleen ..... 39
Table 12 Percentages of CCR2 expression within $CD4^+$ T-cell subtypes in spleen ..... 39

## Danksagung

Am Ende dieser Arbeit möchte ich ein Dankeschön an einige Personen aussprechen, ohne die die Fertigstellung dieser Dissertation nicht möglich gewesen wäre.

Besonders bedanken möchte ich mich bei PD Dr. med. Susanne Krauss-Etschmann für die Möglichkeit an dem interessanten Thema zu arbeiten und so das experimentelle wissenschaftliche Arbeiten zu erlernen und für die Betreuung der Arbeit.

Ein herzliches Dankeschön geht auch an Dr. Yingyan Yu für die gute und enge Zusammenarbeit in der experimentellen Phase des Projektes, für die Einführung in die Arbeit mit den Mäusen und auch für die konstruktiven Diskussionen über die Organisation der Versuche und deren Durchführung.

Bedanken möchte ich mich auch besonders bei meiner Mitdoktorandin Katharina Singer, die mir in der Anfangsphase die Einarbeitung im Labor sehr erleichtert hat.

Ein ganz großes Dankeschön gebührt auch Rabea Imker und Cornelia Dalibor für die viele praktische Unterstützung an den Versuchstagen ohne die viele Versuche kaum realisierbar gewesen wären.

Genauso möchte ich mich bei allen anderen Mitarbeitern der Arbeitsgruppe und im CPC bedanken für die gute Zusammenarbeit und die tolle Arbeitsatmosphäre.

Nicht zuletzt möchte ich mich auch bei meiner Familie bedanken. Meinen Eltern und Geschwistern, die mich bei meinem Studium und der Doktorarbeit immer unterstützt und angespornt haben und ganz besonders auch bei meiner Geda, die immer mitgefiebert und an ich geglaubt hat.

## Eidesstattliche Versicherung

Ich erkläre hiermit an Eides statt,

dass ich die vorliegende Dissertation mit dem Thema

*„ Phenotypic characterization of CCR2$^+$ T cells in experimental pulmonary fibrosis“*

selbständig verfasst, mich außer der angegebenen keiner weiteren Hilfsmittel bedient und alle Erkenntnisse, die aus dem Schrifttum ganz oder annähernd übernommen sind, als solche kenntlich gemacht und nach ihrer Herkunft unter Bezeichnung der Fundstelle einzeln nachgewiesen habe.

Ich erkläre des Weiteren, dass die hier vorgelegte Dissertation nicht in gleicher oder in ähnlicher Form bei einer anderen Stelle zur Erlangung eines akademischen Grades eingereicht wurde.

München, den 25.07.2014

Eva Alice Brudy